Coordination Chemistry Reviews 393 (2019) 79–117

Contents lists available at ScienceDirect

Coordination Chemistry Reviews

journal homepage: www.elsevier.com/locate/ccr

Review

Organometallic and coordination rhenium compounds and their potential in cancer therapy

Elisabeth B. Bauer [a], Allison A. Haase [b], Robert M. Reich [a], Debbie C. Crans [b,c,*], Fritz E. Kühn [a,*]

[a] Molecular Catalysis, Catalysis Research Center and Department of Chemistry, Technische Universität München, Lichtenbergstr. 4, 85747 Garching bei München, Germany
[b] Department of Chemistry, Colorado State University, Fort Collins, CO 80523-1872, United States
[c] Cell and Molecular Biology Program, Colorado State University, Fort Collins, CO 80523-1872, United States

ARTICLE INFO

Article history:
Received 30 November 2018
Received in revised form 29 April 2019
Accepted 30 April 2019
Available online 22 May 2019

This manuscript is dedicated to our friend and colleague Armando Pombeiro on the occasion of his 70th birthday.

Keywords:
Rhenium complexes
Anticancer
Therapeutic applications
Cytotoxicity
IC_{50} values
Clinical applications of Re compounds

ABSTRACT

This review focuses on cytotoxic rhenium compounds in terms of IC_{50} values, their mode of action in biological systems and their status in clinical trials. Biological studies of different rhenium compounds ordered by the oxidation state of rhenium are presented. Numerous rhenium complexes are reported, with the greatest number of compounds containing a $Re(I)(CO)_3^+$ core. A wide range of complexes has been designed using a combination of organometallic ligands, N- or S-based ligands, peptides, multidentate ligands and oxo groups. Design concepts based on membrane permeability and lipophilicity, membrane receptor targets and specific enzyme targets are presented. The cytotoxicity parameter IC_{50} is shown for organometallic compounds, coordination complexes, clusters and Re(oxo) complexes. In addition, a brief summary of *in vivo* studies is given. A further summary of rhenium compounds subjected to clinical trials is presented to provide information about the classes of rhenium compounds that have been tested in human beings and the approaches used in these studies. Moreover, the comparability of the IC_{50} values among the cytotoxicity studies is critically assessed to provide the basis for a summary of the most potent rhenium compounds according to their reported IC_{50} values for each type of cancer. The summary of the structures for the most cytotoxic complexes allows the identification of structural similarities and basic features that could lead to their cytotoxicity and might be useful for future investigations. Finally, the information from the analysis of the rhenium compounds subjected to cellular studies is compared to data on the rhenium compounds that have been involved in *in vivo* evaluation and clinical trials.

Contents

1. Introduction . . . 80
2. Basics of bioinorganic rhenium anticancer studies: rhenium chemistry and compounds . . . 80
   2.1. Elemental rhenium's occurrence and application . . . 80
   2.2. Methods of evaluating cytotoxicity in cell culture . . . 81
3. Organometallic Re(I) compounds . . . 82

Abbreviations: AChE, acetylcholinesterase; BiPy, bipyridine; BSA, bovine serum albumin; Cp, cyclopentadienyl; CQR, chloroquine-resistant; CQS, chloroquine-sensitive; *D. magna*, *Daphnia magna*; DCA, dichloroacetate; DFT, density functional theory; dppf, 1,10-bis(diphenylphosphino)-ferrocene; EC_{50}, half maximal effective concentration; ED_{50}, half maximal effective dose; EGFR, epidermal growth factor receptor; ER, estrogen receptor; GFAAS, graphite furnace atomic absorption spectroscopy; GLUT, glucose transporter; GnRH, gonadotropin-releasing hormone; h, hour; HDAC, histone deactylase; hMAB, humanized monoclonal antibody; HPLC, high-performance liquid chromatography; HSAB, Hard and Soft Acid and Base; IC_{50}, half-maximal inhibitor concentration; *L. minor*, *Lemna minor*; LD_{50}/LC_{50}, half-maximal lethal dose/concentration; MAG_3, mercapto acetyl triglycine; min, minute; MTT, 3-(4,5-dimehtylthiazol-2-yl)-2,5-diphenyltetrazolium bromide; n.a., not active; NAD, nicotinamide adenine dinucleotide; NADH, reduced NAD; NIS, sodium iodide symporter; NIS US, National Institute of Health of the United States; n.d., not determined; MAB, monoclonal antibody; OTf, triflate; PACT, photoactivated chemotherapy; PBR, peripheral benzodiazepine receptor; PDK, pyruvate dehydrogenase kinase; PDT, photodynamic therapy; PEG, polyethylene glycol; PI, propidium iodide; *R. subcapitata*, *Raphidocelis subcapitata*; ROS, reactive oxygen species; SAHA, suberanilohydroxamic acid (also known as Vorinostat); SERM, Selective Estrogen Receptor Modulator; SPECT, single photon emission computed tomography; t, ton (metric); $t_{1/2}$, half-life; TFA, trifluoroacetic acid; TSPO, translocator protein; *V. fischeri*, *Vibro fischeri*.

* Corresponding authors.
E-mail address: fritz.kuehn@ch.tum.de (F.E. Kühn).

https://doi.org/10.1016/j.ccr.2019.04.014
0010-8545/

3.1. Fundamental chemical properties of organometallic Re(I) compounds . . . 82
3.2. $(CO)_3$Re(I)Cp derivatives . . . 82
3.3. $(CO)_3$Re complexes with N-donor ligands . . . 85
3.4. $(CO)_3$Re complexes with pyridine ligands . . . 91
3.5. $(CO)_3$Re complexes with mixed donor ligands . . . 93
4. Re coordination compounds . . . 98
4.1. Coordination compounds of Re(III), Re(IV) and Re(V) . . . 98
5. Re clusters, Re(VII) trioxo compounds and perrhenates . . . 101
5.1. Re cluster compounds . . . 101
5.2. Re(VII) trioxo compounds and perrhenates . . . 105
6. *In vivo* studies of Re compounds . . . 105
6.1. $(CO)_3$Re(I) based compounds . . . 105
6.2. Dirhenium(III) based compounds . . . 106
6.3. Re(V) based compounds . . . 107
6.4. Re cluster and Re(VII) based compounds . . . 108
7. Clinical trials . . . 109
8. Summary of most effective compounds in various cell lines . . . 112
9. Conclusions . . . 115
Acknowledgments . . . 115
Declaration of interest . . . 115
References . . . 115

1. Introduction

Although a vast number of compounds with anticancer effects have been identified, cancer is still among the leading causes for death worldwide [1]. Cancer treatment options depend on type, stage and location of the cancer. Often, all malignant cells are removed by surgery. Alternatively, either with or without surgery, chemotherapeutic agents or hormonal agents are used to treat the cancerous cells followed by continued treatments such as radiotherapy [2]. Increasingly, the biological targets of the chemotherapeutic drugs are identified leading to a better understanding of their mechanism of action. This growing knowledge allows the development of new and more powerful target-specific drugs. This is important, as cells can develop immunity against commonly used, rather unspecific anticancer drugs, like cisplatin [3,4]. It is critical that scientists continue to identify innovative approaches to combat cancer cells, and consequently information on the molecular structures for active compounds are essential for any structural based approaches to drug development.

Diagnosis at an early stage of cancer is also a crucial factor for successful treatment and therefore survival of patients. Thus, diagnostic nuclear medicine using radiolabeled cancer-targeting compounds represents a powerful, non-invasive tool. One of the most widely applied radioactive isotopes in this field is technetium-99m, which emits γ-radiation with an energy of 140 keV and a half-life of 6 h which is ideal for diagnostic imaging. Its congener rhenium has both stable isotopes and radioactive isotopes suitable for therapeutic applications. Due to similar physicochemical properties, Tc and Re are often applied to combine diagnostic and therapeutic ('theranostic') approaches, and such applications have frequently been reviewed [5–12]. Furthermore, Re compounds are promising theranostic candidates due the diagnostic applicable γ-emission of ^{186}Re and ^{188}Re isotopes or by replacing the Re core by ^{99m}Tc. Therapeutic possibilities are provided by cytotoxic Re compounds, based on either non-radioactive Re isotopes or β-emitting ^{186}Re and ^{188}Re. In addition, non-radioactive Re compounds are studied for their medicinal benefits. For example, luminescent Re carbonyl complexes and their application as imaging agents as well as (photo)cytotoxic and photosensitizing agents are summarized in some recent reviews [13–15]. However, the reported anticancer effects of Re and its ability to be used for therapeutic purposes makes this element particularly attractive as a drug component.

Already clinically approved drugs like cisplatin for treatment of cancer and chloroquine for treatment of malaria have been widely applied for decades and resistances to these drugs have been documented and increasingly becoming a problem. In the case of cisplatin, the observed resistance is presumably a consequence of genetic and epigenetic changes of different cellular pathways as well as inherent cellular defense mechanisms activated in response to external toxins [4]. *P. falciparum*, a parasite that causes malaria in humans and is treated with chloroquine, develops resistance over the years of chloroquine treatment by changes in the parasite's chromosome [16]. Therefore, many studies focus on overcoming resistance, and replacing these older drugs.

Thus, in-depth biological studies on Re(I) tricarbonyl complexes are performed by several groups [17,18] and an excellent review reported in 2014 by Gasser *et al.* [19] summarizes the effects of cytotoxic Re(I) carbonyl complexes. In addition covering recent results, this review describes cytotoxic Re complexes in various oxidation states and coordination modes, the limited number of Re compounds in *in vivo* studies, and highlights the class of compounds having advanced to clinical trials. Additionally, where investigated, the studies on the mechanism of action of the complexes and their biological targets are discussed. Thus, the aim of this review is to identify basic concepts and structural features for future investigations on Re based pharmaceuticals.

2. Basics of bioinorganic rhenium anticancer studies: rhenium chemistry and compounds

2.1. Elemental rhenium's occurrence and application

Rhenium is one of the rarest earth metals and the last of the stable elements that has been identified [20,21]. In nature, rhenium is only found in association with other, more common metals such as molybdenum in ores and not as an element [22]. Comparatively high amounts of Re sulfide are associated with molybdenum sulfide ores where Re is obtained by roasting and reduction processes. The most stable natural Re isotopes are ^{185}Re (37.4%, stable) and ^{187}Re (62.6%, β^--radiation, $t_{1/2} = 4.3 \times 10^{10}$ years). Additionally, the most prominent artificial isotopes are ^{186}Re (91%, β^--radiation, $t_{1/2} = 89.3$ h, $E_{max} = 1.07$ MeV; 9% γ-radiation, 137 keV) and ^{188}Re (85%, β^--radiation, $t_{1/2} = 17.021$ h, $E_{max} = 2.12$ MeV; 15%, γ-radiation, 155 keV) [23]. The global annual Re metal production was about 49.4 tons in

2015, which is an increase of 5% compared to 47.1 tons in 2014 [24]. The most common industrial application of Re is in super alloys found in turbine blades, combustion chambers and the exhaust nozzles of jet engines. The second most common application is in industrial catalysis, e.g. the "Rheniforming process" for production of lead-free gasoline [25]. Further industrially relevant catalytic reactions of Re compounds include hydrogenations, dehydrogenations, oxidations, olefin metathesis, aldehyde olefinations and epoxidation reactions [26–28].

Re and its radioactive congener Tc have similar physical properties such as ionic radii, shape, dipole moment and lipophilicity due to lanthanide contraction [29]. However, their chemical properties differ specifically in terms of their thermodynamic stability in high oxidation states and ligand substitution on the metal center, which is responsible for the differences when comparing Re and Tc compounds [11,29]. Nevertheless, the similarity of Tc and Re can be exploited for analysis of Tc compounds with methods requiring non-radioactive compounds as well as for combining therapeutic and diagnostic approaches for medicinal purposes without structural modifications of the compound [8]. Non-radioactive Re complexes are also applied in biological studies, which is a topic thoroughly discussed in this review. In the following, different biologically active Re complexes are described and classified based on the oxidation states of Re.

2.2. Methods of evaluating cytotoxicity in cell culture

To obtain insight into the degree of the compounds' cytotoxicity and/or antiproliferative effects, *in vitro* studies with various cancer cell lines are performed [30]. The most commonly applied assay method to evaluate anticancer effects is the MTT assay. Its name is derived from the yellow reagent 3-(4,5-dimehtylthiazol-2-yl)-2 ,5-diphenyltetrazolium bromide (MTT), which is converted to purple formazan upon transformation by mitochondrial reductase which only occurs in healthy, living cells. The amount of formazan can be quantified through changes in absorbance at 570 nm, which is proportional to the number of viable cells [31].

An alternative assay, the resazurin assay, makes use of the blue, non-fluorescent 7-hydroxy-10-oxidophenoxazin-10-ium-3-one (resazurin), which is also reduced in living cells to yield resofurin, a pink fluorescent dye. This reduction is also proportional to the amount of living cells and can be quantified by either measuring the absorbance or the fluorescence of a cell suspension [32,33]. Resazurin is also used in the alamar blue assay where supplements preventing the formation of resofurin are added to avoid reduction of the dye prior to its application in cell culture. Thus, a longer incubation period is required [32,33]. Another colorimetric method to determine the quantity of living cells in an assay is the crystal violet stain. Crystal violet has a strong affinity to the external surface of the DNA double helix and can stain DNA by intercalation [34]. In the lactate dehydrogenase assay, lactate is oxidized to pyruvate at the same time NAD is reduced to NADH [35,36]. These assays are readily monitored using the absorbance of NADH at 340 nm and belongs to a class of enzyme assays that takes advantage of the chromophore of the NADH/NAD couple. Such assays are used to display many different reactions that either use the NADH/NAD or NADPH/NADP directly or are connected to such a reaction. The reader is referred to other publications to obtain more information regarding assays [32,35,37].

The observed growth inhibition in these cytotoxicity assays is measured by calculating the number of living cells and plotting them against the concentration of the applied drug. For evaluation, a descending sigmoidal dose–response curve will be generated. In there, the concentration of the substance that is needed to inhibit cell growth by 50% is represented by the IC_{50} value. The identification of IC_{50} values is mostly used to determine the cytotoxicity of a drug. In contrast, the half-maximal effective concentration (EC_{50}) is the concentration of the substance that gives half-maximal response/effect, whereas the curve is ascending (see Fig. 1). The difference between IC_{50} (where 'I' stands for inhibition) and EC_{50}

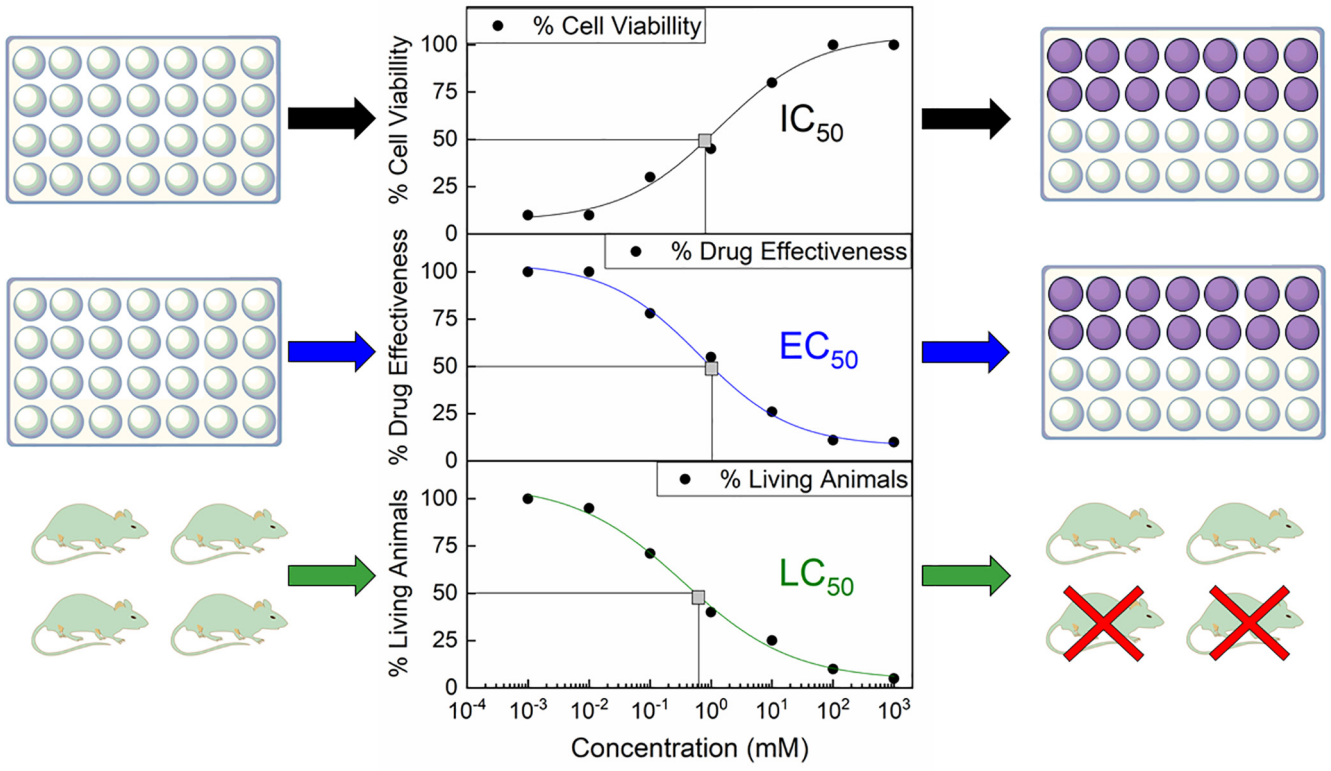

Fig. 1. Schematic representation of EC_{50}, IC_{50} and LD_{50} values.

(where 'E' stands for effect) is just the definition of the starting point and the end of the curve. Accordingly, IC_{50} values can be calculated for antagonists and EC_{50} for agonists. Furthermore, LD_{50} is the concentration of the compound that is lethal to half of the population of the organisms that are being studied. A schematic representation of how these values can be obtained is given in Fig. 1. For calculation of IC/EC_{50} values, different software packages can be used, for example Origin®, SigmaPlot®, Excel® or GraphPad®. They are able to calculate dose–response curves using the 'dose' of the applied substrate in the experimental cell assay (usually the logarithmic scale of the compound concentration) as the x-axis and the 'response' measured by spectrophotometry as the y-axis.

A standard dose–response curve can be calculated by non-linear regression using different calculation approaches. One is the four-parameter logistic equation (see Eq. (1)). The four parameters are the top and the bottom plateaus of the curve, the IC/EC_{50} and the slope factor (Hill slope), which is −1.0.

$$Y = \min + (\max - \min)/(1 + 10(X - \log IC_{50})) \quad (1)$$

This standard assumption is the easiest one for a data set with few data points; a variable slope is only useful with many data points (Eq. (2)).

$$Y = 100/(1 + 10(\log IC_{50} - X)\text{slope}) \quad (2)$$

Ideally, the curve matches the experimental data points [38].

Accordingly, the lower the IC_{50} value, the more cytotoxic the tested compound. Compounds with IC_{50} values >100 μM are termed 'non-toxic'. Compounds with an IC_{50} value between 5 and 100 μM are named 'moderately cytotoxic' and cytotoxic compounds have IC_{50} values <5 μM. Moreover, incubation times of 24 h represent the acute toxicity of the compound, whereas an incubation time of 72 h rather represents systemic influence of the test compound on cell growth, namely the antiproliferative properties of the compound. Some researchers will provide one or more times depending on the assay.

IC_{50} values provide preliminary insights into biological effects and the biological potency of the molecules in certain cell lines. In such assays, different biochemical processes occur and various receptors are presented by the cells. Hence, determination and comparison of IC_{50} values are measures for biological characteristics and profiles of potential drugs. Many issues complicate the observation and interpretation of cell growth studies, because it is usually assumed that the compound investigated readily penetrates the membrane and the compound reaches the active site in the cell. However, if the drug is not soluble in water, a DMSO solution is used for *in vitro* studies to administer the drug. If precipitation takes place when mixing the test solution with cell medium, the drug uptake will be delayed/reduced and thus the effect on cell growth will not be as large as anticipated. Therefore, drug precipitation will result in lower measurement of drug toxicity compared to a soluble drug. Nevertheless, cell culture evaluations have been used for many years, providing a well-known tool for comparing various compounds. However, caution must be used when comparing the values in various publications, as reported by Di *et al.* [30] and Sebaugh *et al.* [39]. It is every researcher's responsibility to consider published IC_{50} values when evaluating properties of compounds as potential drugs. Since many drugs are hydrophobic, they have limited cell culture media solubility and this fact may delay cellular uptake, which will result in reduced measurement of toxicity. Considering that many compounds under evaluation as potential drugs are very hydrophobic, such systematic errors in measurements are a widespread problem that should not be neglected.

Many studies include control drugs to provide a reference for their assays. Examples of control drugs that are used are cisplatin, chloroquine or, for specific drug-conjugated metal complexes, the corresponding ligand. These benchmark systems are well known with regard to their mechanism of action and their biological effects and therefore provide a valuable baseline to evaluate the potential of new compounds. Appropriate study designs will include growth studies in diseased, normal, and drug-resistant cell lines with the potential drug under investigation and the proper controls.

3. Organometallic Re(I) compounds

3.1. Fundamental chemical properties of organometallic Re(I) compounds

Synthesis and characterization of organometallic Re carbonyl complexes started in the early 1940's when Walter Hieber *et al.* studied the substitution of halogen Re pentacarbonyl complexes [40]. The $Re(I)(CO)_3^+$ core is very stable even in the presence of coordinating solvents or in solutions of dilute hydrochloric acid. Only sulfuric acid and nitric acid are capable of oxidizing the Re core and consequently decomposing these compounds [40].

The basic Re carbonyl chemistry and the synthetic procedures are well established. Depending on the nature of the ligands, the kinetically inert Re carbonyl complexes can exhibit distinct phosphorescence/luminescence properties and are therefore increasingly applied as photosensitizers and bioimaging agents [15]. Accordingly, investigations are ongoing to develop non-toxic imaging agents. Two reviews focusing on bioimaging, photocytotoxicity and photophysical properties of Re complexes were recently published [14,15].

Moreover, numerous cytotoxic Re(I) tricarbonyl complexes have been synthesized and evaluated for their anticancer properties since the first cytotoxic $Re(I)(CO)_3$ complexes, namely $[Re_2(\mu\text{-}OH)_3(CO)_6]$, $[Re_2(\mu\text{-}OH)(\mu\text{-}OPh)_2(CO)_6]$, $[Re_2(\mu\text{-}OMe)_2(\mu\text{-}dppf)_2(CO)_6]$, and $[Re_2(\mu\text{-}OPh)_2(\mu\text{-}dppf)_2(CO)_6]$ (dppf = 1,10-bis(diphenylphosphino)-ferrocene) were reported in 2000 by Yan *et al.* [41]. A review by Gasser *et al.* published in 2014 summarizes the biological evaluation of different $Re(I)(CO)_3$ based complexes [19]. The general structural feature of the rhenium complexes is the octahedral coordination geometry of the rhenium core providing three vacant coordination sites besides the three coordinated carbonyls. Considering the 'Hard and Soft Acid and Base' (HSAB) concept developed in 1963 by Pearson [42], the Re(I) carbonyl core is recognized as a hard Lewis acid. Accordingly, DFT calculations as well as experimental data determined the stability of Re(I) carbonyl complexes resulting in complex stabilities in the order N > S > O for donor atoms of the coordinating ligands stabilizing the $Re(I)(CO)_3^+$ core [43]. Therefore, predominantly Re(I) tricarbonyl complexes of pyridine, bipyridine and phenanthroline based ligands are found in literature, as the following sections show. However, convenient structural modifications of the Re complexes are possible, creating task-specific compounds for desired application, e.g. by changing the solubility and/or introducing certain functionalities. For biological applications, the relatively small and compact size of the Re carbonyl moiety compared to chelates and coordination complexes can be advantageous as well as the kinetic stability and inertness of the $Re(I)(CO)_3$ core [5].

In the following biomedical studies with different classes of Re (I) complexes will be summarized.

3.2. $(CO)_3Re(I)Cp$ derivatives

Cyrhetrene $[(CO)_3Re(\eta^5\text{-}C_5H_5)]$ based compounds are increasingly applied in biological studies due to their photo-physical and electrochemical properties, high stability in water and air, lipophilicity and specific biological activities [44,45]. This class of

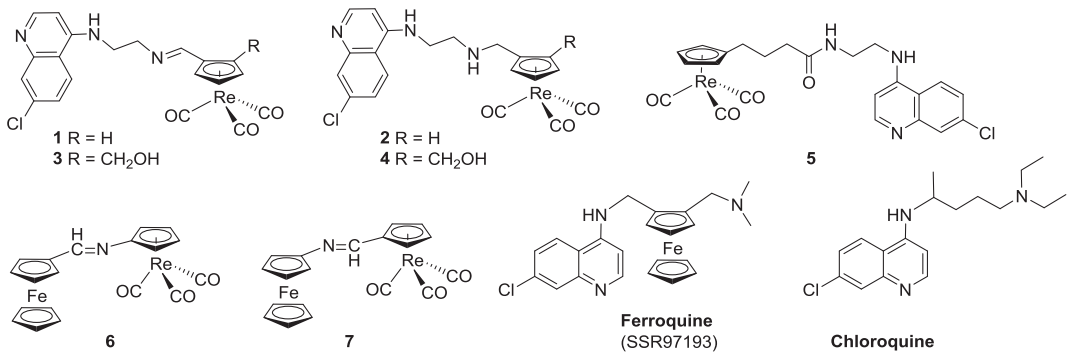

Fig. 2. Structures of $(CO)_3Re(I)Cp$ based compounds **1** to **5** (corresponding IC_{50} values are given in Table 1) and **6** and **7** (corresponding IC_{50} values are given in Table 2). Additionally, the structures of the reference drugs ferroquine and chloroquine are given.

Table 1
Antimalarial activity given as IC_{50} values in μM for different $(CO)_3Re(I)Cp$ based complexes with diamine appendages, **1** to **5** and the reference drugs ferroquine and chloroquine.

Compound [ref.]	Anti-malarial activity (*P. falciparum*)	
Strain	Chloroquine-sensitive 3D7	Chloroquine-resistant W2
1[a] [46]	0.064 ± 0.014	2.563 ± 0.772
2[a] [46]	0.497 ± 0.042	0.267 ± 0.083
3[a] [46]	0.085 ± 0.017	2.167 ± 0.306
4[a] [46]	5.500 ± 0.557	2.533 ± 0.153
Ferroquine[a] [46]	0.0034 ± 0.0006	0.0068 ± 0.0007
Chloroquine[a] [46]	0.023 ± 0.005	0.563 ± 0.085
Strain	D10	Dd2
5[b] [47]	0.27 ± 0.05	0.37 ± 0.06

[a] IC_{50} determination using microdilution radioisotope assay of Dejardins [46].
[b] IC_{50} determination using lactate dehydrogenase assay [47].

compounds is often studied as antimalarial [46,47] and anticancer agents [44,48–52]. The compounds shown in Fig. 2 are conjugated to a chloroquine moiety, which was a very successful organic antimalarial agent for decades until resistances to it were developed [47]. Therefore, research focused on chloroquine derivatives, like ferroquine, a ferrocene-chloroquine conjugate (structure given in Fig. 2), which is currently in phase II clinical trials [53]. Cyrhetrene-chloroquine conjugates **1** to **5** (Fig. 2) were studied for their biologic activity. The IC_{50} values against chloroquine-sensitive (CQS) and chloroquine-resistant (CQR) strains of *Plasmodium falciparum* are given in Table 1.

Klahn *et al.* published antimalarial studies on this class of compounds in 2010 with different linkers between the chloroquine entity and cyrhetrene (Fig. 2, compounds **1**–**4**). Additionally, the influence of metallocene substitution on antimalarial activity was studied by modification of the cyclopentadienyl ring with an electron-withdrawing group. The highest activities are shown by **1** and **3**, respectively, against the CQS strain (Table 1). Compound **2** displays higher cytotoxicity in the CQR strain exceeding even chloroquine. Attempts to correlate the lipophilicity with growth inhibition did not yield an obvious association [46].

Nordlander *et al.* synthesized compound **5** in order to compare the influence of the metal center on the antimalarial activity. However, a comprehensive evaluation of this study is difficult as the experimental section contains too little information about the assay procedure [47]. Even though the IC_{50} values are reported in the low micromolar range, the full potential of these compounds remains unclear due to solubility issues and the difficulties in carrying out an evaluation with such compound properties [47].

Further studies from the Klahn group focus on investigations of ferrocene-cyrhetrene derivatives **6** and **7** and their anticancer activity (Fig. 2 and Table 2) [44]. Compound **7** is both more stable and more active in cancer cell lines than **6,** although like cisplatin, is more cytotoxic to normal cells. Due to structural differences, the comparison of the IC_{50} values of **6** and **7** to **1**–**4** are based on function and show that **1** to **4** have significantly lower IC_{50} values and therefore are more potent than **6** and **7** [44].

$(CO)_3Re(I)Cp$ compounds **8** and **10** conjugated to the cell-penetrating peptide sC18 were synthesized, tested *in vitro* and compared to the corresponding Mn complexes **9** and **11** by Schatzschneider *et al.* [48]. The corresponding IC_{50} values are given in Table 3, the structures in Fig. 3. The results indicate that the exchange of the metal center has no influence on the cytotoxicity. However, the change of the linker from keto (**8** and **9**) to aliphatic (**10** and **11**) slightly decreases the IC_{50} value from about 60 μM to about 40 μM [48]. The peptide itself is non-toxic [54].

Table 2
IC_{50} values [μM] determined for $(CO)_3Re(I)Cp$ based complexes with imine appendages, **6** and **7**, in cancer and non-cancer cell lines applying a colorimetric assay with an incubation time of 72 h.

Compound [ref.]	Human cancer cell lines			Human non-cancer cell line
	MCF-7	MDA-MB-231	HCT-116	BJ
6 [44]	>30	>30	>30	71 ± 2
7 [44]	12 ± 5.2	7.4 ± 1.5	7.8 ± 3.3	21 ± 2
Cisplatin [44]	12 ± 2.8	13 ± 1.8	14 ± 1.0	23 ± 2

Table 3
Cytotoxicity and antiproliferative properties given as IC_{50} values in [μM] of $(CO)_3Re(I)Cp$ compounds with cell-penetrating appendages **8** to **14**.

Compound [ref.]	Human cancer cell lines				Murine cell line
	MCF-7	A431	HeLa	A375	B16F1
8[a] [48]	59.2 ± 7.3				
9[a] [48]	56.9 ± 2.1				
10[a] [48]	40.8 ± 8.9				
11[a] [48]	43.8 ± 6.4				
12[b] [49]	9.47	13.7	14.4	14.7	9.82
13[b] [49]	15.2	17.1	13.3	23.3	12.6
14[b] [49]	11.4	17.3	8.34	12.5	15.2
SAHA[b] [49]	3.74	4.44	4.45	4.58	3.67

[a] Resazurin assay read after 24 h of incubation time [48].
[b] MTT assay read after 72 h of incubation time [49].

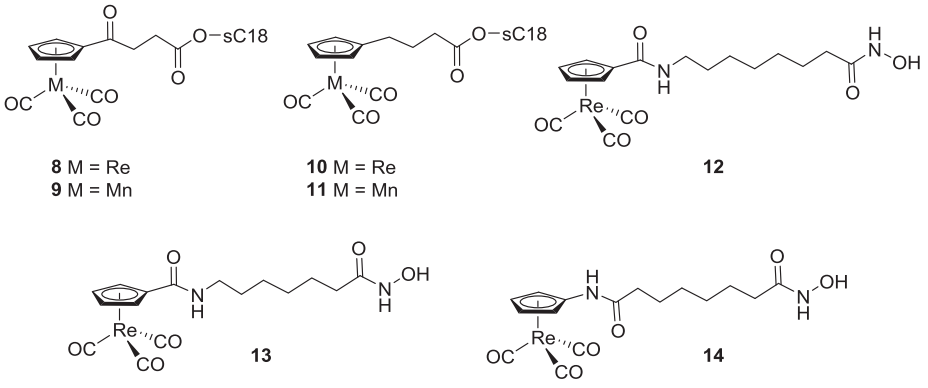

Fig. 3. Structures of $(CO)_3Re(I)Cp$ compounds with cell-penetrating appendages **8** to **14**. Corresponding IC_{50} values are given in Table 3.

In 2012, Alberto *et al.* examined the influence of the substitution of phenyl rings and different linker length of $(CO)_3Re(I)Cp$ based complexes on the biological activity by investigating histone deacetylase (HDAC) inhibition of SAHA conjugated compounds **12**–**14** (Fig. 3) [49]. It was shown that this modification does not alter the antiproliferative effect against different cancer cell lines. Complex **12** is the most active organometallic compound, though the organic compounds have lower IC_{50} values (1.6–5 μM). Compared to the activity of SAHA in HeLa cells, compound **12** has an IC_{50} value about twice of that of SAHA [49]. Additionally, the authors present a new versatile synthesis for [^{99m}Tc(I)$(CO)_3$(Cp-R)] imaging complexes. The published method involves amide-coupled *Thiele's* acids dimers $(HCp\text{-}R)_2$ with two R substituents leading to two different ^{99m}Tc labeled compounds *via* metal-mediated *retro Diels-Alder* reaction [49].

A comparison of the IC_{50} values of the compounds within Table 3 is problematic, because the incubation times are quite different, and it has been shown that the results of this type of study depend on incubation times [30]. Although compound **9** has a higher IC_{50} value after 24 h, it might be in the same range as **12** after 72 h.

The compounds studied by Metzler-Nolte *et al.* are based on $(CO)_3Re(I)Cp$ imines and conjugated to piperazine derivatives (compounds **15**–**22** in Fig. 4), which are assumed to target GSK-3β kinase [50]. These compounds were evaluated for their ability to inhibit growth of HT-29 and PT-45 cells. The results of the growth inhibiting studies are the IC_{50} values given in Table 4. For

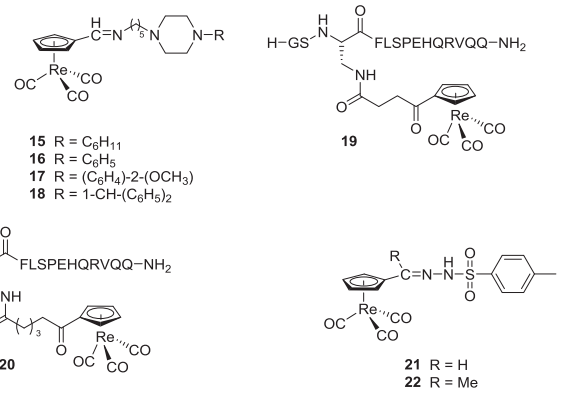

Fig. 4. Structures of $(CO)_3Re(I)Cp$ based complexes with imines or carbonyl appendages **15** to **22**. Corresponding IC_{50} values are given in Table 4.

the HT-29 growth inhibition, the results are in the same order of magnitude as cisplatin, which was also tested in the same study for comparison and gives an IC_{50} value of 32.6 ± 0.7 μM for cisplatin. In contrast, the compounds are almost inactive in PT-45 cells. Overall, complex **18** shows the lowest IC_{50} value for both cell lines [50].

Luyt *et al.* published Re(I)Cp carbonyl complexes conjugated to a specific peptide (ghrelin) with varying linker length (compounds

Table 4
IC_{50} values in [μM] of $(CO)_3Re(I)Cp$ based complexes with imines or carbonyl appendages **15** to **22**.

Compound [ref.]	Human cancer cell lines		Compound [ref.]	Chinese hamster cell line	Human cancer cell line
	HT-29	PT-45		CHO-K1	H1299
15[a] [50]	97.27 ± 0.06	na	**19**[b] [51]	0.035	
16[a] [50]	72.78 ± 0.04	na	**20**[b] [51]	0.174	
17[a] [50]	76.38 ± 0.05	90.16 ± 0.05	**21**[c] [52]		37.5 ± 6.6
18[a] [50]	30.48 ± 0.03	25.82 ± 0.03	**22**[c] [52]		24.3 ± 8.3
Cisplatin[a] [50]	32.6 ± 0.7	2.2 ± 0.3	**Cisplatin**[c] [52]		12.8 ± 5.6

(na = not active).
[a] MTT assay read after 72 h of incubation time [50].
[b] Radio ligand binding assay; no incubation time given [51].
[c] MTT assay read after 24 h of incubation time [52].

19 and **20** in Fig. 4) [51]. Compound **19**, with a shorter linker, has a significantly lower IC_{50} value than complexes with a longer linker (see Table 4). Thus, the linker length clearly influences the binding affinity to the receptor [51].

Concha *et al.* investigated the biological behavior of $(CO)_3Re(I)$ Cp tosylhydrazone complexes **21** and **22** (Fig. 4) [52]. These compounds were tested in MTT assays in comparison to the corresponding Mn and FeCp complexes as well as cisplatin. The resulting IC_{50} values are higher than that for cisplatin. The results of the study indicate that the electronic effect of the hydrazone substituent has much more influence on the biological activity than the metal center. This shows the importance of the applied ligand system [52].

Jaouen *et al.* modified Tamoxifen, one of the best-evaluated Selective Estrogen Receptor Modulators (SERMs), which are used to treat hormone dependent breast cancer, with organometallic moieties [55–57]. For a description on the mechanism of action of SERMs, the reader is referred to the publication by Jaouen *et al.* [55]. Modifications of Tamoxifen with cyclopentadienyl moieties of Fe, Ti, Re or ^{99m}Tc were studied to improve the therapeutic efficacy of this class of drugs [55]. Re(I) carbonyl derivatives of Tamoxifen (isomers of compound **23** in Fig. 5) are active in ERα positive breast cancer cells and inactive in ERα negative cells, similar to the parent drug. In brief, two different sub-types of estrogen receptor (ER) were discovered to play an important role in many physiological functions in the human body as well as in the evolution of breast cancer, namely ERα and ERβ. ERα is considered to be responsible for increased proliferation in breast tumors and in contrast, ERβ is thought to prevent proliferation. Accordingly, treatment of breast cancer should be possible applying ERα-antagonists or ERβ-agonists, respectively [58]. To evaluate whether a compound is acting as an agonist or antagonist, different cell models were applied. In the present study, the MVLN cell line with high ERα expression and the MDA-MB-231 cell line without ERα expression (but supposedly ERβ expression) were used. The results shown in Table 5 display no effect of incubating an isomeric mixture of Re complex **23** as well as Tamoxifen on MDA-MB-231 cells, however both tested compounds show antiproliferative effects in MVLN cells. This indicates an anti-oestrogenic effect (control is set at 100%; a value above 100% indicates an oestrogenic effect and a value lower than 100% an anti-oestogenic effect) [56].

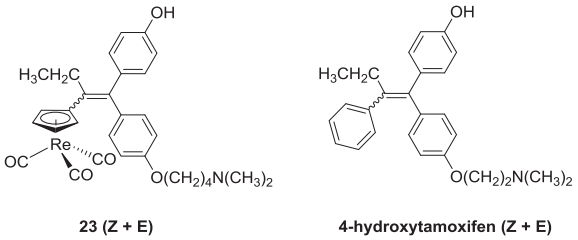

Fig. 5. Structure of $(CO)_3Re(I)Cp$ based Tamoxifen derivative **23** and 4-hydroxytamoxifen.

Table 5
Antiproliferative activity of compound **23** and 4-hydroxytamoxifen on MVLN (high ERα expression) and MDA-MB-231 (no ERα expression, supposedly ERβ expression) breast cancer cell lines in % of luciferase induction after 24 h of culture [56].

Compound [ref.]	Molarity	Human cancer cell line	
		MVLN	MDA-MB-231
23 [56]	1×10^{-6}	55.5	n.d.
23 [56]	1×10^{-7}	51.5	91
4-Hydroxytamoxifen [56]	1×10^{-7}	51.5	88

n.d. = not determined.

Replacing the non-radioactive Re core by either ^{188}Re or ^{186}Re for therapeutic purposes and by ^{99m}Tc for diagnostic applications provides theranostic use of these Tamoxifen derivatives [59].

3.3. $(CO)_3Re$ complexes with N-donor ligands

Efforts have been made to design complexes with improved cytotoxic activity for treatment of cancer. One approach taken is to add a ligand, which will provide additional toxicity to the complex. For example, the ligand is derived from organic drugs with known anticancer properties like doxorubicin or the ligand system, can be tuned resulting in increased cytotoxicity upon photolysis. Examples for such systems are shown in Fig. 6.

The $(CO)_3Re(I)$ core is known to have photosensitizing properties and it was shown that the cytotoxicity increased upon irradiation. Patra *et al.* studied $(CO)_3Re(I)$ based complexes with iminedipyridyl ligands **24** to **27** for their cytotoxicity in healthy and cancerous cell lines (Fig. 6 and Table 6) [60]. Moderate growth inhibition was observed with the lowest IC_{50} value of 7.8 ± 1.9 μM for complex **24** against HeLa cells, which is even lower than that determined for cisplatin in this cell line (see Table 6). However, no toxicity in HepG2 and healthy cells was observed, indicating that these compounds possess the potential to have a good and safe activity profile suitable for treatment of cervical cancer [60].

Paulo *et al.* studied the (photo)cytotoxicity of a series of $(CO)_3Re(I)$ based complexes with iminedipyridyl ligands including a heter-

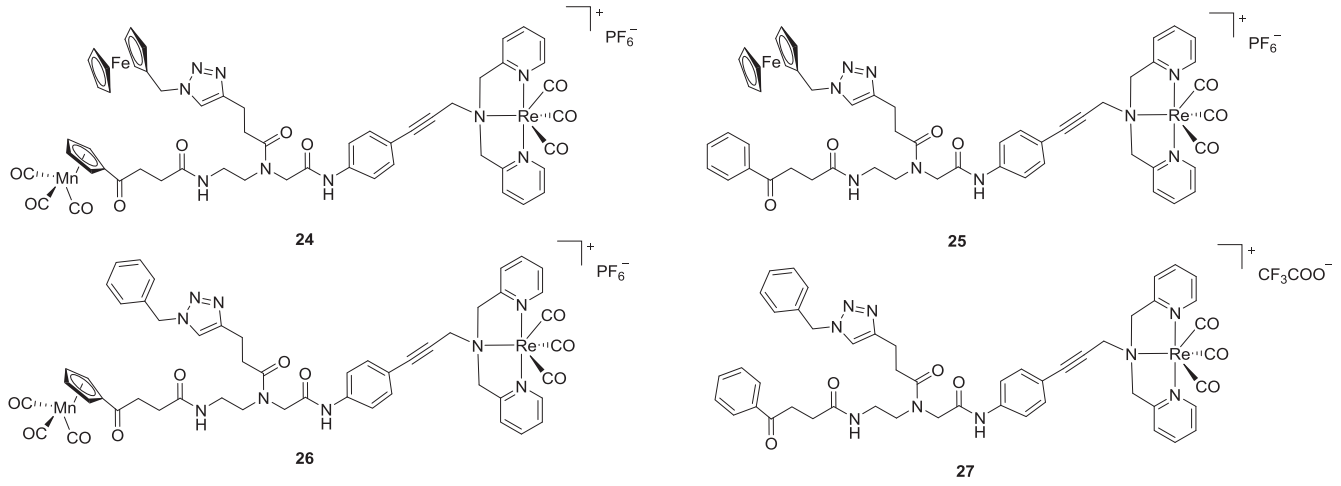

Fig. 6. Structures of $(CO)_3Re(I)$ based complexes with iminedipyridyl ligands **24** to **27**. Corresponding IC_{50} values are given in Table 6.

Table 6
IC_{50} values [μM] of different $(CO)_3Re(I)$ based complexes with iminedipyridyl ligands determined in different human cell lines.

Compound [ref.]	Human cancer cell lines		Human non-cancer cell line
	HepG2	HeLa	MRC-5
24[a] [60]	>100	7.8 ± 1.9	>100
25[a] [60]	>100	10.2 ± 2.0	22.8 ± 3.1
26[a] [60]	>100	8.0 ± 1.0	n.d.
27[a] [60]	52.7 ± 9.7	26.3 ± 0.8	36.9 ± 5.0
Cisplatin[a] [60]	5.5 ± 0.5	11.5 ± 2.9	7.9 ± 1.2

n.d. = not determined.
[a] MTT assay read after 48 h of incubation time [60].

obimetallic complex **29** shown in Fig. 7. The Re complexes **28** and **29** are cytotoxic in the dark as well as upon irradiation against cisplatin resistant cells. For both complexes, the IC_{50} values decreased upon irradiation to less than half compared to the IC_{50} values in the dark. The IC_{50} value in healthy cells in the dark is slightly higher than the values obtained by irradiation (Table 7). For cisplatin, a contradictory effect was observed leading to higher IC_{50} values upon irradiation, which is explainable by the shorter incubation time [61].

Superior cytotoxicity has been found for $(CO)_3Re(I)$ complexes (and include two $(CO)_3Re(I)Cp$ complexes) with doxorubicin conjugates **30**–**34** reported by Alberto *et al.* One of these complexes, **33**, has an IC_{50} value of 0.34 μM in HeLa cells (Table 7). Moreover, it was shown by confocal microscopy and ICP-MS that in contrast to the parent drug and compounds **30**–**32**, complexes **33** and **34** accumulate to a much higher extent in mitochondria (2% and

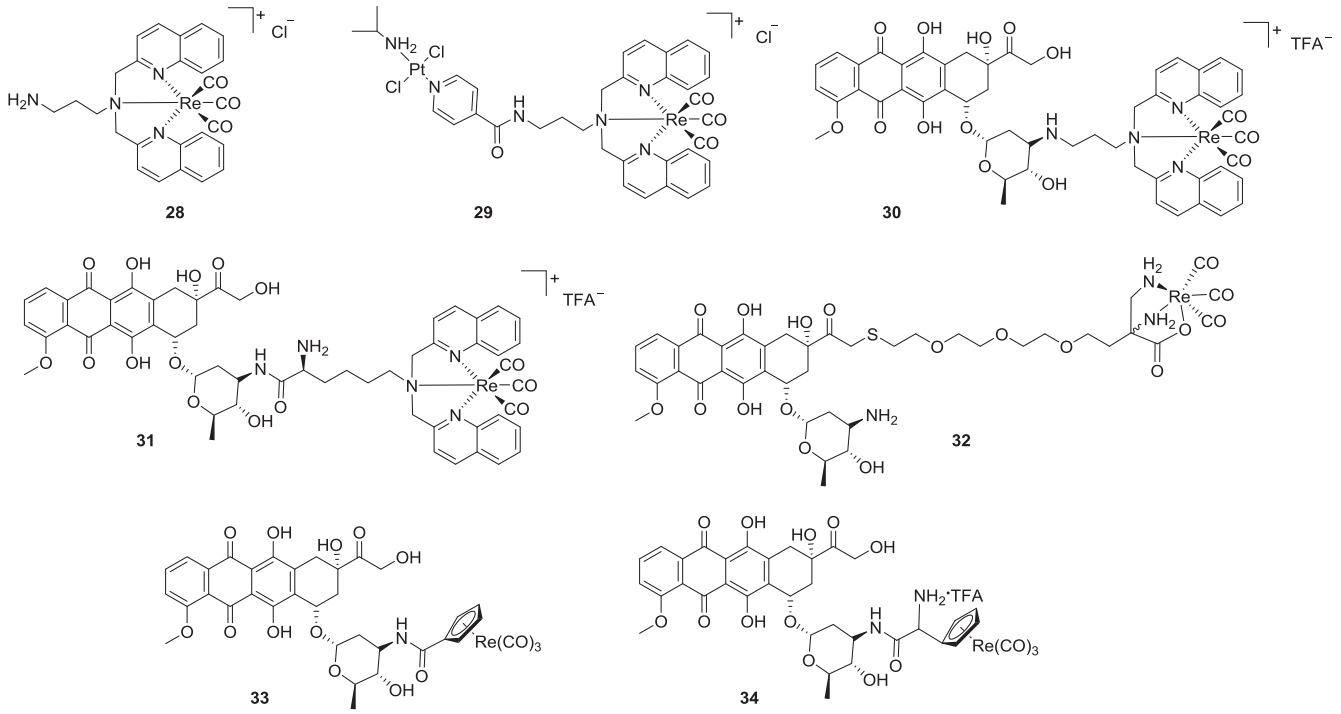

Fig. 7. Structures of a series of $(CO)_3Re(I)$ based complexes with iminedipyridyl ligands (**28** to **32**) and two $(CO)_3Re(I)Cp$ complexes with doxorubicin conjugates (**33** to **34**). The corresponding IC_{50} values are given in Table 7.

Table 7
IC_{50} values in [μM] determined for $(CO)_3Re(I)$ based complexes with iminedipyridyl ligands (**28** to **32**) and two $(CO)_3Re(I)Cp$ complexes with doxorubicin conjugates (**33** and **34**).

Compound [ref.]	Human non-cancer cell line		Human cancer cell line			Murine cell line
	MRC-5	RPE1-hTERT	HeLa	A2780	A2780R	B16F1
28[a] [61]	121 ± 10.1		155 ± 22/20.1 ± 6.5	46.1 ± 6.5/7.8 ± 1.6	198 ± 20.5/19.3 ± 2.1	
29[a] [61]	22.0 ± 5.3		42.8 ± 4.7/13.5 ± 4.1	28.7 ± 4.2/18.4 ± 5.2	27.8 ± 4.7/16.5 ± 2.7	
Cisplatin[a] [61]	8.4 ± 2.1		10.2 ± 2.3/35.2 ± 4.6	1.7 ± 0.5/9.3 ± 2.1	9.5 ± 2.3/27.5 ± 3.1	
30[b] [62]			19.7 ± 2.1			11.4 ± 4.9
31[b] [63]			6.2 ± 2.3			
32[b] [63]			12.2 ± 2.4			
33[b] [64]		1.82 ± 0.54	0.34 ± 0.03			
34[b] [64]		1.27 ± 0.53	1.65 ± 0.26			
Doxorubicin [62]			0.093 ± 0.02			0.095 ± 0.01

[a] Resazurin assay in the dark, read after 48 h of incubation/4 h incubation with complex followed by 10 min irradiation with wavelength of 350 nm (2.58 J cm^{-1}) [61].
[b] Resazurin assay read after 48 h of incubation time [62–64].

30%, respectively). This is important and suggests that some cytotoxic action may involve the critical energy production in the mitochondria. All these compounds were found to be inhibitors of human topoisomerase with a comparable affinity to the parent drug. Comparison of *in vivo* bio-distribution of doxorubicin and its conjugates with Re (complex **32**) and ^{99m}Tc showed that the metal coordination does not significantly alter the bio-distribution [62–64].

Gasser *et al.* reported two $(CO)_3Re(I)$*N,N*-bis(quinolinoyl) complexes (**35** and **36**, Fig. 8) and their potential application in photodynamic therapy (PDT). However, PDT can only treat surface cancers or those accessible by endoscopy. The investigated complexes contain two different targeting peptides (NLS and bombesin) for an increased selectivity towards cancer cells, which is connected *via* a photolinker (**36-NLS/bombesin** to **38** in Fig. 8). Upon irradiation, the bio-conjugates are separated from the Re moiety and singlet oxygen is generated which results in IC_{50} values ~ 9 μM, which is lower than the value determined for cisplatin (Table 8). Notably, precursors **28** and **35** are similar except for their length (one CH_2 group) and have comparable IC_{50} values against MRC-5 and HeLa cells (see Tables 7 and 8, respectively). The most cytotoxic complexes against HeLa and PC3 cancer cell lines were found to be the bombesin conjugates **36-bombesin** and **38**, which additionally have the highest IC_{50} values in healthy cells. The investigation of the mode of action of **37** reveals that this compound induces a combination of apoptosis and necrosis [19,65–67].

Furthermore, vitamin B_{12} conjugates with $(CO)_3Re(I)$phenanthroline **40** and **41** were studied in PC3 cells by Santoro *et al.* [68]. Table 8 shows the IC_{50} values for complex **40** and the Re(I) starting material **39**. Due to the instability of **40**, it can be assumed that both IC_{50} values represent the toxicity of **39** with different axial ligands, because MeOH is not strongly bound to Re(I) and may be replaced by water or chlorine when dissolved in the cell medium [68]. Similar observations were noted in a study published by Wilson *et al.* [69]. Further investigations concerning the axial ligand and IC_{50} determination of additional cell lines might be promising for **39** and **41** [68].

Luengo *et al.* published heterometallic Re(I)/Au(I) complexes **42**–**47** (Fig. 9) in 2017. Their cytotoxic properties in A549 cells show double the activity for trimetallic complexes **45**–**47** than for bimetallic compounds (see Table 9). This finding may be attributed to an increased cellular uptake resulting from a beneficial balance of the charge and lipophilicity. These compounds can be tracked and further studied for their location/accumulation in cells by fluorescence microscopy for a better understanding of their biological behavior and targets [70].

A549 cells were also used by Maislus *et al.* for evaluation of the biologic properties of β-carboline compounds **48**–**51** (Fig. 9), which have suitable photochemical properties for investigations using fluorescence microscopy. It was shown that **51** exhibits the lowest IC_{50} value (10 μM) compared to all compounds given in Table 9, which is comparable to cisplatin (8 μM). Therefore, further evaluation of this compound in cisplatin-resistant and healthy cells would be of interest [71].

Ye *et al.* studied the inhibitory effect of histone deactylase (HDAC) inhibitor conjugated to Re(I) carbonyl complex **52** (Fig. 10 and Table 10). The inhibition of HDAC was measured in nuclear extracts from HeLa cells as well as on the isolated enzyme human recombinant HDAC7. The corresponding IC_{50} values are given in Table 10 and are in high nanomolar range, which is comparable to the parent drug SAHA. Studies were performed with this compound to determine its mode of action. According to the results, the mechanism could not be identified, however, the biological response is not identical to the one resulting from SAHA or cisplatin treatment. SAHA is an organic small molecule causing cell death by inhibiting HDAC, and cisplatin is a small inorganic drug causing cell death by binding to DNA and inhibiting its replication. Further studies of **52** in cisplatin/SAHA resistant cell lines were performed to verify the different mode of action [72]. In Table 3, results are summarized with the $(CO)_3Re(I)Cp$ based complexes with cell-penetrating appendages, **12**–**14**, also modified with the SAHA moiety. These IC_{50} values are in the range of 8.3 to 23.3 μM, which is significantly higher than the nanomolar values determined for **52**. However, the nanomolar values are obtained on nuclear extracts, which are not directly comparable to intact cell measurements. Accordingly, values for SAHA are 0.078 μM (cell-based measurement) and 4.45 μM (isolated enzyme) [49,72].

Water-soluble porphyrin conjugates **53** and **54** were studied *in vitro* for their photocytotoxicity. Complex **54** shows no toxicity in the dark; however, it exhibits moderate activity upon irradiation, which is also observed for the corresponding organic deriva-

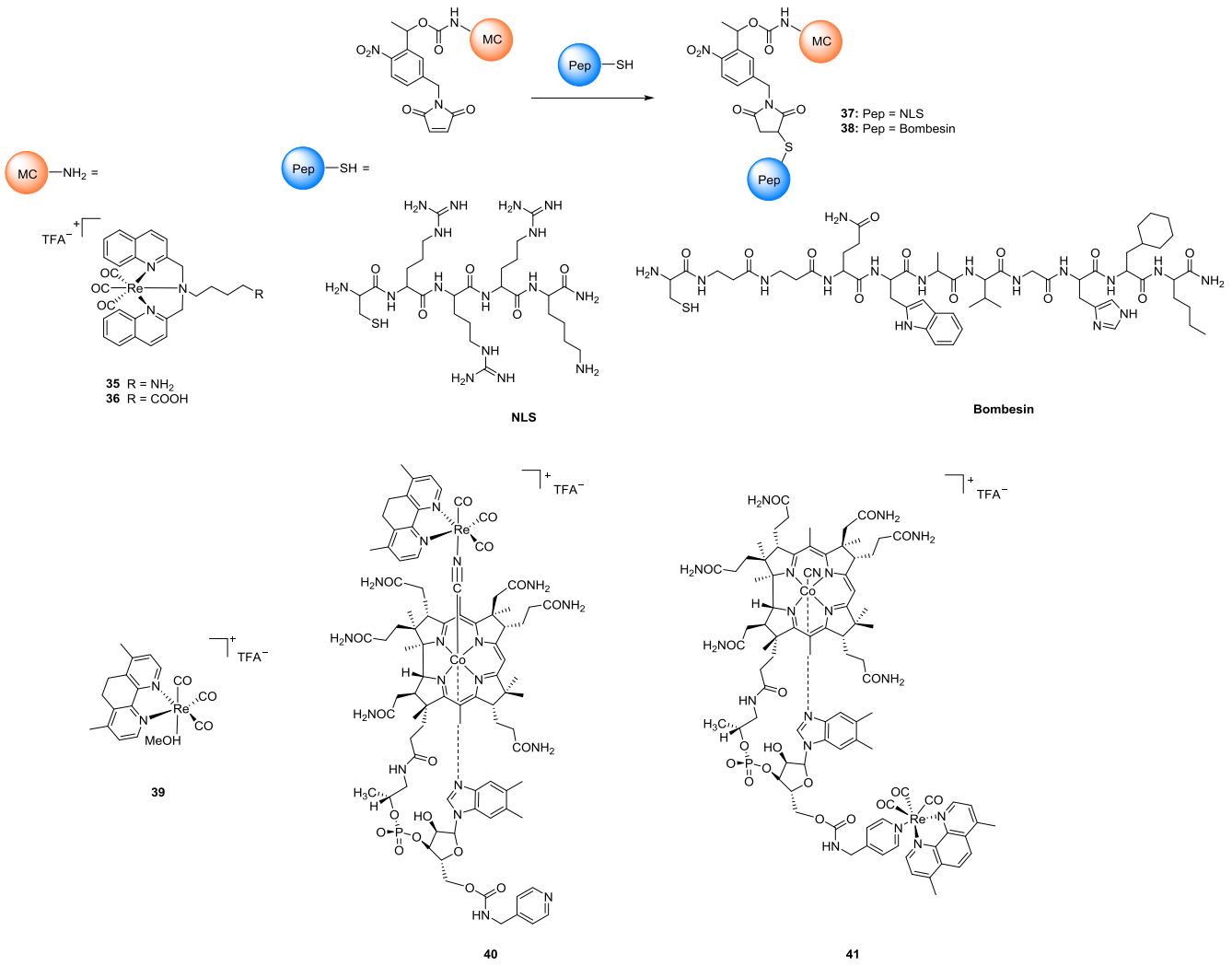

Fig. 8. Structures of $(CO)_3Re(I)$ complexes with NLS and bombesin ligands to form complexes **35** to **41**. Corresponding IC_{50} values are given in Table 8.

Table 8
IC_{50} values in [μM] determined for $(CO)_3Re(I)$ complexes with NLS and bombesin ligands **35** to **41**.

Compound [ref.]	Human non-cancer cell line		Human cancer cell lines	
	3T3	MRC-5	HeLa	PC3
35[a] [66]		>100/40.3 ± 5.4*	187.1 ± 17.9/17.3 ± 2.9*	>100/>100*
36[a] [65]		>100	>100/9.3 ± 2.2*	
36-NLS[a] [66]		17.8 ± 1.8/13.0 ± 2.5*	35.1 ± 1.8/18.3 ± 1.4*	n.d.
37[a] [66]		36.2 ± 0.6/20.5 ± 5.5*	14.5 ± 5.2/9.3 ± 0.8*	n.d.
36-bombesin[a] [66]		44.1 ± 9.9/41.6 ± 15.9*	>100/5.3 ± 1.0*	>100 /13.6 ± 1.7*
38[a] [66]		72.3 ± 3.6/23.3 ± 0.6*	>100/9.7 ± 4.4*	>100/19.2 ± 2.4*
Cisplatin [66]		10.5 ± 2.8/47.8 ± 1.5*	9.2 ± 0.6/26.8 ± 1.7*	
39[b] [68]	45 ± 3			4 ± 2
40[b] [68]	47 ± 7			7 ± 1
41[b] [68]	200			15 ± 2

n.d. = not determined.
* 10 min irradiation with UV-A light (350 nm, 2.58 J cm^{-1}) [66].
[a] Resazurin assay read after 48 h of incubation time [65,66].
[b] Trypan blue assay read after 48 h of incubation time [68].

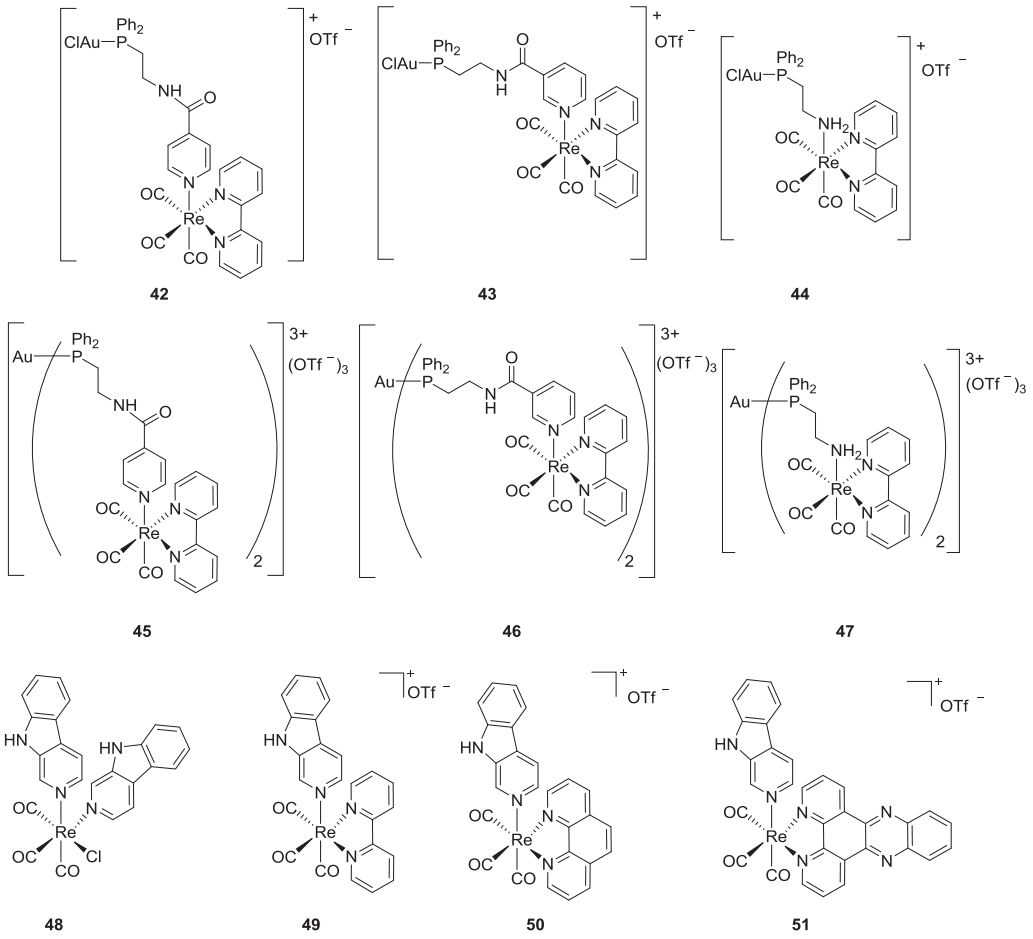

Fig. 9. Structures of $(CO)_3Re(I)$ complexes with (bi)pyridine ligands **42**–**51**. Corresponding IC_{50} values are given in Table 9.

Table 9
IC_{50} values in [μM] determined for $(CO)_3Re(I)$ complexes with (bi)pyridine ligands **42** to **51** using the MTT assay and read after 24 h of incubation.

Compound [ref.]	Human cancer cell line A549
42 [70]	75.25 ± 10.67
43 [70]	67.80 ± 4.11
44 [70]	64.69 ± 3.32
45 [70]	42.44 ± 4.03
46 [70]	36.09 ± 16.99
47 [70]	35.82 ± 1.82
48 [71]	85 ± 1
49 [71]	88 ± 1
50 [71]	65 ± 1
51 [71]	10 ± 1

tive. Thus the observed activity is at least in part due to the ligand of the Re(I) complex. The cytotoxicity of compounds **53** and **54** is significantly higher upon irradiation both in cancerous and healthy cells (see IC_{50} values in Table 10). The influence of further metal complexation of the porphyrin moiety remains to be determined, but would be of interest for understanding the potential modulation of the activity of this system [73].

$(CO)_3Re(I)$ based β-elemene conjugates **55**–**57** were synthesized and tested *in vitro* by Ren *et al.* [74]. These systems showed comparable cytotoxic activity in the cancer cell lines (see Table 10). Furthermore, the radioactive ^{188}Re analogues were synthesized [74] although no further evaluation of their biological activity has been reported so far.

Policar *et al.* evaluated the influence of the length of the side chain on lipophilicity, cellular uptake and antiproliferative effect of the luminescent compounds **58** to **60**. The results reveal that the higher the lipophilicity, the greater the cell uptake and therefore the highest antiproliferative effect with the lowest IC_{50} (of 3.3 μM) is found for the compounds with the C_{12} side chain **60** (see Fig. 11 and Table 11) [75]. A purity of 95% in HPLC analysis using water/acetonitrile indicates that these are relatively stable coordination complexes with regard to ligand exchange compared to other Re coordination complexes [69,75].

Complexes **61** to **63** published by Lo *et al.* are shown to selectively react with azide-functionalized proteins making them useful for imaging of azide-labeled biomolecules. However, these complexes exhibit a cytotoxicity of 3–10 μM in the Chinese hamster cell line CHO and therefore displays higher cytotoxicity than cisplatin (Table 11). Additionally, an increased cellular uptake is possible when the cells are pretreated with an azide-modified glycoprotein-labeling probe [76].

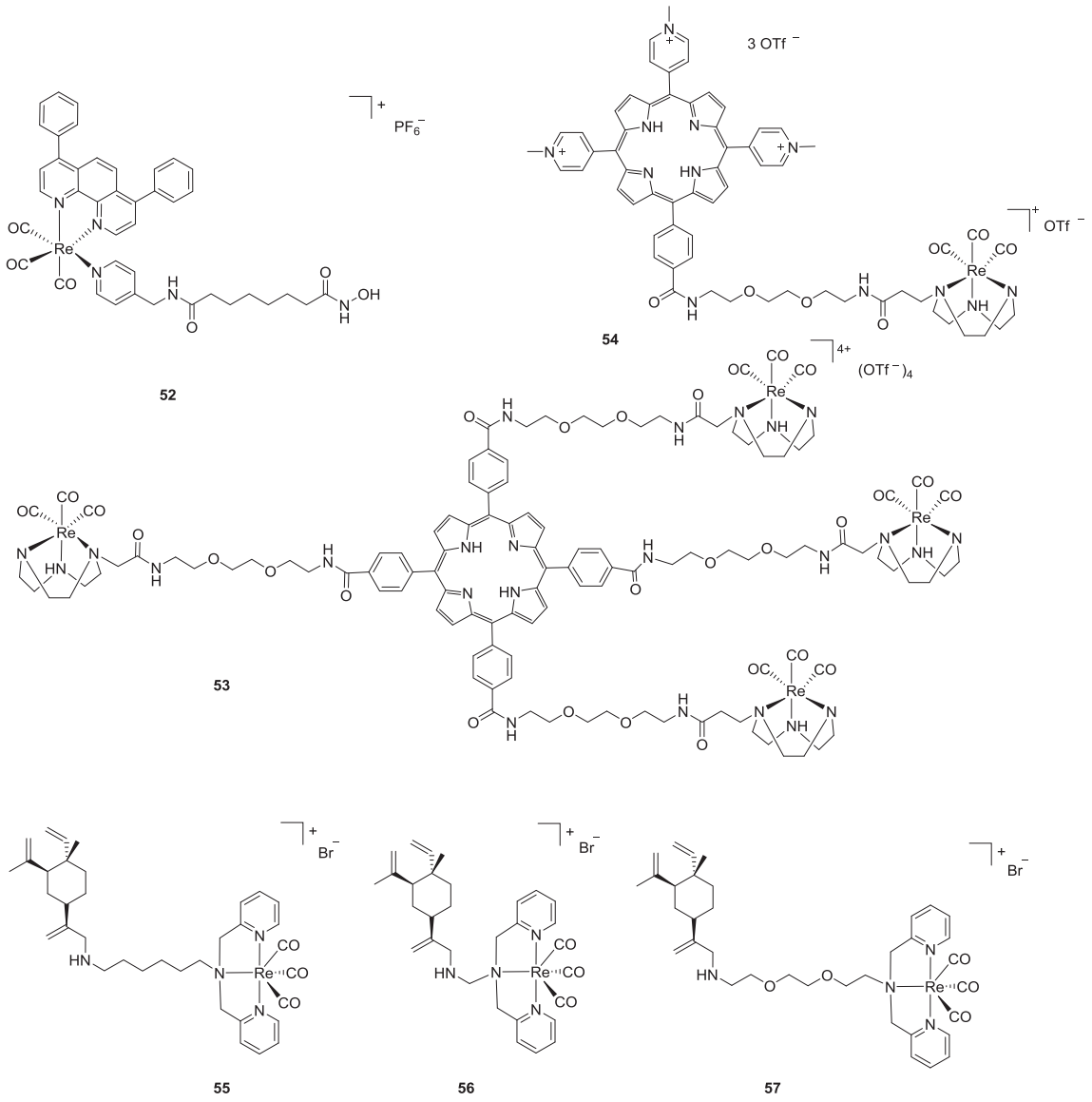

Fig. 10. Structures of $(CO)_3Re(I)$ complexes with long tethers **52**–**57**. Corresponding IC_{50} values are given in Table 10.

Table 10
IC_{50} values in [μM] determined for $(CO)_3Re(I)$ complexes with long tethers **52** to **57**.

Compound [ref.]	Human cancer cell lines				Human non-cancer cell line
	HeLa	HDAC7	H460M2	LLC	HBL-100
52[a] [72]	0.106 ± 0.007	0.682 ± 0.060			
SAHA[a] [72]	0.0786 ± 0.006	0.529 ± 0.048			
53[*] [73]	>100/1.4 ± 1.3[*]		7.4 ± 2.0/0.5 ± 0.2[*]		33.7 ± 14.5/0.5 ± 0.1[*]
54[*] [73]	>100/73 ± 19[*]		>100/12 ± 5[*]		>100/42.8 ± 5.3[*]
55[b] [74]	10.9 ± 1.2			5.0 ± 1.9	
56[b] [74]	11.2 ± 1.5			5.1 ± 1.3	
57[b] [74]	10.5 ± 2.9			4.8 ± 2.3	

[a] MTT assay; no incubation time given [72].
[*] Irradiation with wavelength of 650 nm with a total light dose of 10 J cm^{-1}; MTT assay read 24 h post-irradiation [73].
[b] WST-1 assay read after 24 h of incubation time [74].

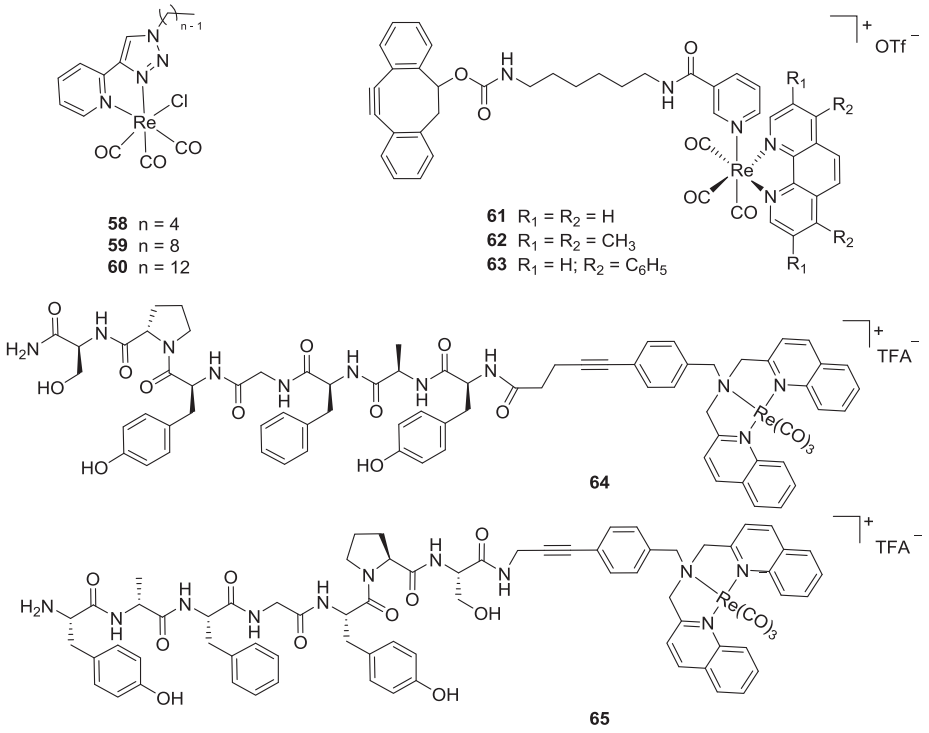

Fig. 11. Structures of $(CO)_3$Re(I) complexes with lipophilic appendages **58**–**65**. Corresponding IC_{50} values are given in Table 11.

Table 11
IC_{50} values in [nM] determined for $(CO)_3$Re(I) complexes with lipophilic appendages **58** to **65**.

Compound [ref.]	Human cancer cell lines MDA-MB-231	Chinese hamster cell line CHO	Human non-cancer cell lines HEK293
58[a] [75]	19000 ± 300		
59[a] [75]	4000 ± 200		
60[a] [75]	3300 ± 100		
61[b] [76]		9550 ± 1550	
62[b] [76]		3500 ± 30	
63[b] [76]		2940 ± 20	
Cisplatin[b] [76]		25490 ± 54	
64[c] [77]			0.076 ± 0.001
65[c] [77]			4.4 ± 0.4

[a] Methylene blue staining read after 5 d of incubation time [75].
[b] MTT assay read after 48 h of incubation time [76].
[c] Forskolin-stimulated cAMP accumulation assay [77].

Metzler-Nolte *et al.* reported complexes **64** and **65** combining the opioid peptide dermorphin with a Re carbonyl core. By evaluating their biological effects, the authors discovered in a blocking group scan that not only the N-terminal domain is a ligand binding site but also the C-terminal domain. The binding affinities of these complexes to the opioid receptor give IC_{50} values in the nano- to subnanomolar range (see Fig. 11 and Table 11). Moreover, a dose-dependent analgesic effect was observed in the preliminary *in vivo* studies which potentially paves the way to complexes that binds as substrates for opioid receptors [77].

3.4. $(CO)_3$Re complexes with pyridine ligands

The following section covers Re(I) carbonyl complexes coordinated to ligands derived from the fundamental pyridine structure, starting with Mao's publications from 2016 to 2018 [78–80]. These phosphorescent compounds can be divided into two structural groups: the phenanthroline (**66a**-**f**) and diphenyl-phenanthroline (**67a**-**j**) coordinated complexes (Fig. 13). Comparison of the IC_{50} values given in Table 12 shows that diphenyl-phenanthroline coordinated complexes are more active than the phenanthroline based ones. These complexes have a higher lipophilicity and therefore show an increased cell uptake leading to increased cytotoxicity. The increased cell uptake was confirmed by confocal microscopy. In addition, the IC_{50} values are lower in cisplatin-sensitive and cisplatin-resistant cell lines than the values determined for cisplatin (21.5 and 65.6 μM, respectively). Complex **67e** displays a low IC_{50} value (0.52 μM) in HeLa cells and shows toxicity against other cancer cell lines, particularly when compared to healthy cells (see Table 12). The selectivity towards cancer cells is further verified by co-incubation and imaging experiments (Fig. 12). The high cytotoxicity of compounds **67a**-**j** is caused by selectively targeting the mitochondria, inducing mitochondrial damage and caspase-dependent apoptosis [78,79]. Moreover, evidence for selective apoptotic cell death was observed for complexes **67d** and **67e**. Therefore, A549 cells were stained with Hoechst, a cell-permeable blue dye, which readily stains the nucleus of living cells (see Fig. 12, 'Hoechst' column). These pre-stained cancerous A549 cells were co-cultured with healthy, non-stained LO2 cells followed by treatment of these co-cultured A549/LO2 cells with the Re complexes. Finally, annexin V/PI double staining was performed on these co-cultured cells. Annexin V is a protein with high affinity to phosphatidylserine, another protein that is only present on the surface of apoptotic cells. By modification of annexin V with a fluorescent tag (a green fluorescent dye shown in Fig. 12), apoptotic

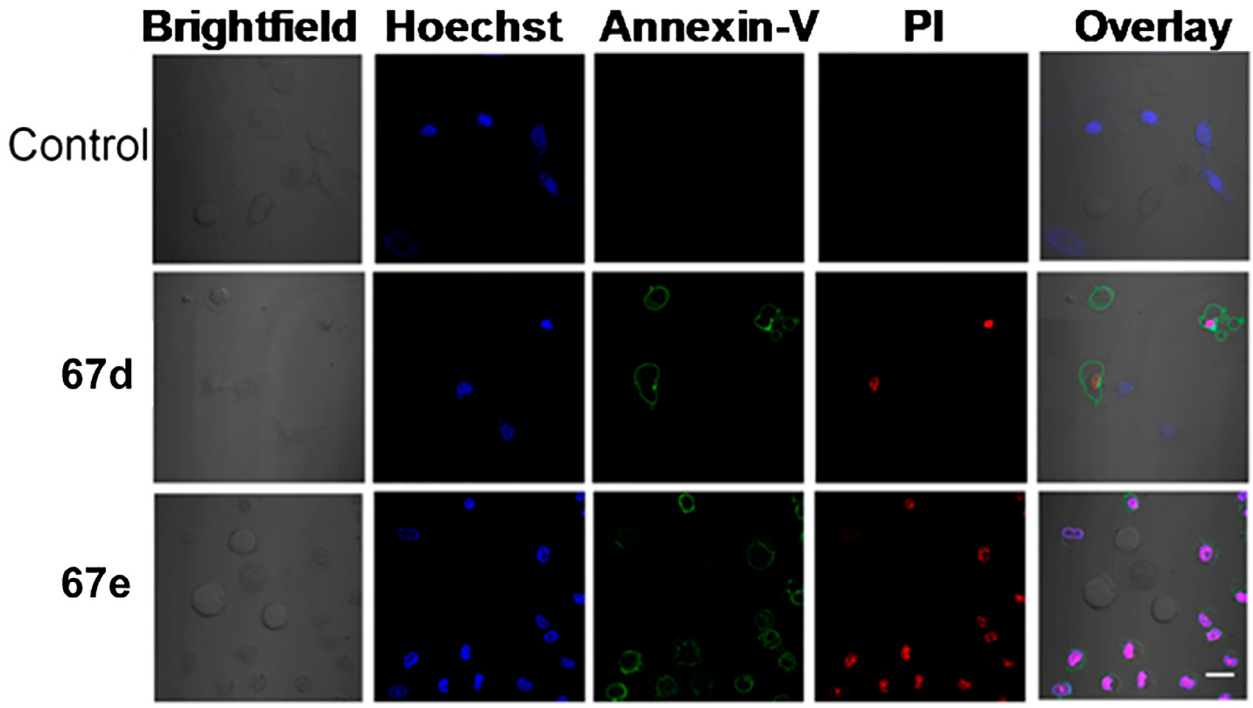

Fig. 12. Confocal microscopic images of A549 cells pre-stained with Hoechst following treatment and co-incubation of pre-stained A549 and LO2 cells with 5 μM of either complex **67d** or **67e**. Final annexin V/PI staining shows the capability of complex **67e** to selectively induce apoptosis in cancer cells. Reprinted with permissions from ACS Appl. Mater. Interfaces, 9 (2017) 13900–13912. Copyright 2018 American Chemical Society.

cells can be displayed using fluorescence microscopy. Propidium iodide (PI) is a cell impermeable, red fluorescent dye that intercalates with DNA. PI only stains apoptotic and/or necrotic cells, because apoptotic and necrotic cells have a decreased nuclear and plasma membrane integrity and thus PI is able to pass through these membranes and intercalate with the DNA of these cells and stain them. This means that PI cannot pass the membranes of living or early apoptotic cells and therefore are not stained. Accordingly, these fluorescent markers are applied in fluorescence microscopic experiments to distinguish between living and dying/dead cells.

In Fig. 12, the confocal microscopic images of A549 (blue nuclei)/LO2 co-cultured cells treated with complexes **67d** (referring to **2b** in the figure) and **67e** (referring to **3b** in the figure) and stained with different fluorescent labels are presented. Considering the different staining properties of the applied labels, **67d** displays lower selectivity of killing healthy and cancerous cells compared to complex **67e**, because not all three labels (Hoechst in blue, annexin V in green and PI in red) are always located in the same cells when looking at the overlay. Nevertheless, this experiment reveals a good selectivity of compound **67e** in killing cancer cells rather than healthy cells [78].

In addition, a recent study of Mao *et al.* shows submicromolar IC_{50} values for the mitochondria-targeting compound **67j**, which is coordinated to dichloroacetate (DCA), a metabolic modulator. This complex is shown to inhibit the pyruvate dehydrogenase kinase (PDK) and therefore selectively target and kill the PDK-overexpressing cells NCI-H1229 and RKO as indicated by the IC_{50} values (see Table 12). This compound also shows high anticancer and anti-angiogenetic activity compared to its DCA-free analogue. Therefore, this study shows that targeting the metabolism of cancer cells is a highly effective and selective method for cancer treatment as well as understanding the mechanism of action [80].

Gasser *et al.* studied the fluorescent complex **68** in detail for its anticancer activity, showing an activity comparable to **66** and **67** (Fig. 13) [81]. However, the selectivity towards cancer cells over healthy cells was not determined. Experiments on a biosensor-chip micro bioreactor reveals that this complex is also targeting the mitochondria and inhibits the mitochondrial respiration [81].

Red light emitting, CF_3 functionalized complexes **69** and **70** (Fig. 13) were biologically evaluated by Mueller *et al.* [82]. The IC_{50} values in Table 12 show a certain selectivity for different cell lines and activity in a range of 4–84 μM. Additionally, the position of CF_3 is shown to strongly influence the cytotoxicity, thus, the IC_{50} values are comparable to the structurally related complexes **67a-j** [78–80].

In a further publication, Gasser *et al.* showed an enhanced cytotoxicity of luminescent Re carbonyl complexes **71** (Fig. 14), when coupled to a lipid-modified peptide, which is known to increase cell permeability. The IC_{50} values of precursor **71** and the peptide-conjugate **72** are given in Table 13, which is, for **72**, in the range of cisplatin (9.1 ± 2.8 μM) [83].

Lo *et al.* reported a series of Re(I) carbonyl complexes **73**–**78** (Fig. 14). Their study shows that the glucose-free compounds (**73**–**75**, for IC_{50} values see Table 13) have lower IC_{50} values compared to the D-glucose conjugated $(CO)_3$Re-complexes (**76**–**78**). Moreover, the cytotoxicity of the compounds can be related to the respective lipophilicities and thus the cellular uptake of these complexes. Additional biological evaluation of glucose-conjugates indicates a strong affinity for the GLUT receptor [84]. A further publication by Lo *et al.* describes trifunctional complexes **79**–**81**. These luminescent fluorine-containing Re(I) carbonyl complexes contain different functional groups for conjugation with biomolecules, like bovine serum albumin (BSA) or glutathione, and therefore are precursors rather than bioactive molecules. However, compound **81** is not stable in aqueous solution and was therefore not submitted for cytotoxicity evaluation [85].

Table 13 shows how different results can be obtained in the same cell line for the same compound, like cisplatin. Therefore, these values just represent a basis for evaluating cytotoxic effects,

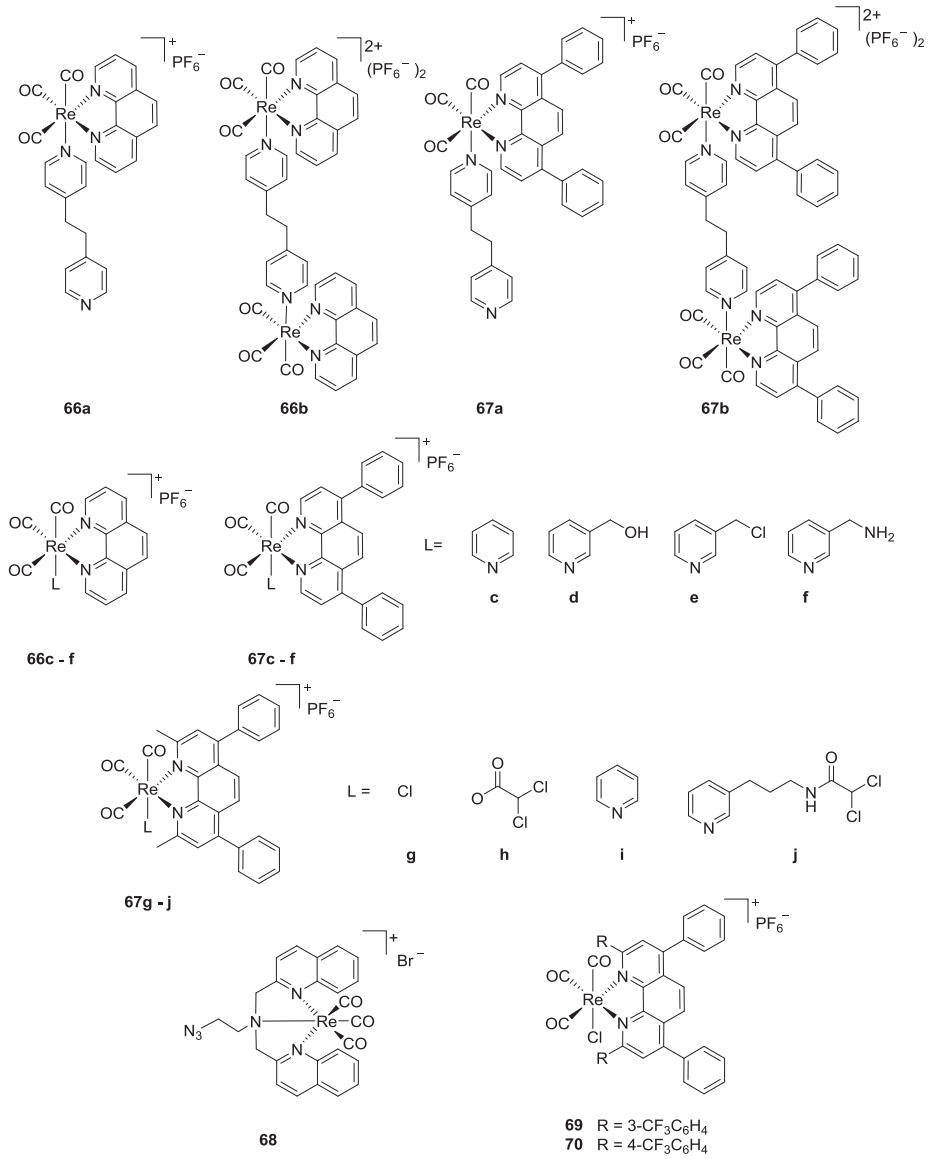

Fig. 13. Structures of compounds **66a**-**70**. Corresponding IC_{50} values are given in Table 12.

however, these compounds need to be further studied *in vivo* to reveal their effects in animals and human.

Lo *et al.* performed biological and photophysical studies on $(CO)_3Re$ polypyridine complexes **82**–**89** and the influence of the modification with a PEG appendage for their potential application as non-toxic multicolor probes in fluorescence lifetime imaging microscopy (FLIM). In particular, the non-toxic compound **85** has an IC_{50} value >1151 μM, and can potentially be applied as a FLIM imaging agent [85]. The PEG conjugation does not significantly affect the luminescence properties and the cytotoxicity of these compounds [86]. A follow-up study by Lo *et al.* evaluated the biological activity of a highly photo-cytotoxic $(CO)_3Re(I)$-fructose conjugate **90** (Fig. 15), which can enter the cell via the fructose transporter and ultimately accumulates in the mitochondria. However, the fructose-free complex **91** also exhibits a higher photocytotoxicity (see Table 14) [87]. In summary, Lo *et al.* investigated several luminescent, structurally related $(CO)_3Re(I)$ polypyridine complexes exhibiting cytotoxicity in the range of 3.5–90 μM in MTT assays using HeLa cells for applications such as imaging, and as antibacterial and anticancer agents [15,88].

Wang *et al.* reported photocytotoxic compounds **92** and **93** (Fig. 15). The photophysical and cytotoxic properties of these compounds were examined resulting in micromolar IC_{50} values (Table 14). The observed IC_{50} value for complex **93** decreases upon irradiation with 365 nm LED light [89].

Rajagopal *et al.* showed that compounds **94**–**96** (Fig. 16) are able to bind to the groove of calf thymus DNA. The determined binding constants are one order of magnitude higher for compounds **95** and **96** than for **94**, indicating the importance of the lipophilic alkyl chains on the bipyridine ligand. This trend can also be observed for the IC_{50} values (Table 15). Additionally, the comparison of the IC_{50} values in cancerous and healthy cells indicates a good selectivity towards the cancer cells [90]. Co-incubation of healthy cells with cancerous cells and *in vivo* studies could further confirm this selectivity.

3.5. $(CO)_3Re$ complexes with mixed donor ligands

Mandal *et al.* screened a library of Re carbonyl complexes with mixed donor ligands against breast cancer cells for their cytotoxic properties. In Table 16, the most potent compounds and the corresponding IC_{50} values are listed. These compounds, in particular compounds **97** to **99** (Fig. 17), have remarkably low IC_{50} values in the submicromolar range in MCF-7A, MCF-10A and MDA-MB-

Table 12
IC_{50} values [μM] of $(CO)_3Re(I)$ based (poly)pyridine compounds tested in different cell lines.

Compound [ref.]	Human non-cancer cell lines	Human cancer cell lines								
	LO2	HeLa	A549	A549cisR	HepG2	MCF-7	U2OS	THP-1	RKO	NCI-H1229
66a[a] [79]	>100	44.7 ± 4.0	>100	>100	39.8 ± 3.7					
66b[a] [79]	12.4 ± 1.2	2.0 ± 0.2	4.6 ± 0.3	1.6 ± 0.1	3.1 ± 0.3					
66c[a] [78]	>100	>100	>100	>100						
66d[a] [78]	>100	>100	>100	>100						
66e[a] [78]	>100	64.6 ± 2.2	75.8 ± 2.3	37.3 ± 1.1						
66f[a] [78]	47.9 ± 1.5	52.5 ± 3.0	39.8 ± 0.7	36.5 ± 1.8						
67a[a] [79]	56.2 ± 4.7	9.1 ± 0.8	11.7 ± 4.1	11.5 ± 1.0	12.0 ± 1.1					
67b[a] [79]	10.2 ± 1.0	1.7 ± 0.1	2.0 ± 0.2	1.9 ± 0.1	2.1 ± 0.2					
67c[a] [78]	3.1 ± 0.5	0.95 ± 0.11	3.9 ± 0.7	1.2 ± 0.5						
67d[a] [78]	7.6 ± 0.9	1.7 ± 0.4	5.5 ± 0.6	2.7 ± 0.5						
67e[a] [78]	18.7 ± 1.1	0.52 ± 0.07	3.4 ± 0.6	0.75 ± 0.12						
67f[a] [78]	6.4 ± 0.7	5.9 ± 0.9	22.4 ± 1.2	8.5 ± 1.1						
67g[b] [80]	30.0 ± 1.1		18.1 ± 2.3	17.8 ± 2.2		32.1 ± 2.1			14.2 ± 1.7	12.4 ± 1.4
67h[b] [80]	21.0 ± 3.2		15.0 ± 1.4	15.9 ± 2.1		14.4 ± 1.2			9.7 ± 1.1	3.7 ± 0.2
67i[b] [80]	20.0 ± 3.5		11.0 ± 1.2	13.0 ± 3.4		7.6 ± 1.1			9.1 ± 0.8	2.9 ± 0.1
67j[b] [80]	22.0 ± 2.1		4.1 ± 0.9	4.3 ± 0.7		4.0 ± 1.2			2.2 ± 0.2	0.8 ± 0.1
Cisplatin[a] [78]	29.9 ± 2.1	8.9 ± 1.0	21.5 ± 2.5	65.6 ± 1.6						
$Re(CO)_5Br$[c] [81]					>100	76.9 ± 3.8	>100			
68[c] [81]					29.8 ± 1.0	8.6 ± 0.2	16.9 ± 1.5			
Cisplatin[c] [81]					3.9 ± 1.0	2.7 ± 0.1	8.2 ± 1.5			
69[d] [82]		4.56 ± 3	3.62 ± 0.8					33 ± 16		
70[d] [82]		83 ± 80	4.76 ± 2.5					14 ± 4.1		

[a] MTT assay read after 48 h of incubation time [78,79].
[b] MTT assay read after 24 h of incubation in the dark [80].
[c] Resazurin assay read after 48 h of incubation time [81].
[d] MTS assay read after 72 h of incubation time [82].

231 cell lines. Such high cytotoxic activity of the $(CO)_3Re(I)$-phenyl-phenanthroline compounds was also observed for the $(CO)_3Re(I)$ complexes previously discussed, like **67j**. As stated before, the authors attribute the effect to the lipophilicity of these complexes, which is important for cell membrane penetration and their ability to intercalate with DNA [91]. However, this is not the case for all of these compounds, e.g. the diphenyl-phenanthroline coordinated complex **97** is the most active one in MCF-7 cells, however, the diphenyl-phenanthroline based complex **111** is the least active (see Table 16). For MCF-10A cells, the phenanthroline-based complex **98** has the lowest IC_{50} value and the diphenyl-phenanthroline coordinated **104** displays the highest IC_{50} value. Overall, the exchange of the axial ligand seems to have less influence on the activity than the changes on the phenanthroline moiety. This can be seen by looking at complexes **102** and **103** (additional benzyl moiety on the axial ligand), which shows less significant changes in IC_{50} values in all cell lines, as compared to **103** (diphenyl-phenanthroline) and **109** (phenanthroline).

Yan *et al.* studied Re phosphine compounds **112–118**, $[NBu_4][ReO_4]$ and $[NEt_4]_2[ReBr_3(CO)_3]$ (Fig. 18) for their cytotoxic effects in cultured cell line suspensions (Table 17) and in solid tumor cultures (Table 18). However, the authors determined ED_{50} values (mean effective dose of the compound) in μg per ml and not the molar concentration. Recalculation of these values to EC_{50} values (molar concentration) using the molecular weight of the compounds results in values that are more comparable. Since the EC_{50} values are easier to compare, the presented discussion is based on the recalculated EC_{50} values. However, both values are included in Tables 17 and 18 in the order ED_{50}/EC_{50} value to show the difference in the values and the importance of using the molar concentration and not the dose of a test compound.

The recalculated EC_{50} values range from 0.93 to 18.00 μM. Compound **116** displays the lowest EC_{50} values in almost all tested cell lines except for A549, 1-A9 and T-molt$_4$, where compound **115** shows the lowest values (see Tables 17 and 18). In cultured cell line suspensions, the lowest observed EC_{50} value is 0.93 μM for

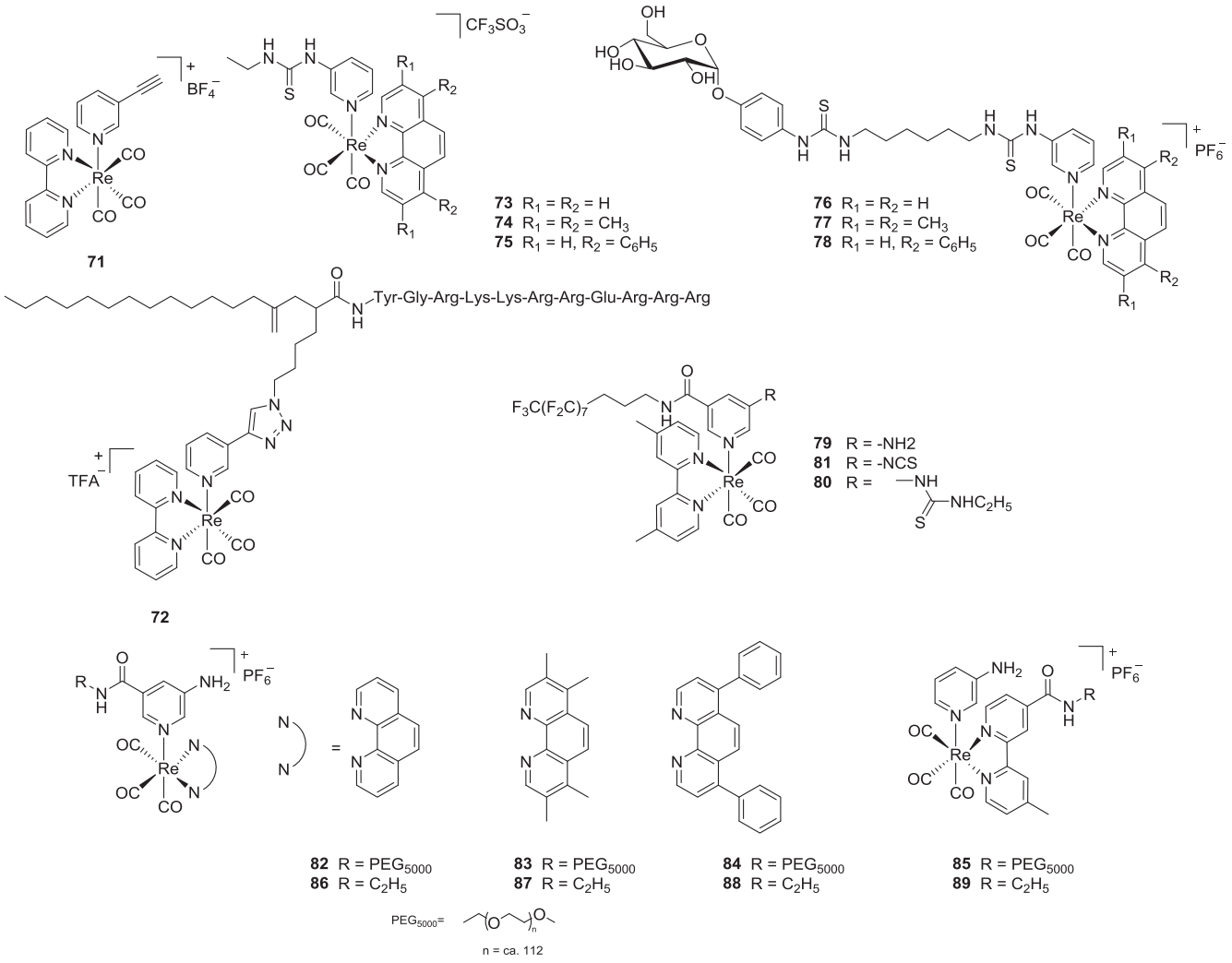

Fig. 14. Structures of $(CO)_3Re(I)$ based (poly)pyridine compounds **71**–**89**. Corresponding IC_{50} values are given in Table 13.

compound **116** in HeLa-S3 cells. In healthy cells, this compound has an EC_{50} value of 5.99 μM (see Table 17). In solid tumor cultures, the lowest EC_{50} value is observed for complex **116** (0.99 μM in MCF-7, see Table 18).

In summary, all compounds given in Tables 17 and 18 have low ED/EC_{50} values in the same range, despite the fact that the structures have few common characteristics other than the $Re(CO)^{3+}$ core [92,93].

A detailed study on the cytotoxicity, reactivity and mechanism of action of $(CO)_3Re(I)BiPy^+$ compounds **119**–**121** (see Fig. 20) was reported by Wilson *et al.* [69,85]. When chloride is coordinated instead of a water molecule to these Re complexes, the compounds display a decreased water-solubility. However, the axial water/chloride ligand can easily be exchanged. The evaluation of the cytotoxicity of water-coordinated complexes **119**–**121** in HeLa cells reveals low IC_{50} values (see Table 19). These compounds were then further tested in different wild type and cisplatin resistant cells resulting in comparable or even lower IC_{50} values with complex **121** being the most active complex (data not shown). Moreover, these complexes are less toxic against the normal cell line MRC-5 than cisplatin (0.43 μM). Complex **121** was analyzed for its cytotoxicity, nucleobase and amino acid binding, in the annexin V/PI assay, ROS assay, JC-1 assay, western blot for protein expression, cellular uptake assays and it was screened in a cell viability test in the presence of different inhibitors as well as a NCI-60 tumor cell panel-screen. Together, these studies indicate that the complex is able to overcome cisplatin resistance and induces caspase-independent cell death [69]. Fluorescence microscopy making use of the luminescence of complex **121** in the yellow light region was performed to evaluate the intracellular localization of the Re compound (Fig. 19). The images in Fig. 19 show distribution of complex **121** all over the cytosol and formation of cytoplasmic vacuoles. More information about the nature of these vacuoles was obtained using transfection methods to express organelle-specific proteins fused with a fluorescent protein (RFP-Rab5 and RFP-2xFYVE) and a lysosomal tracker (LysoTrack) (see Fig. 19). The results indicate either that the complex labels a wide range of different endosomes and lysosomes or that the vacuoles have lysosomal characteristics and are part of an endosome-lysosome fusion process [69]. More information on the investigation of the mechanism of action of these compounds require further experimental methods.

Re(I) pyridocarbazole complexes **122**–**125** (see Fig. 20) are shown to have suitable properties for photodynamic therapy (PDT) induced by a red light. Moreover, these compounds exhibit nanomolar affinity (see Table 19) for protein kinase Pim1, which potentially enables selective targeting of Pim1 expressed in cancer cells [94]. Cyz *et al.* biologically evaluated compounds **126**–**129**

Table 13
IC_{50} values [μM] of $(CO)_3Re(I)$ based (poly)pyridine compounds tested in HeLa cells.

Compound [ref.]	Human cancer cell lines HeLa
71[a] [83]	29.9 ± 6.1
72[a] [83]	13.0 ± 2.0
Cisplatin[a] [83]	9.1 ± 2.8
73[b] [84]	22.8 ± 5.2
74[b] [84]	7.7 ± 0.6
75[b] [84]	2.8 ± 0.4
76[b] [84]	>150
77[b] [84]	90.0 ± 7.6
78[b] [84]	68.9 ± 2.3
Cisplatin[b] [84]	27.6 ± 1.8
79[b] [85]	8.70
80[b] [85]	17.02
82[b] [86]	26.3 ± 1.6
83[b] [86]	11.9 ± 1.6
84[b] [86]	6.6 ± 0.4
85[b] [86]	>1151.7
86[b] [86]	15.0 ± 4.8
87[b] [86]	5.0 ± 0.4
88[b] [86]	3.6 ± 0.4
89[b] [86]	159.1 ± 8.0

[a] Resazurin assay read after 48 h of incubation time [83].
[b] MTT assay read after 48 h of incubation time [84–86].

(Fig. 20, Table 19). Comparing the IC_{50} values, compounds **126** and **127** are slightly more active than **128** and **129**. Additionally, these compounds were shown to initiate apoptosis [95].

The EGFR inhibiting compound **130** was evaluated in A431 cells by Permettis *et al.* showing a slightly lower IC_{50} value (2.0 μM, see Table 19) than the parent compound (4.8 μM) [96].

Mieczkowski *et al.* studied the cytotoxicity of complexes **131**–**136** against ovarian cancer cell lines and healthy cells [97]. The results against wild type and cisplatin resistant cell lines indicate that complex **133** has low IC_{50} values in both cancer cell lines and a high value in healthy cells (see Table 20). Interestingly, the difference between compounds **131**–**133** is the substitution of a coordinated halogen resulting in a dramatically different cytotoxicity [97].

An additional publication by Wilson *et al.* studied the photocytoxicity of structurally comparable compounds **137** and **138** (Fig. 21) to their previous publication (compounds **119**–**121** in Fig. 20) which are highly cytotoxic (1.2 μM) when exposing the cells to visible light. Importantly, complexes **137** and **138** are not toxic in the dark, but after irradiation at 365 nm, IC_{50} values of 2.2 μM in wild type cells and 3.2 μM in cisplatin resistant cells are observed for complex **138** (see Table 20). Interestingly, the complexes **137** and **138** are shown to release CO upon irradiation with UV light and are therefore useful for photodynamic therapy (PDT) or photoactivated chemotherapy (PACT) [98].

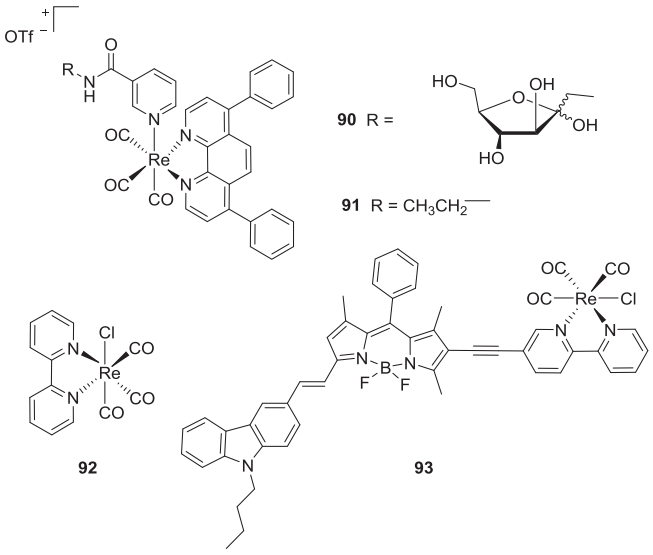

Fig. 15. Structures of compounds **90**–**93**. Corresponding IC_{50} values are given in Table 14.

Wong *et al.* reported a study on the cytotoxicity of **139** (Fig. 21) and its interaction with calf thymus DNA. The IC_{50} values obtained by MTT assays in HepG2, HeLa and KB-3–1 cells are 30–50 μM with less toxicity towards normal cells (Table 20). The observed changes in pH in solid tumor cell lines was shown to have no influence on the effects of these compounds. For multi-drug resistant KB-V-1 cells, the IC_{50} value is about 4 times higher, but considering the cell lines resistance to other drugs, the observed effects are still promising [99]. Moreover, in Table 20 the varying IC_{50} values for cisplatin evaluated in the same cell line is observed. For A2780cisR this value ranges from 5 to 30 μM.

Natile *et al.* evaluated bimetallic Re(I) carbonyl complexes **140** and **141** conjugated to a translocator protein (TSPO) (Fig. 21 and Table 20). Structurally, **141** has two $Re(CO)_3$ moieties, whereas **140** has one $Re(CO)_3$ and one PtCl moiety. Interestingly, for these complexes the biological evaluation indicates a slightly higher cytotoxicity for the ligand (9.0 μM), than for the Re complexes. However, the heterobimetallic complex **140** exhibits only a slightly higher IC_{50} value than the Re-free analogue, and both maintain antiproliferative activity in cisplatin resistant cells [101]. Of these compounds, the ligand is the most active [100]. Overall, of the compounds in Table 20, the most active compounds are the irradiated photoactivated complexes **133**, **137** and **138** with IC_{50} values of 2–4.6 μM in A2780 and A2780cisR cell lines.

Manimaran *et al.* reported three studies on Re(I) metallacycles **142**–**151** (Fig. 22) [102–104]. These complexes were tested in different cancer cell lines as well as in normal blood cells for their IC_{50} values (see Table 21). A great selectivity towards cancer cell lines was observed since the complexes are inactive (IC_{50} values > 100 μM) in normal blood cells. Overall, the tested compounds have a moderate activity comparable to cisplatin (26 μM in A549 cells), which was included in the assay studies. The lowest IC_{50} value is observed for complex **151** in MCF-7 cells. Morphological observations on cells treated with complexes **142** and **146** indicate that these compounds induce apoptosis [102–104].

Desmaële *et al.* synthesized four Re carbonyl complexes with diseleno-ether ligands. Due to water insolubility and limited solubility in DMSO only complex **152** was tested *in vitro*. The complex shows cytotoxicity in MCF-7 cells (see Table 21) and moderate to no activity in the other tested cell lines [105]. Therefore, this complex was further evaluated in breast-cancer-bearing mice showing

Table 14
IC_{50} values [μM] determined in MTT assays for $(CO)_3Re(I)$ based (poly)pyridine complexes in different human and murine cell lines.

Compound [ref.]	Murine cell lines		Human non-cancer cell lines	Human cancer cell lines			
	LLC	NIH/3T3	HEK293T	MDA-MB-231	HepG2	A549	MCF-7
90 [87]		2.1 ± 0.3	6.7 ± 0.7	4.9 ± 0.4	33.9 ± 0.9	26.8 ± 2.1	9.6 ± 0.6/2.0 ± 0.04[b]
91 [87]		1.8 ± 0.3	2.1 ± 0.2	2.3 ± 0.2	5.7 ± 0.4	2.6 ± 0.3	3.9 ± 0.3/0.3 ± 0.01[b]
92 [89]	18.72/17.65[a]						
93 [89]	20.63/12.93[a]						

[a] Irradiated with LED 365 nm [89].
[b] Irradiated with light (wavelength > 365 nm) for 4 h [87].

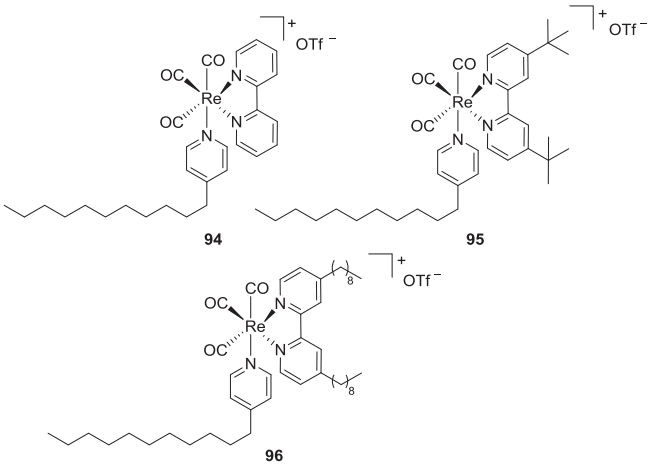

Fig. 16. Structures of $(CO)_3Re(I)$ complexes with a bipyridine ligand and a hydrophobic appendage **94–96**. Corresponding IC_{50} values are given in Table 15.

Table 15
IC_{50} values [μM] determined for $(CO)_3Re(I)$ complexes with a bipyridine ligand and a hydrophobic appendage **94–96** in different human cell lines.[a]

Compound [ref.]	Human cancer cell lines		Human non-cancer cell line
	Raji	Jurkat	PBMC
94 [90]	31 ± 05	37 ± 2.2	117 ± 3
95 [90]	23 ± 1	28 ± 1.1	135 ± 5
96 [90]	15 ± 1.7	18 ± 0.2	93 ± 2.5

[a] MTT assay read after 72 h of incubation time [90].

Table 16
IC_{50} values in μM of different $(CO)_3Re(I)$ based complexes having mixed donor ligands determined in different breast cancer cell lines.[a]

Compound [ref.]	Human cancer cell lines		
	MCF-7A	MCF-10A	MDA-MB-231
97 [91]	0.337 ± 0.303	1.78 ± 0.173	0.248 ± 0.336
98 [91]	0.425 ± 0.226	0.023 ± 0.02	6.39 ± 0.362
99 [91]	0.849 ± 0.255	2.51 ± 0.187	0.716 ± 0.242
100 [91]	0.958 ± 0.261	1.47 ± 0.177	1.06 ± 0.375
101 [91]	1.25 ± 0.607	12.1 ± 0.554	6.17 ± 0.767
102 [91]	1.27 ± 0.228	3.46 ± 0.186	1.27 ± 0.361
103 [91]	1.31 ± 0.297	2.79 ± 0.250	1.08 ± 0.198
104 [91]	1.33 ± 0.29	6.38 ± 0.316	0.591 ± 0.145
105 [91]	1.51 ± 0.243	3.02 ± 0.133	1.23 ± 0.197
106 [91]	1.54 ± 0.179	1.59 ± 0.351	2.78 ± 0.373
107 [91]	1.55 ± 0.285	5.7 ± 0.337	3.09 ± 0.284
108 [91]	1.56 ± 0.420	2.65 ± 0.253	1.7 ± 0.314
109 [91]	1.58 ± 0.263	1.66 ± 0.229	1.86 ± 0.318
110 [91]	1.65 ± 0.171	6.31 ± 0.240	1.03 ± 0.181
111 [91]	1.7 ± 0.226	3.63 ± 0.403	1.53 ± 0.143

[a] Alamar blue assay read after 72 h of incubation time [91].

that a cure is possible with a treatment dose of 10 mg/kg/d for 4 weeks [106]. More details on the *in vivo* evaluation is given in section **6.1**.

Yan *et al.* evaluated the cytotoxicity of complexes **153–158** (Fig. 23) in cancerous and healthy cell lines. The most cytotoxic compound is **157** with an IC_{50} value of 1.0 μM in MOLT-4 cells but also 9 μM was found in normal fibroblasts. Combined, **156** has the better cytotoxic overall profile with an IC_{50} value of 7 μM in MOLT-4 cells and no toxicity in healthy cells (see Table 22). Increasing incubation time from the 24 h, which was used in the assay, may still reveal some cytotoxicity. Moreover, the complex was shown to dimerize in DMSO solution by the loss of bromide and coordination of the OH group to the second Re atom, which might also happen *in vitro*. Additionally, the phenolic OH groups interacts *via* proton transfer with guanosine and induces apoptosis in cancer cells [107].

A Re dimer **159** was reported by Policar *et al.* and tested against breast cancer cell lines showing good antiproliferative properties (see Table 22). A comparison with complexes **153–158** cannot be made due to varying incubation times used in the study; however, compound **159** has a lower IC_{50} value in MCF-7 cells than the other compounds. Tamoxifen, which is used as reference drug for MCF-7 cells, was shown to have higher IC_{50} values (11.2 μM in MCF-7 and 13.4 μM in MDA-MB-231 cells) [108].

Further bromide $(CO)_3Re(I)$ hydrazine complexes **160–162** (Fig. 24), which form dimers in solution, were reported by Gambino *et al.* [109]. These compounds were tested *in vitro* against *Trypanosoma cruzi* and healthy cells (see IC_{50} values in Table 23). The comparison of the IC_{50} values shows a good selectivity for *T. cruzi* over healthy cells and an increased cytotoxicity compared to the reference drug Nifurtimox (20.1 μM). Compounds **160** and **162** have comparable cytotoxicity of about 2 μM, compound **161** has a lower value of 1.3 μM, however, it exhibits an increased toxicity

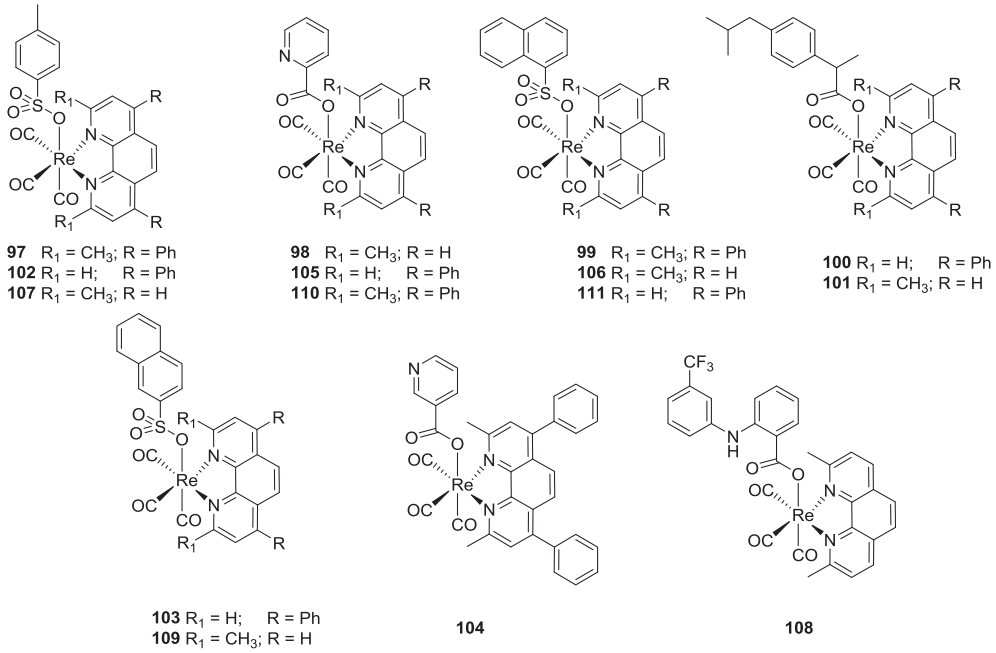

Fig. 17. Structures of different $(CO)_3Re(I)$ based complexes **97–111** having mixed donor ligands. Corresponding IC_{50} values are given in Table 16.

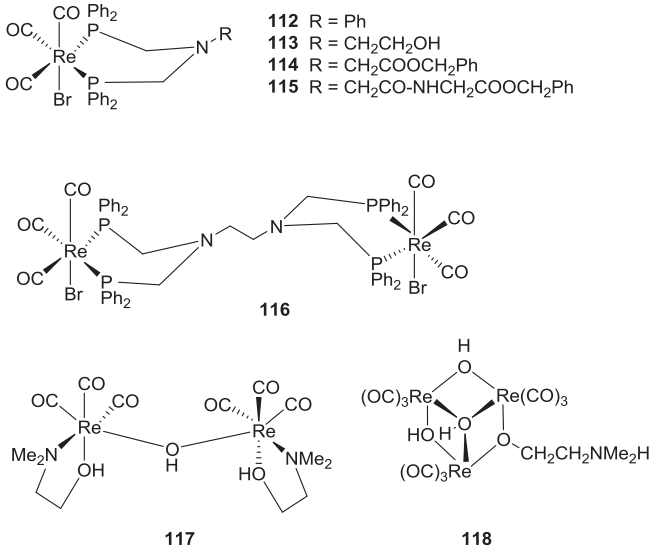

Fig. 18. Structures of $(CO)_3Re(I)$ compounds **112–118**. Corresponding ED/EC_{50} values are given in Table 17 (cultured cell line suspensions) and **18** (solid tumor cultures).

against healthy cells. Therefore, the biological profile of **160** and **162** is better. Additionally, the authors were able to show that these compounds inhibit the respiration system of mitochondria [109]. Targeting the mitochondria was also shown to increase cytotoxicity by Mao *et al.*, who introduced two groups of $(CO)_3Re(I)$ containing phenanthroline (**66a-f**) and diphenyl-phenanthroline compounds (**67a-j**) discussed in Table 12 [78–80].

Massi *et al.* published a very detailed biological study on $(CO)_3$-Re(I) carbene complexes **163–165**, which are modified with indomethacin, an anti-inflammatory drug, and tested their antiproliferative activity against different pancreatic cancer cell lines and healthy HEK cells (see Table 23). In the same setup, ruthenium complexes with the same indomethacin-based ligand system were also examined and showed no activity. The determined IC_{50} values for the $(CO)_3Re(I)$ carbene based complexes are in the low micromolar range (similar to cisplatin) for all three cancer cell lines and are slightly higher for healthy cells. Further biological studies were performed to investigate the origin of the varying biological effects observed for these compounds. A series of these complexes were subjected to an anticancer screen, the results of which showed that the most influential structural variation involves the lability of the ancillary bromide ligand. Furthermore, it was shown that complexes **163–165** inhibit phosphorylation of Aurora-A kinase and thus induces partial cell cycle arrest at the G2/M phase (in about 26% of the cells) [110]. Wilson *et al.* similarly observed cell cycle arrest of the G2/M phase induced by compound **121** reaching about 50% of the cells [69].

4. Re coordination compounds

In coordination compounds, Re is mostly reported in oxidation states III, IV and V [111–113] as well as Re(VII) in trioxo complexes [114]. It was initially assumed that Re(IV) and (V) complexes were disproportionating in aqueous solution, until Davison *et al.* reported highly stable Re(V) and Tc(V) oxobis(dithiolato) complexes [115]. The increased complex stability opened up the applications of Re coordination complexes in medicinal chemistry and underscore the importance of the ligand system as a crucial drug component for medical application as evidenced by the compounds that are in clinical trials (see below).

4.1. Coordination compounds of Re(III), Re(IV) and Re(V)

The following paragraph describes the cytotoxic effects of Re coordination complexes, where Re exists in oxidation states III, IV or V. A detailed biological study on this class of compounds was reported by Lippard *et al.* [116]. The structures of the studied Re (V)oxo phenanthroline complexes **166** and **167** are given in Fig. 26. The cytotoxic properties of complexes **166** and **167** were compared to cisplatin, which was evaluated in the same assay, showing that **166** and **167** exhibit lower IC_{50} values in most of the cell lines (see Table 24). In A2780 cisplatin resistant cells, both complexes have low IC_{50} values compared to cisplatin

Table 17
ED/EC_{50} values of different $(CO)_3Re(I)$ based complexes having mixed donor ligands determined in different cell line suspensions ([μg/ml]/[μM]; EC_{50} values are recalculated by considering the molecular weight of the respective compound).[a]

Compound [ref.]	Human cancer cell lines						Murine cell lines		Human non-cancer cell lines
	HL-60	T $molt_3$	T $molt_4$	HuT-78	THP-1	HeLa-S^3	L1210	P388	RMPI 1788
112 [92]	3.42/4.07	3.27/3.89	4.52/5.38	2.60/3.09	2.10/2.50	2.69/3.20	2.36/2.81	2.72/3.24	6.78/8.07
113 [92]	3.33/4.12	4.70/5.82	4.36/5.40	2.96/3.67	3.28/4.06	2.32/2.87	1.72/2.13	2.91/3.60	7.02/8.70
114 [92]	2.14/2.35	5.17/5.67	4.32/4.74	2.55/2.80	3.30/3.62	2.68/2.94	1.92/2.11	2.30/2.52	7.60/8.34
115 [92]	3.37/3.48	3.01/3.11	3.64/3.76	3.53/3.64	5.21/5.38	2.85/2.94	2.80/2.89	3.61/3.73	6.86/7.08
116 [92]	2.05/1.32	3.06/1.97	6.16/3.97	2.70/1.74	3.87/2.49	1.45/0.93	2.90/1.87	2.02/1.30	9.31/5.99
117 [93]	3.01/4.09	3.17/4.31	5.44/7.39	3.48/4.73	4.93/6.70	3.02/4.10	3.09/4.20	2.49/3.38	8.50/11.55
118 [93]	5.97/6.28	3.74/3.93	5.64/5.93	3.58/3.76	2.86/3.01	2.75/2.89	3.15/3.31	2.48/2.61	6.70/7.05
$[NBu_4][ReO_4]$ [93]	3.56/7.23	3.59/7.29	4.96/10.07	2.54/5.16	2.10/4.26	3.12/6.33	3.65/7.41	2.69/5.46	7.18/14.57
$[NEt_4]_2ReBr_3(CO)_3]$ [93]	3.83/4.97	3.96/5.14	4.60/5.97	3.17/4.11	2.85/3.70	2.42/3.14	2.65/3.44	4.55/5.91	8.00/10.38

[a] Measurements were carried out using the Trypan blue exclusion method.

Table 18
ED/EC_{50} values of different $(CO)_3Re(I)$ based complexes having mixed donor ligands determined in different solid tumor cultures in [μg/ml]/μM using crystal violet/MeOH (EC_{50} values are recalculated by considering the molecular weight of the respective compound).

Compound [ref.]	Human cancer cell line									
	KB	A549	1-A9	MCF-7	UM 86	HCT-8	HSO	SK2	PL	HepG2
112 [92]	6.88/8.19	8.02/9.55	7.71/9.18	3.52/4.19	8.99/10.71	5.45/6.49	4.59/5.47	6.11/7.28	3.90/4.64	4.76/5.67
113 [92]	4.88/6.04	4.02/4.98	3.39/4.20	2.01/2.49	6.49/8.04	10.69/13.24	5.32/6.59	4.18/5.18	7.30/9.04	5.07/6.28
114 [92]	4.34/4.76	8.51/9.33	8.92/9.78	2.37/2.60	9.05/9.93	3.95/4.33	5.86/6.43	3.45/3.78	5.06/5.55	4.02/4.41
115 [92]	6.45/6.66	3.24/3.34	3.72/3.84	2.42/2.50	6.67/6.88	4.55/4.70	7.72/7.97	13.3/13.73	8.61/8.89	4.49/4.63
116 [92]	5.49/3.53	6.82/4.39	7.39/4.76	1.53/0.99	7.78/5.01	5.65/3.64	5.00/3.22	2.87/1.85	4.95/3.19	3.74/2.41
117 [93]	3.71/5.04	5.53/7.52	6.07/8.25	3.60/4.89	4.89/6.65	3.51/4.77	7.11/9.66	2.85/3.87		
118 [93]	6.74/7.09	5.76/6.06	2.48/2.61	3.11/3.27	7.28/7.66	6.33/6.66	13.12/13.80	4.15/4.36		
$[NBu_4][ReO_4]$ [93]	7.79/15.81	8.87/18.00	4.18/8.48	7.99/16.22	8.26/16.77	8.04/16.32	12.48/25.33	3.82/7.75		
$[NEt_4]_2ReBr_3(CO)_3]$ [93]	7.27/9.44	8.35/10.84	5.37/6.97	2.17/2.82	8.15/10.58	10.92/14.17	6.74/8.75	4.46/5.79		

(IC_{50} = 0.042 μM and 8.42 μM, respectively, see Table 24). However, **166** and **167** show lower IC_{50} values in healthy MRC-5 cells than cisplatin.

Studies investigating the mechanism of action of these compounds were performed. The mechanism of cell death induced by the test compounds was investigated by staining A549 cells with the fluorescent dyes Hoechst, a cell-permeable bisbenzimide dye staining the cell nucleus, and propidium iodide (PI), a cell impermeable DNA intercalating dye. The differences in cell permeability of these dyes are used in fluorescence microscopy experiments to distinguish between intact living cells and dying, necrotic or late-apoptotic cells with a damaged plasma membrane. Furthermore, necrostatin-1 (5-(indol-3-ylmethyl)-3-methyl-2-thio-hydantoin), a compound inhibiting apoptosis, is used to further investigate the cell death caused by compounds **166** and **167**.

In Fig. 25, the fluorescence microscopy images of Hoechst/PI stained A549 cells incubated with different concentrations of **166** and **167** and necrostatin-1 are shown [116].

In summary, the images suggest a necrotic cell death induced by complexes **166** and **167**, which can be blocked with necrostatin-1. In combination with further investigations, the results show that these complexes induce mitochondrial damage and necrosis as evidenced by RIP1-RIP3-dependent ROS production. Cell cycle analysis shows an arrest in the G1 phase [116].

Abram *et al.* evaluated the biological activity of complexes **168**–**176** (Fig. 27) in MCF-7 breast cancer cells [117]. The activities of these '3 + 1' compounds were found to be strongly influenced by the lability of the monodentate ancillary ligand Cl, CN or SCN; the more labile the monodentate ligand, the more cytotoxic the complex. Thus, the chloride and cyanide coordinated complexes **168** and **172**, **173** have the lowest IC_{50} values (0.41 μM (**168**) and 0.6 μM (**172** and **173**); see Table 25). Coordination of chelating ligands significantly increases the IC_{50} value to 376 μM for complex **176** [117].

Complexes **177**–**186** (Fig. 27) were examined *in vitro* and *in vivo* for the binding affinity towards the 5-HT_2 serotonin receptor [118]. The most potent complexes are **182** and **183** (see Table 25). The corresponding ^{99m}Tc compounds exhibit comparable activity and bio-distribution with high liver uptake, renal excretion and low brain uptake. The bio-distribution of the Re compounds was not

Table 19
IC_{50} values [μM] determined for $(CO)_3Re(I)$ complexes **119**–**130** in different human cell lines.

Compound [ref.]	Human cancer cell lines							Human non-cancer cell line
	A549	A549cisR	HeLa	KinasePim 1	A375	K562	A431	MRC-5
119[a] [69]	5.2 ± 4.0	3.9 ± 4.6	5.8 ± 3.4					10.7 ± 0.5
120[a] [69]	9.7 ± 4.1	5.7 ± 1.8	8.8 ± 2.4					6.0 ± 1.9
121[a] [69]	6.7 ± 4.9	5.4 ± 1.8	1.2 ± 0.2					4.1 ± 0.9
Cisplatin[a] [69]	3.0 ± 1.8	12.4 ± 8.5	3.0 ± 1.2					0.43 ± 0.14
122[b] [94]				0.084				
123[b] [94]				0.673				
124[b] [94]				0.058				
125[b] [94]			10.0/0.03[c]	0.075				
126[d] [95]					0.9	3.4		
127[d] [95]					0.7	3.0		
128[d] [95]					1.3	7.5		
129[d] [95]					1.8	7.8		
130[a] [96]							2.0 ± 0.98	

[a] MTT assay read after 72 h of incubation time [69,96].
[b] radioactive assay: measured by the degree of phosphorylated substrate peptide P70 S6 after 30 min of incubation at room temperature with an ATP concentration of 10 μM [94].
[c] EC_{50} value; dark/ irradiated with 580 nm LED light; determined after 24 h incubation with MTT assay [94].
[d] MTT assay read after 48 h of incubation time [95].

evaluated. However, compounds targeting the brain receptors require the ability to cross the blood–brain barrier, which limits the application of these complexes [118].

In Table 26, some examples of theranostic Re/^{99m}Tc approaches are presented. Jurisson *et al.* evaluated the binding affinity of Bombesin-conjugates **187** and **188** (Fig. 28) *in vitro*. The ligand system was studied for complexation of non-radioactive Re, ^{99m}Tc and carrier-added as well as non-carrier-added ^{186}Re showing adequate complexation properties and stabilities for these metals. The very low IC_{50} values (see Table 26) and the biological profile of the tested compounds are promising for the development of a combination of imaging and therapeutic agent for prostate cancer [119,120].

Cyclometalated complexes **189** and **190** (Fig. 28) were evaluated for potential theranostic applications and biological activity by Gilon *et al.* [121]. These complexes were designed to address Gonadotropin-releasing hormone (GnRH) receptors. This receptor is overexpressed on different cancer types, for example on breast, prostate and ovarian cancers. In order to evaluate the potential of these compounds, the IC_{50} values on rat pituitary cortex membrane were determined. The highest affinity of 50 nM (see Table 26) was found for **189**. For comparison a higher affinity was found for native GnRH (10 nM) [121].

Vomero *et al.* evaluated the biological application of peripheral benzodiazepine receptor (PBR) targeting complexes **191** and **192** (Fig. 28). Although these complexes have very low IC_{50} values (see Table 26), the bio-distribution of the corresponding ^{99m}Tc complex show no distinct accumulation of these complexes. Therefore, the properties of these complexes must be further optimized to maintain this high affinity towards the receptor and simultaneously show a better bio-distribution [122].

Pirmettis *et al.* studied quinazoline coordinated complexes **193** and **194** (Fig. 29) for their ability to target epidermal growth factor receptor (EGFR) [123]. The EGFR is known to be overexpressed on certain solid tumors. The authors report that the Re compounds significantly inhibit autophosphorylation of EGFR and have low IC_{50} values (see Table 27). Another interesting aspect mentioned in the paper is the substitution of the chloride and one fluoride in complex **193** with bromide and a proton, respectively. This results in complex **194** and lead to significantly increased antiproliferative activity (see Table 27) [123]. It would be very interesting to determine if the single exchange of the chloride by bromide would similarly influence the biological activity.

The cytotoxicity of a metal-cyclized peptide has been presented by Jurisson *et al.* [124]. The Re-core is coordinated to the thioacetic acid modified terminal amino acid and a cysteine residue as determined by NMR studies with the stability of the complex being supported by quantum chemical calculations [124]. The authors synthesized four different isomers of the Re(V) octreotide analogues, but were only able to separate three of them, namely **195**–**197** (Fig. 29). Thus, one of the evaluated compounds is a mixture of two isomers, where one of them is complex **196**. The other isomer could not be structurally characterized in similar detail as the others due to overlapping signals in the NMR studies. Regardless, the compounds were evaluated for their binding affinity to the somatostatin receptor overexpressing rat cells. The determined IC_{50} values are in the high nanomolar range with the lowest value being 130 nM for complex **196**. The benchmark system In-DOTA-Tyr^3-octreotide, when tested in the same assay, has an IC_{50} value of 8 nM. Importantly, these complexes have one of the lowest IC_{50} values reported for cyclized Re(V) octreotide analogues and other Re compounds presented in this review. Furthermore, these

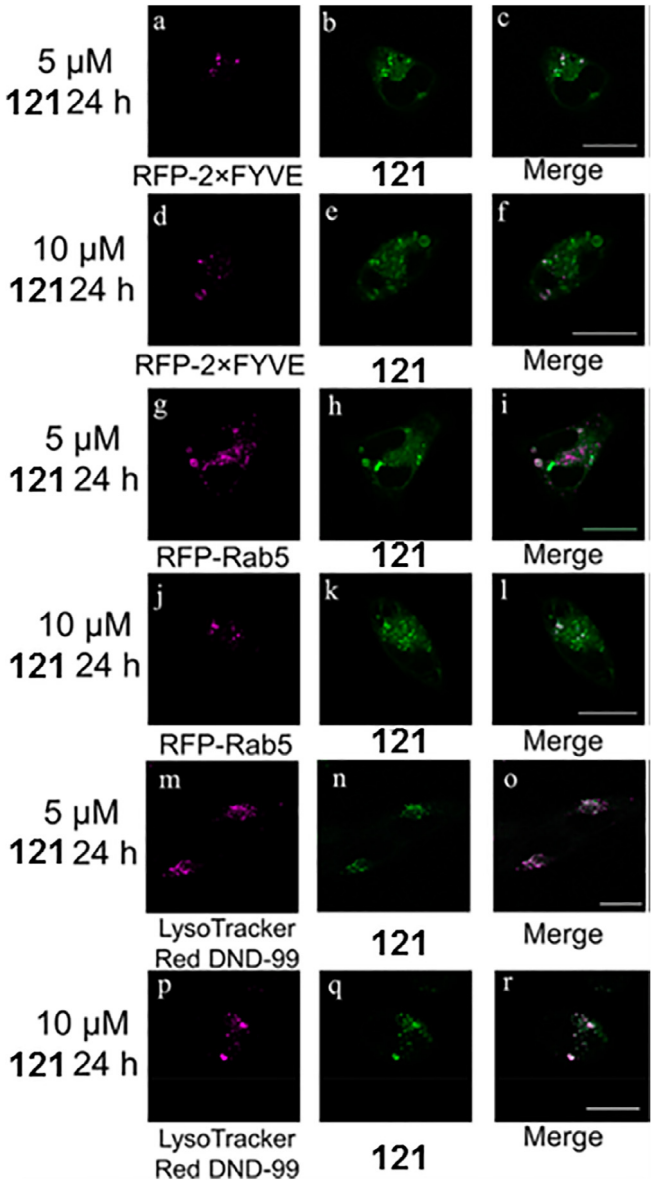

Fig. 19. Confocal microscopic images of HeLa cells treated with different concentrations of compound **121** and stained or transfected with the specified dye or plasmid. Reprinted with permissions from J. Am. Chem. Soc., 139 (2017) 14302–14314. Copyright 2018 American Chemical Society.

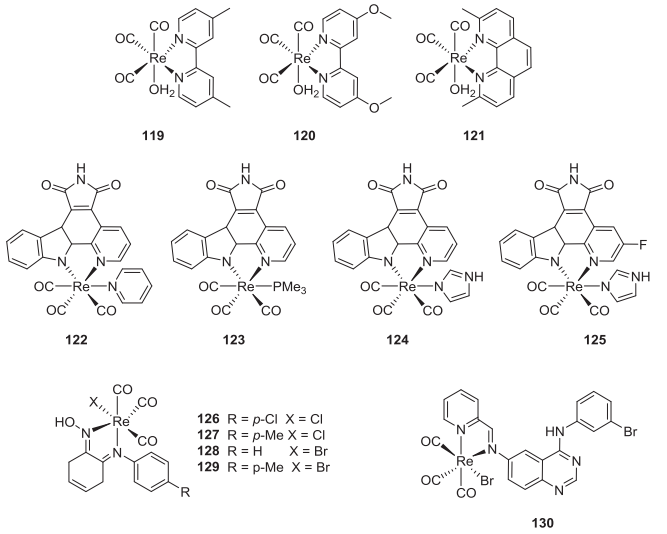

Fig. 20. Structures of $(CO)_3Re(I)$ compounds **119–130** bearing dinitrogen based ligands. Corresponding IC_{50} values are given in Table 19.

complexes are more stable than non-cyclized metal-coordinated peptides, and thus provide a good basis for theranostic approaches with cyclized Re-peptides [124].

5. Re clusters, Re(VII) trioxo compounds and perrhenates

Finally, octahedral water-soluble hexarhenium cluster compounds have been assumed applicable for medicinal purposes due to their favorable properties. Based on their luminescence and X-ray contrast properties, these clusters may be applied as imaging agents in the future [125]. Moreover, Re clusters were found to generate reactive singlet oxygen upon irradiation with UV-light and therefore are studied for their potential in photodynamic therapy of actinic keratosis or basal cell carcinoma [126].

Biological studies involving Re(VII) trioxo compounds have been performed to evaluate potential (eco)toxic effects of methyltrioxorhenium (MTO), a widely applied homogenous epoxidation catalyst [127]. In addition, perrhenate based ionic liquids (ILs), which are promising catalysts for oxidation and epoxidation reactions, have been studied *in vitro* to get insight in to potential (eco)-toxic effects [128]. It had turned out, however, that in perrhenate containing ILs the toxicity depends largely on the cations and MTO is converted to perrhenate in aqueous, particularly basic environments, reducing its toxicity relatively quickly [127,128]. The area of ecotoxicity determines the influence of chemicals polluting the environment and ecosystem. Chemical pollution is of big concern in modern environmental risk management, as ecosystems are still exposed to steadily increasing amounts of hazardous chemicals eventually leading to chronic effects. First, pollutant interactions can be observed on the cellular level e.g. by gene activation, activation of different signaling pathways or stress-specific responses. Additionally, organisms and populations of different species show different, complex reactions upon exposure to different pollutants. To get insight into the effect of a compound that is frequently exposed to an ecosystem by the industry, different species and microorganisms are studied in *in vitro* tests. Additionally, these results may give insights into the mechanism of action of these compounds [129]. Furthermore, cancer cells are included in these studies, since compounds previously declared as 'toxic' were found to have anticancer properties depending on the applied dose [130].

5.1. Re cluster compounds

Re clusters are increasingly investigated for their potential biological application in blue-light PDT (light irradiation up to 500 nm) due to their photosensitizing properties and the ability to generate singlet oxygen. Blue-light PDT is widely used in treatment of cancer affecting the skin like basal cell carcinoma and squamous cell carcinoma [126]. For application in blue-light PDT, cluster compounds should be stable, water-soluble, and luminescent, have a high cellular uptake, show photo-induced cytotoxicity, and low dark toxicity. The compounds described in the following will be evaluated for such properties.

Studies on the cluster compounds $Na_4[\{Re_6S_8\}(CN)_6]$, $Na_4[\{Re_6Se_8\}(CN)_6]$ and $Na_4[\{Re_6Te_8\}(CN)_6]$ studied by Shestopalov *et al.* [125,126] showed that the cytotoxicity and the cellular uptake kinetics of the compounds are strongly dependent on the chalco-

Table 20
IC_{50} values [μM] determined for $(CO)_3Re(I)$ heteroatom containing complexes **131–141** in different cell lines.

Compound [ref.]	Human cancer cell lines						Rat	Human non-cancer cell lines	
	HeLa	KB-31	KB-V-1	A2780	A2780cisR	HepG2	C6[b]	CCD-19Lu	HEK293T
131[a] [97]				7.75 ± 0.07	8.91 ± 0.17				6.61 ± 0.48
132[a] [97]				19.04 ± 1.12	26.61 ± 2.37				15.76 ± 4.74
133[a] [97]				2.02 ± 0.19	4.29 ± 0.27				22.24 ± 1.07
134[a] [97]				18.34 ± 1.36	24.97 ± 0.43				16.67 ± 1.34
135[a] [97]				13.74 ± 0.53	20.40 ± 2.55				15.84 ± 3.31
136[a] [97]				18.09 ± 0.77	48.45 ± 2.02				63.36 ± 1.17
Cisplatin[a] [97]				8.32 ± 0.88	30.2 ± 0.94				3.44 ± 0.48
137[a] [98]	>200/26.4 ± 9.2*			>200/4.6 ± 1.4*	>200/29.9 ± 7.7*				
138[a] [98]	>200/5.9 ± 1.4*			>200/2.2 ± 1.1*	>200/3.2 ± 0.7*				
Cisplatin[a] [98]				0.18 ± 0.07	5.14 ± 1.1				
139[a] [99]	50.3 ± 0.2	43.5 ± 2.2	195 ± 1			30.9 ± 1.1		112 ± 3	
Cisplatin[a] [99]	11.6 ± 0.2	22.1 ± 3.6	39.1 ± 1.7			10.5 ± 0.5		129 ± 1	
140[c] [100]				10.6 ± 0.3	19.1 ± 0.6		4.5 ± 0.1		
141[c] [100]				n.d.	n.d.		19.2 ± 0.6		
Cisplatin[c] [100]				2.9 ± 0.4	9.2 ± 0.4		0.7 ± 0.2		

[a] MTT assay read after 24 h of incubation time [97,99].
* 1h irradiation with light of wavelength 365 nm, MTT assay [98].
[b] Cell line with high expression of TSPO.
[c] MTT assay read after 72 h of incubation time [100].

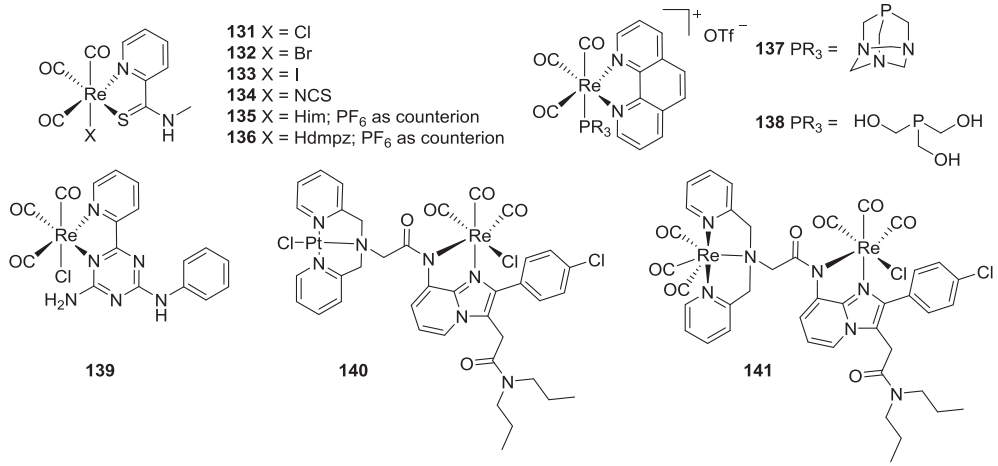

Fig. 21. Structures of $(CO)_3Re(I)$ heteroatom containing compounds **131–141**. Corresponding IC_{50} values are given in Table 20.

gen atoms. The cytotoxicity was found to decrease in the order S > Se > Te whereas the cellular accumulation in contrast increases in the order S < Se < Te in Hep-2 cells. However, photocytotoxicity and reactive oxygen species (ROS) production increases in the order Te < S < Se and thus breaks the periodic table trend. Nevertheless, the Se complex was able to reduce cell viability to 63% at a concentration of 100 μM [125,126]. The hexarhenium cluster $Na_4[\{Re_6Te_8\}(CN)_6]$, studied by Mironov *et al.*, was found to be completely non-toxic *in vitro* (see Table 28) and *in vivo* it was not taken up by cells. The low toxicity of this cluster represents a good start for the development of X-ray contrast agents based on hexarhenium cluster complexes [131] although evaluating strategies to get the compound into cells should be considered a high priority. In conclusion, the reported data form a good basis for further development of biological applicable cluster compounds [125,126,131].

Other hexarhenium clusters $K_2H_8[\{Re_6Se_8\}(P(CH_2CH_2CONH_2)(CH_2CH_2COO)_2)_6]$ and $K_4[\{Re_6(\mu3\text{-}Se_8\}(BTA)_6]$ having benzotriazolate apical ligands were photochemically and biologically evaluated by Brylev *et al.* [132]. The compounds display red

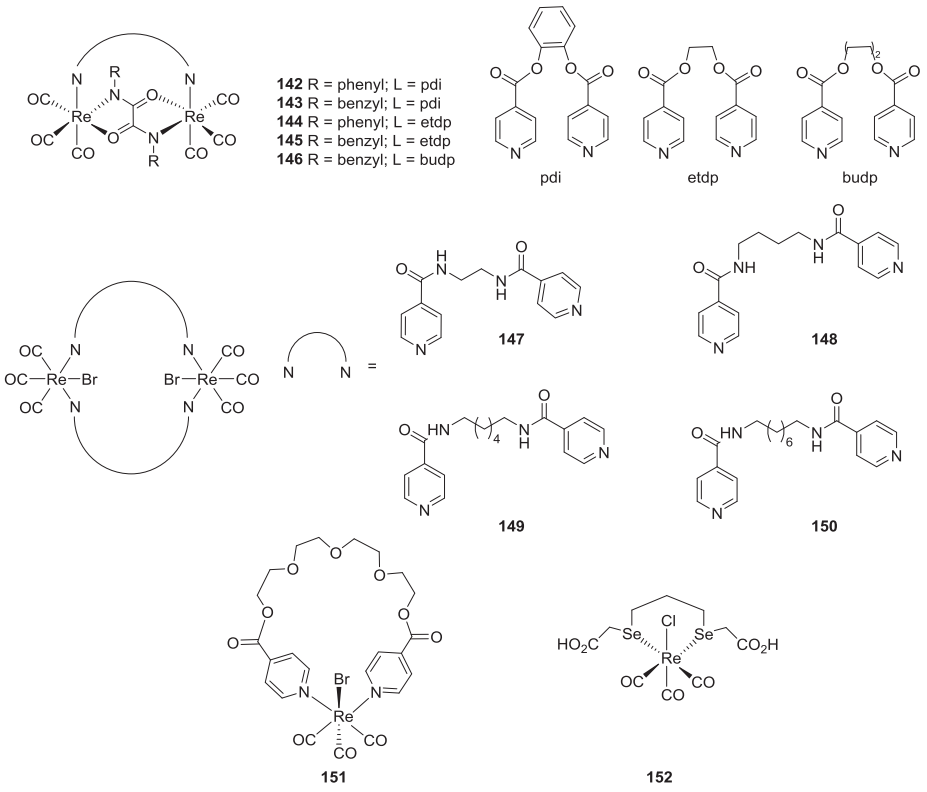

Fig. 22. Schematic illustration of structures of binuclear $(CO)_3Re(I)$ compounds and two appended monomeric complexes **142–152**. Corresponding IC_{50} values are given in Table 21.

Table 21
IC_{50} values [μM] determined for $(CO)_3Re(I)$ complexes **142–152** in different human cancer cell lines.

Compound [ref.]	Human cancer cell lines						
	HeLa	A549	HCT-15	HT-29	MCF-7	HepG2	K562
142[a] [104]	>100	95.72 ± 8.2	20.80 ± 1.9				
143[a] [104]	54.19 ± 2.4	56.15 ± 2.9	n.a.				
144[a] [104]	19.81 ± 2.5	88.49 ± 1.2	n.a.				
145[a] [104]	40.49 ± 1.9	65.23 ± 7.2	n.a.				
146[a] [104]	64.50 ± 1.9	29.65 ± 1.4	30.53 ± 1.3				
Cisplatin[a] [104]	39.84 ± 6.4	25.89 ± 1.8	23.93 ± 2.8				
147[a] [102]	23.4 ± 1.4	>100	48.2 ± 3.4			30.1 ± 1.6	27.3 ± 1.3
148[a] [102]	63.4 ± 3.1	41.4 ± 2.2	42.2 ± 3.1			23.3 ± 1.2	>100
149[a] [102]	22.8 ± 2.5	>100	46.9 ± 3.1			29.4 ± 2.8	26.4 ± 1.9
150[a] [102]	21.2 ± 2.7	24.7 ± 2.9	22.1 ± 2.3			27.3 ± 2.6	24.1 ± 1.7
Cisplatin[a] [102]	20.94 ± 2.1	18.63 ± 3.8	17.92 ± 2.9			21.91 ± 3.4	23.65 ± 2.2
151[a] [103]	17.56 ± 5.7	18.2 ± 5.7	n.a.		11.9 ± 1.4	20.2 ± 9.2	n.a.
152[b] [105]	75.1	131.5		>500	4.75		

(n.a. = not active).
[a] MTT assay read after 48 h of incubation time [102–104].
[b] No incubation time given; MTT assay [105].

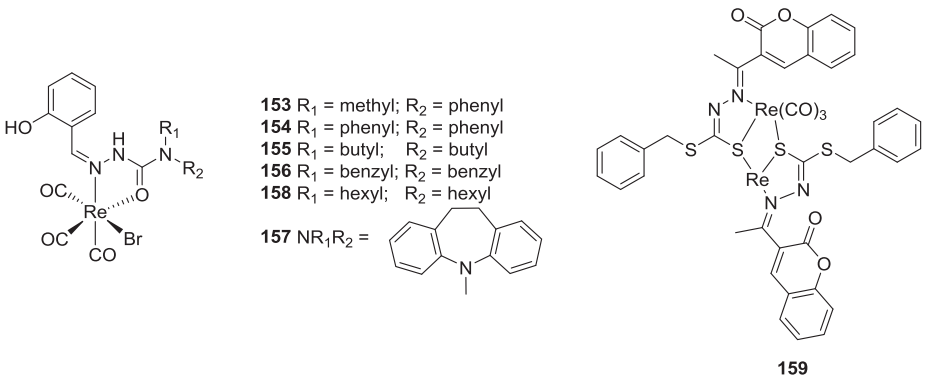

Fig. 23. Structures of an asymmetric binuclear Re(I) compounds and phenol containing monomeric complexes **153**–**159**. Corresponding IC_{50} values are given in Table 22.

Table 22
IC_{50} values [μM] determined for asymmetric binuclear Re(I) compounds and phenol containing monomeric complexes **153**–**159** in different human cell lines.

Compound [ref.]	Human cancer cell lines			Human non-cancer cell line
	MOLT-4	MCF-7	MDA-MB-231	Fibroblast
153[a] [107]	24 ± 6	>125		>125
154[a] [107]	15 ± 1	>125		>125
155[a] [107]	15 ± 1	>125		>125
156[a] [107]	7.3 ± 0.4	24 ± 4		>125
157[a] [107]	1.0 ± 0.1	35 ± 4		9 ± 1
158[a] [107]	22 ± 2	>125		>125
Cisplatin[a] [107]	18 ± 1	71 ± 8		28 ± 2
159[b] [108]		19.41	8.61	
Tamoxifen[b] [108]		11.20	13.40	

[a] MTT assay read after 24 h of incubation time [107].
[b] MTT assay read after 72 h of incubation time [108].

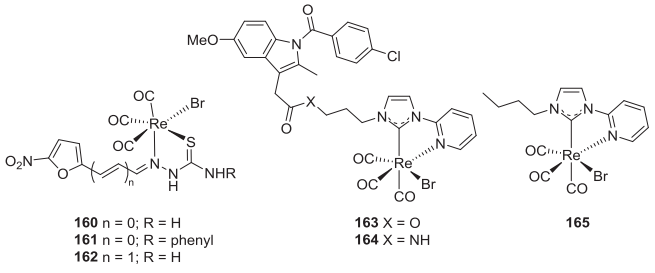

Fig. 24. Structures of $(CO)_3Re(I)$ carbene or hydrazine compounds **160**–**165**. Corresponding IC_{50} values are given in Table 23.

phosphorescence and high quantum yields, which is beneficial for imaging applications. In addition, the compounds taken up by the cells accumulate in the cytoplasm. The IC_{50} indicate no acute cytotoxicity although long-time toxicity of the complexes are possible. Compared to $Na_4[\{Re_6S_8\}(CN)_6]$, $Na_4[\{Re_6Te_8\}(CN)_6]$, $K_2H_8[\{Re_6Se_8\}(P(CH_2CH_2CONH_2)(CH_2CH_2COO)_2)_6]$ and $K_4[\{Re_6(\mu3\text{-}Se_8\}(BTA)_6]$ these clusters are 4–7 fold more toxic [132].

Ramirez-Tagle *et al.* evaluated the biological activity of cluster $Re_6Se_8I_6^{3-}$ [133]. The authors determined the IC_{50} and the IC_{max} value in healthy and cancer cells. Results show that the concentration, at which all cancer cells are killed (IC_{max} see Table 28), is in the same concentration range, where half of the healthy cells are

Table 23
IC_{50} values [μM] determined for $(CO)_3Re(I)$ carbene or hydrazine complexes **160**–**165** in different biological systems.

Compound [ref.]	Human non-cancer cell line	Antimicrobial	Compound [ref.]	Human cancer cell lines			Human non-cancer cell line
	EA.hy926	*T. cruzi* (Dm28c strain)		HPAF-II	ASPC1	CFPAC	HEK293T
160[a] [109]	36.9 ± 0.7	2.4 ± 0.2	**163**[b] [110]	6.0 ± 2.0	7.9 ± 1.4	6.0 ± 1.8	11.8 ± 2.3
161[a] [109]	14.3 ± 0.6	1.3 ± 0.3	**164**[b] [110]	4.8 ± 0.8	9.4 ± 3.5	5.4 ± 1.4	8.6 ± 0.3
162[a] [109]	43.6 ± 1.1	2.01 ± 0.03	**165**[b] [110]	5.6 ± 0.6	4.0 ± 1.2	5.7 ± 2.8	14.8 ± 2.4
Nifurtimox[a] [109]	20.1 ± 0.8	–	**Carboplatin**[b] [110]	8.7 ± 4.3	6.8 ± 2.0	7.4 ± 1.2	45

[a] MTT assay read after 24 h of incubation time [109].
[b] Resazurin assay read after 72 h of incubation time [110].

Table 24
IC_{50} values [μM] of Re(V) oxo based coordination compounds **166** and **167** tested in different human cell lines determined by MTT assay with an incubation time of 72 h.

Compound [ref.]	Human cancer lines										Non-cancer cell line	
	A549	A549 (confluent)	HeLa	U2OS	NTERA-2	A2780	A2780CP70	DU 145	HT-29	MDA-MB-231	MCF-7	PC3	MRC-5
166 [116]	0.207 ± 0.004	8.61 ± 0.749	0.445 ± 0.004	0.274 ± 0.006	0.23 ± 0.028	0.67 ± 0.040	0.042 ± 0.015	2.840 ± 0.381	0.085 ± 0.011	0.475 ± 161	0.285 ± 0.035	0.27 ± 0.014	1.35 ± 0.228
167 [116]	0.157 ± 0.015	5.25 ± 1.98	0.695 ± 0.021	0.209 ± 0.031	0.255 ± 0.035	0.150 ± 0.01	0.056 ± 0.002	1.37 ± 0.084	0.095 ± 0.02	1.74 ± 0.275	0.805 ± 0.021	0.78 ± 0.01	0.709 ± 0.076
Cisplatin [116]	3.23 ± 0.467	9.42 ± 1.93	4.10 ± 0.113	4.60 ± 0.600	0.385 ± 0.049	0.700 ± 0.200	8.42 ± 0.205	>100	29.6 ± 1.32	43.6 ± 7.07	9.74 ± 0.537	10.3 ± 0.919	5.30 ± 0.600

killed (IC_{50} value for healthy cells). Compared to the clusters discussed above, this cluster is the most cytotoxic. However, the cluster displays good cellular uptake and non-intercalating DNA interactions [133].

Hexahydroxohexarhenium clusters $K_4[\{Re_6S_8\}(OH)_6]$, $K_4[\{Re_6Se_8\}(OH)_6]$ and the corresponding polymeric form (Re-cluster-polymer hydride) were studied for their potential application as imaging agents [134]. Choy *et al.* showed that they are not taken up by the cells; however, $K_4[\{Re_6Se_8\}(OH)_6]$ can be internalized by energy-dependent endocytosis. Conjugation of $K_4[\{Re_6Se_8\}(OH)_6]$ with an amphiphilic diblock co-polymer forming a Re cluster-polymer hydride enhanced its cellular uptake. All three clusters display high IC_{50} values of 250–300 μM indicating no toxicity for 72 h (Table 28) [134].

A general schematic illustration of such hexarhenium cluster compounds is given in Fig. 30.

5.2. Re(VII) trioxo compounds and perrhenates

The organometallic catalyst methyltrioxorhenium (MTO), its *tert*-butylpyridine (TBP) conjugate and different perrhenate (ReO_4^-) based ionic liquids have been tested for their (eco)toxicity in different biological systems like bacteria, algae, flea, rat and human cell lines (see Table 29 and Fig. 31). Stolte *et al.* showed that MTO has submicromolar to low micromolar EC_{50} values in aquatic organisms and therefore exhibits acute ecotoxicity. However, in mammals there is moderate to no toxicity as reflected by the EC_{50} values of 100 μM and 45.3 μM in rat and human cells, respectively [128]. Furthermore, it is important to note that the acute toxicity of MTO is time-limited due to hydrolysis to the non-toxic ReO_4^- (EC_{50} values > 100 μM) [127,135]. Investigations on perrhenate based ionic liquids **202**–**205** indicate a strong influence of the corresponding cation on the biological activity and no toxicity to the polar and anionic perrhenate [128]. Among the tested ionic liquids, **204** has an IC_{50} value of 0.045 μM (see Table 29) presumably due to a long alkyl sidechain appendage leading to a highly more lipophilic compound. This explains, why for ammonium perrhenate, which is evaluated in the same cell system, no toxicity was observed for 48 h although chronic toxicity of ReO_4^- has not yet been eliminated [128].

6. *In vivo* studies of Re compounds

Once cell culture studies are completed, the compounds displaying beneficial biological profiles are selected for *in vivo* studies. Several appropriate *in vivo* animal model systems have been used, including Wistar rats [116,136] and naive C57Bl6 mice [69]. There are several studies reported and some of them are addressed in the following paragraphs. Two reviews focusing on $^{186/188}$Re radiopharmaceuticals [137,138] and one discussing *in vivo* studies of non-radioactive Re complexes were recently published [139] and the reader is referred to these reviews for further information. Like the discussion of the *in vitro* data, the compounds evaluated in *in vivo* studies are ordered according to their oxidation state and the nature of the Re-core. Re labeled biomolecules are not discussed in this work and therefore the reader is referred to other publications [140–148].

6.1. $(CO)_3$Re(I) based compounds

Compound **121**, which is already discussed in Table 19, was further evaluated *in vivo*. A simultaneous injection of **121** and the corresponding ^{99m}Tc complex in the same mouse revealed a similar bio-distribution of both compounds and their excretion through renal and hepatobiliary pathway. Metabolite analysis showed the

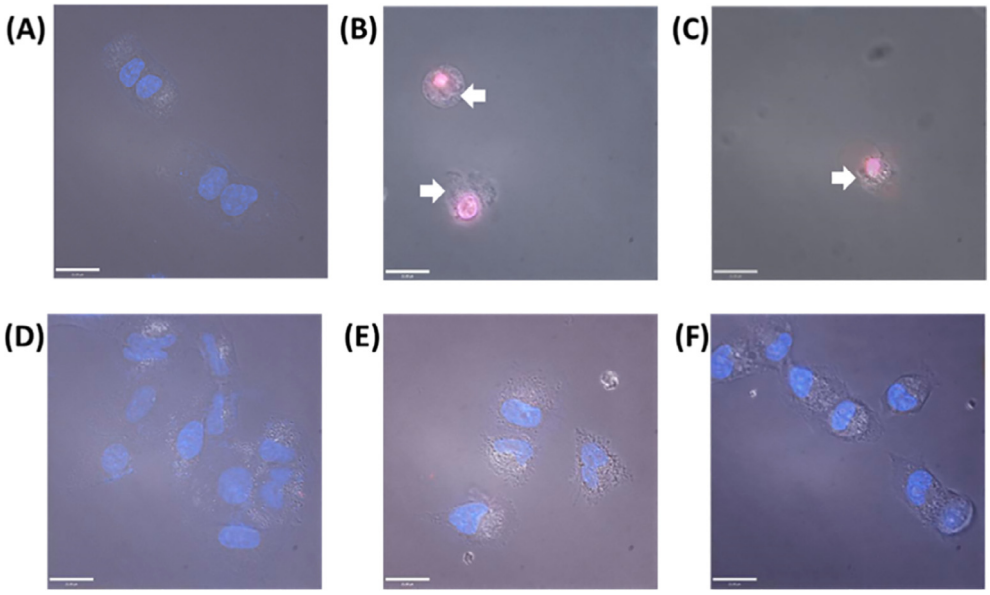

Fig. 25. Fluorescence microscopy images of: (A) untreated A549 cells, (B) cells treated with 20 μM **166** for 12 h, (C) cells treated with 20 μM **167** for 12 h, (D) cells treated with necrostatin-1, (E) cells co-incubated with **166** and necrostatin-1, (F) cells co-incubated with **167** and necrostatin-1. Reprinted with permissions from J. Am. Chem. Soc., 137 (2015) 2967–2974. Copyright 2018 American Chemical Society.

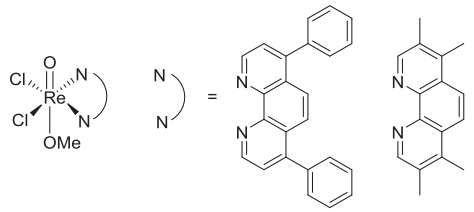

166 167

Fig. 26. Structures of Re(V) oxo based coordination compounds **166** and **167**. Corresponding IC_{50} values are given in Table 24.

presence of **121** (and its chloride analogue, where the axial water ligand is substituted by chloride) up to 120 min in blood and urine. Nevertheless, also two distinct metabolites formed, which were not further analyzed. Overall, compound **121** displays sufficient stability, fast blood clearance and no non-specific accumulation in any organs, which makes this compound a promising candidate for further *in vivo* tumor targeting studies [69].

Collery *et al.* extensively studied the *in vivo* effects of Re(I) diselenoether complex **152** [106]. As shown in Table 21, complex **152** shows cytotoxicity in MCF-7 cells with an IC_{50} value of 4.75 μM, however, is non-toxic in A549 and HT-29 cells. Additionally, it was shown that the compound is able to inhibit cell proliferation of MDA-MB-231 cells at a concentration of 10 μM over a period of 48 h and the effect is retained even after removal of the Re complex. Therefore, the complex was evaluated *in vivo* in MDA-MB-231 bearing mice resulting in remarkably reduced tumor volume compared to mice treated with cisplatin. After one month of treatment, a complete cure of the mice was observed. The investigation on the mechanism of action indicate a beneficial interaction of the redox chemistry of the Se ligand, which is suggested to be liberated in the cells. The Re core is proposed to interact with the DNA in a method similar to cisplatin and therefore is able to induce cell death. Experiments show that treatment with **152** (reducing the tumor volume) resulted in significantly increased tumor growth upon additional administration of a single dose of cisplatin at day 41 of the experiment. Therefore, it is assumed that the Re complex is potentially replaced by cisplatin [106,149,150]. However, further studies confirming this assumption are needed. Overall, the studies show that **152** is a very promising candidate for breast-tumor treatment.

6.2. Dirhenium(III) based compounds

Shtemenko *et al.* evaluated the biological activity of quadruple-bonded dirhenium(III) carboxylates (see Fig. 32) [136,151–155]. A recent review summarizes these findings in detail [156]. Nevertheless, dirhenium compounds are rarely studied in anticancer studies and need to be mentioned in this review. Its absence from biological studies is mostly due to low solubility and instability in aqueous solution. However, encapsulation of these clusters in liposomes stabilizes the quadruple bond and therefore makes it possible to evaluate these compounds in biological studies [156]. Shtemenko *et al.* were able to show that these dirhenium clusters exhibit antihemolytic properties shifting the maximum rate of hemolysis *in vitro* from about 1.5 min to 6 min [153]. Additionally, co-encapsulation of dirhenium cluster and cisplatin in a ratio of 1:4 displays the highest antitumor activity compared to cisplatin and the liposomal form of the rhenium cluster. During a 21 day experiment in tumor-bearing mice, the rhenium-platinum liposome was able to reduce the total tumor volume from 60–100 mm^3 to 0–2 mm^3 indicating its strong anticancer effect [136,154,156]. Increasing antitumor efficiency was shown by introducing different substituents for the dicarboxylates in the order methyl (**206**) < ethyl (**207**) < propyl (**208**) < butyl (**209**) [156]. Additionally, no toxic effects were observed in kidneys, liver and on the production in morphology of red blood cells during *in vivo* experiments. Moreover, it was shown that the dirhenium compounds were able to bind covalently to DNA, like cisplatin and the investigations done by Collery *et al.* [106] on Re(I) diselenoether complexes. However, the Re cluster compounds display different redox behavior leading to antioxidative properties *in vivo* in contrast to pro-oxidative effect of cisplatin [156]. Furthermore, due to the δ-component of the quadruple bond, the cluster is able to scavenge an unpaired electron and therefore reduce oxidative stress in cells. In summary, the liposomal encapsulated quadruple-bonded Re cluster shows synergistic effects with cisplatin leading to antihemolytic, antirad-

Table 25
IC_{50} values [μM] determined for complexes **168**–**186** in different human cell lines.

Compound [ref]	Human cancer cell line MCF-7	Compound [ref]	Frontal cortical tissue for 5-HT_2 receptor binding
168[a] [117]	0.41 ± 0.02	**177**[b] [118]	>100
169[a] [117]	1.51 ± 0.17	**178**[b] [118]	1.289
170[a] [117]	1.7 ± 0.3	**179**[b] [118]	0.845
171[a] [117]	2.0 ± 0.2	**180**[b] [118]	>100
172[a] [117]	0.6 ± 0.3	**181**[b] [118]	0.029
173[a] [117]	0.6 ± 0.3	**182**[b] [118]	0.019
174[a] [117]	2.3 ± 0.3	**183**[b] [118]	0.014
175[a] [117]	22.4 ± 0.3	**184**[b] [118]	0.023
176[a] [117]	376 ± 2	**185**[b] [118]	0.378
Cisplatin[a] [117]	1.6 ± 0.1	**186**[b] [118]	0.352

[a] No incubation time given; CV staining assay [117].
[b] Competition binding assay using [^{3}H]ketanserine [118].

ical, antioxidative and antitumor properties representing a new perspective for the development of new potent anticancer agents [156].

6.3. Re(V) based compounds

Re(V) oxo compounds **166** and **167** (Table 24), were tested *in vivo* in C57BL/6 mice to evaluate toxicity and the side effects of these compounds. After the administration of a single dose, mice were monitored for further 6 days showing no acute toxicity or weight loss. Although IC_{50} values in MRC-5 cells indicate a higher cytotoxicity compared to cisplatin (1.35 μM and 0.71 μM, respectively; cisplatin 5.3 μM), the *in vivo* data indicates a lower toxicity. Therefore, this study shows that IC_{50} values can be seen as indictor of *in vivo* behavior, however, they do not display the complete toxicity profile of a compound [116]. The stability of **166** in whole blood was evaluated at different time points over a period of 6 h by analysis of octanol extracts from aliquots of blood incubated with **166** at 37 °C using GFAAS. The determined half-life is 29.1 min, which is comparable to cisplatin (21.6 min). However, decomposition of the investigated Re complex to water-soluble perrhenate is not covered using this method and is a possible explanation for the observed tolerance in mice.

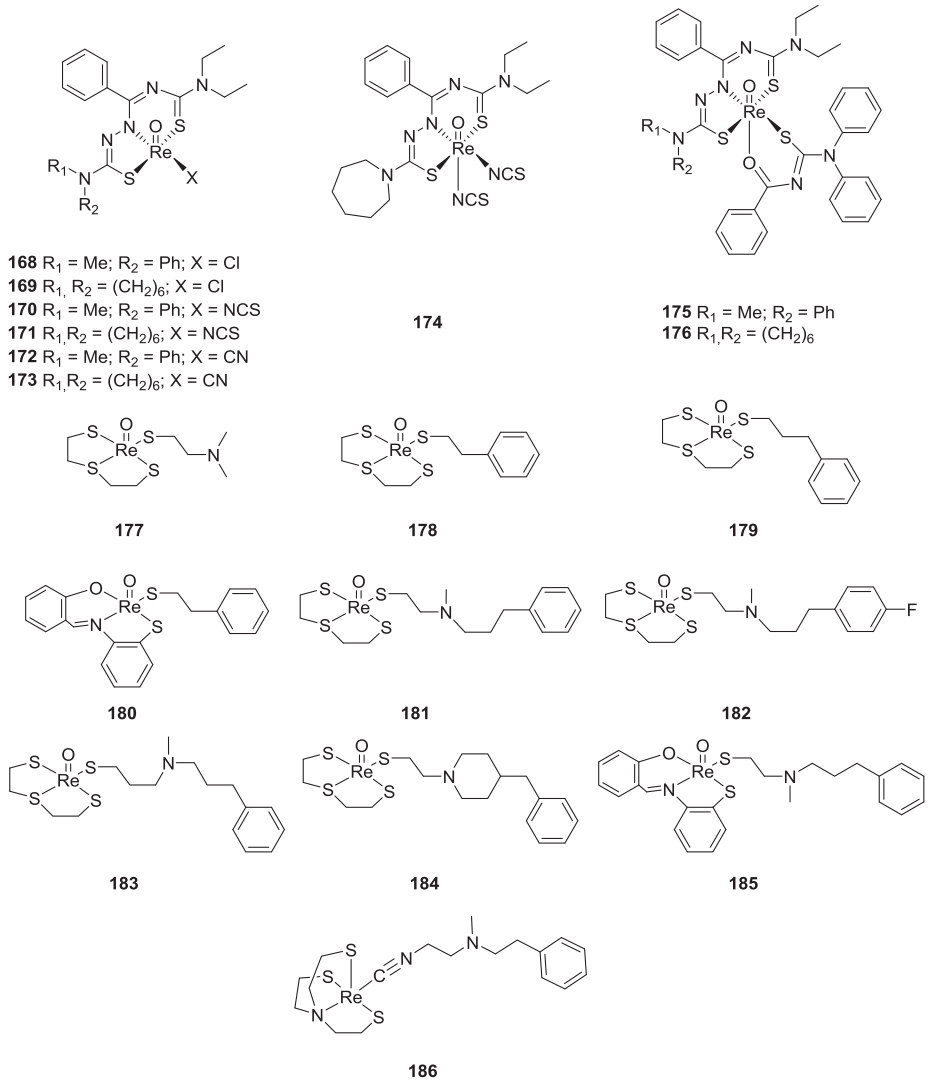

Fig. 27. Structures of compounds **168**–**186**. Corresponding IC_{50} values are given in Table 25.

Table 26
IC_{50} values [μM] determined for Re(oxo)-N,S-donor ligands coordination compounds **187–192** in different cell lines.

Compound [ref.]	Human cancer cell line PC3 [nM]	Compound [ref.]	Rat Pituitary membrane [μM]	Compound [ref.]	Rat Cerebral cortex membrane suspension [μM]
187[a] [119]	2.0 ± 0.7	**189**[b] [121]	0.05	**191**[c] [122]	0.127 ± 0.015
188[a] [120]	1.0 ± 0.2	**190**[b] [121]	1.00	**192**[c] [122]	0.187 ± 0.019

[a] Competition assay with [^{125}I]-Tyr-BBN(NH_2) [119].
[b] Competition assay with [^{125}I]-GnRH [121].
[c] Competition assay with [^{3}H]-PK11195 [122]

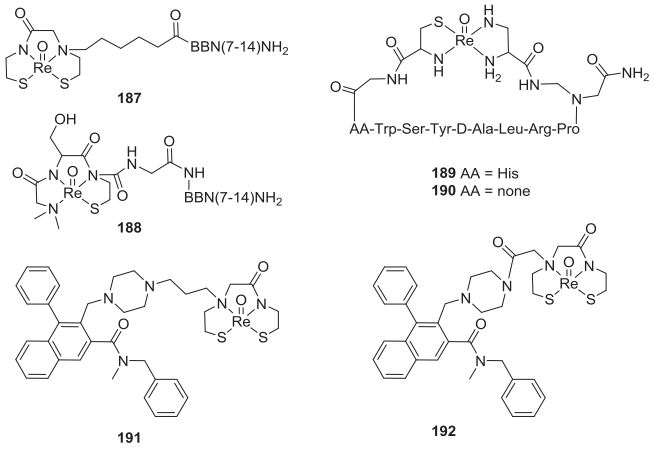

Fig. 28. Structures of Re(oxo)-N,S-donor ligands coordination compounds **187–192**. Corresponding IC_{50} values are given in Table 26.

6.4. Re cluster and Re(VII) based compounds

The sodium iodide symporter (NIS), a membrane glycoprotein, transfers iodide from blood to cells and is mainly expressed in the thyroid. NIS-mediated uptake is extensively studied for $^{99m}TcO_4^-$, ^{125}I and ^{131}I for diagnosis and therapy of NIS expressing tumors. A study by Li *et al.* published in 2016 used NIS transfected HeLa cells and studied $^{188}ReO_4^-$ uptake *in vitro* and *in vivo* [157]. It was shown that $^{188}ReO_4^-$ displays a better distribution and excretion profile compared to ^{125}I. $^{188}ReO_4^-$ reached a maximum uptake level in NIS transfected tumor cells after 0.5 h and decreased faster than ^{125}I, however transferring a higher energy dose to the tumor. Furthermore, $^{188}ReO_4^-$ provides γ-radiation for imaging and β-radiation for therapy displaying a new possibility for NIS gene therapy [157].

Non-toxic hexarhenium cluster (IC_{50} values given in Table 28; about 400 μM) $Na_4[\{Re_6S_8\}(CN)_6]$, $Na_4[\{Re_6Se_8\}(CN)_6]$ and $Na_4[\{Re_6Te_8\}(CN)_6]$ were further evaluated for their toxicity *in vivo* in BALB/C mice [158,159]. After applying a dose of 500 mg (Re)/kg of the Te or S containing cluster, one mouse treated with the Te containing cluster died whereas the others showed no sign of intoxication. The Se containing cluster administered in the same dose led to the deaths of two mice. The surviving mice did not show signs of weight loss or intoxication. Morphological analysis of the liver, kidneys, spleen, lungs and heart of the mice after two weeks of injection showed adverse morphological changes in the liver for the animals treated with $Na_4[\{Re_6S_8\}(CN)_6]$ and $Na_4[\{Re_6Se_8\}(CN)_6]$. This is contrary to the very high IC_{50} values of about 400 μM for these cluster compounds (see Table 28). For the Te containing cluster, no morphological changes could be observed and

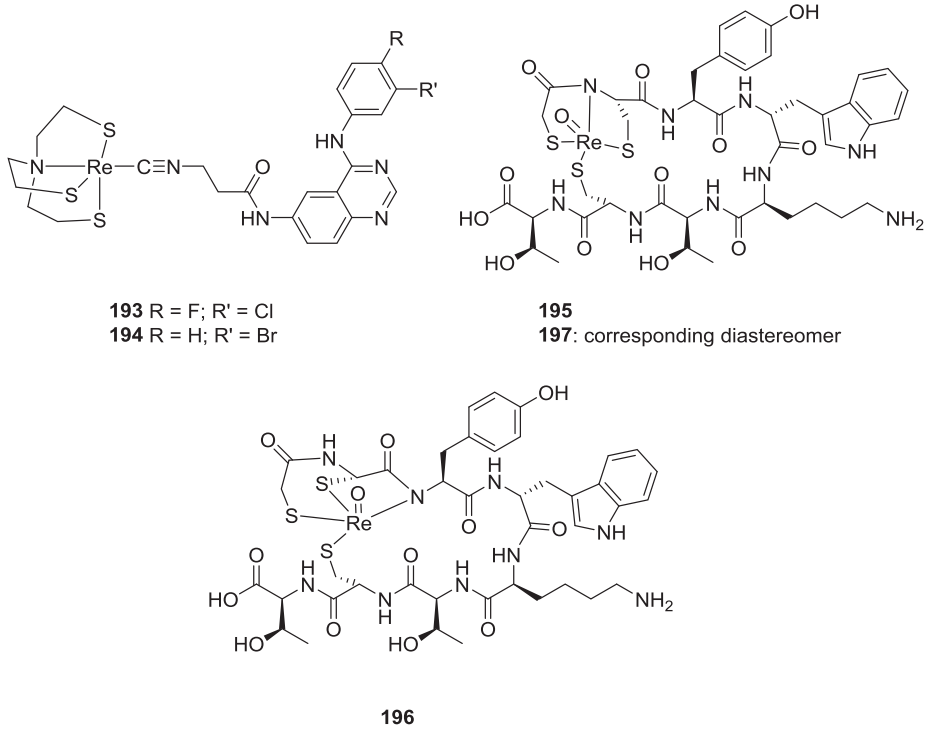

Fig. 29. Structures of Re(III) and Re(V) based coordination compounds **193–197**. Corresponding IC_{50} values are given in Table 27.

Table 27
IC_{50} values [μM] of Re(III) and Re(V) based coordination compounds tested in different human cancer cell lines.

Compound [ref.]	Human cancer cell lines A431	Rat AR42J
193[a] [123]	6.4 ± 1.8	
194[a] [123]	2.9 ± 0.3	
195[b] [124]		1.5 ± 0.7
196[b] [124]		0.13 ± 0.08
197[b] [124]		0.4 ± 0.1
196 + Isomer[b] [124]		0.5 ± 0.2
^{nat}In-DOTA-Tyr^3-octreotide[b] [124]		0.008 ± 0.003

[a] MTT assay read after 72 h of incubation time [123].
[b] 1 h incubation time using competition assay with [^{125}I]-Tyr-somatostatin-14 [124].

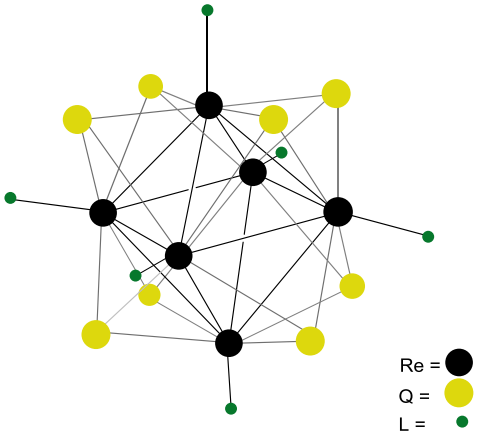

Fig. 30. General scheme of hexarhenium Re_6 chalcogenide cluster compounds discussed in Table 28. (Q = S/Se/Te; L = ligand) [132]

therefore this compound is considered safe in application [159]. This low toxicity is also displayed by the higher IC_{50} values of 4500 μM in Hep-2 cells (Table 28). Bio-distribution studies in rat using the $K_4[\{Re_6S_8\}(CN)_6]$ cluster showed the highest accumulation in liver and kidney medulla. Moreover, accumulation in the spleen was observed suggesting this compound is a suitable imaging (e.g. as an X-ray contrast agent) and therapeutic agent for lymphoproliferative disorders [158].

7. Clinical trials

The ultimate goal of developing new Re-based anticancer compounds is their application in therapeutic/clinical treatment. Cell culture studies of anticancer Re compounds are often used as important initial pre-screening steps ahead of animal and human studies. Many steps of translational research are necessary before studies in humans are possible. Although the field of Re based anticancer agents may be in its infancy, some Re compounds have been investigated in human beings and these will be summarized below.

After extensive studies in cell culture and animal model systems, some compounds show varying degrees of effectiveness and selectivity in killing cancer cells and only a few compounds are continued to human studies. Information on potential progress on compounds being evaluated in human beings are thus relevant to the topic of the current review. Studies in humans are referred to as clinical trials beginning with Phase I and progressing to Phase II and III trials. Phase I clinical trials focus on determining the safety of the compounds in normal subjects, Phase II focuses on determining the proper dose to use in patients and involves a limited number of subjects and a short time period. Phase III studies focus on the treatment of patients for a specific clinical condition (e.g. melanoma) and involves a larger number of subjects for longer periods. The summary of Re compounds in clinical trials (Table 30) shows that the compounds studied are mainly radioactive Re complexes. This may be due to non-invasive dosimetry and imaging of the radioactive compounds *in vivo* by well-established medical equipment, the single photon emission computed tomography (SPECT), as applied for ^{99m}Tc imaging [160]. Since many reviews that focus on Re and Tc radiopharmaceuticals are published [5,11,137,159–175], this review focuses on characterizing the effects of different classes of non-radioactive Re complexes. The ultimate goal is to compare such studies with the compounds that have been selected for clinical trials. Once the analysis of the com-

Table 28
IC_{50} values in [μM] of Re based cluster compounds in different human cell lines.

Compound [ref.]	Human tumor cell lines			Human non-cancer		
	HeLa	Hep-2	HepG2	MRC-5	EA hy 926	HUVEC
$Na_4[\{Re_6S_8\}(CN)_6]$[a] [126]	401 ± 7	417 ± 4		471 ± 13		
$Na_4[\{Re_6Se_8\}(CN)_6]$[a] [126]	410 ± 5	478 ± 8		551 ± 21		
$Na_4[\{Re_6Te_8\}(CN)_6]$[a] [131]		4800 ± 0.3				
$K_2H_8[\{Re_6Se_8\}(P(CH_2CH_2CONH_2)(CH_2CH_2COO)_2)_6]$[b] [132]		123.7 ± 0.8				
$K_4[\{Re_6(\mu3\text{-}Se_8\}(BTA)_6]$[b] [132]		122.6 ± 2.1				
$Re_6Se_8I_6^{3-}$[b] [133]			58.5 ± 5/146.3 ± 23[c]		88.7 ± 6/286.8 ± 34[c]	147 ± 11/457.5 ± 46[c]
$K_4[\{Re_6S_8\}(OH)_6]$[b] [134]	262.3 ± 8.1					
$K_4[\{Re_6Se_8\}(OH)_6]$[b] [134]	297.8 ± 9.5					
Re cluster- polymer hydride[b] [134]	251.7 ± 5.2					

[a] MTT assay read after 48 h of incubation [126,131].
[b] MTT assay read after 72 h of incubation time [132–134].
[c] Determined IC_{max}.

Table 29
EC_{50} values [μM] of Re(VII) trioxo compounds and perrhenate tested in different cell lines. The corresponding structures are given in Fig. 31.

Compound [ref.]	Marine bacteria *V. fischeri*	Green algae *R. subcapitata*	aquatic plant *L. minor*	Water flea *D. magna*	AChE [IC_{50}]	Rat cancer cell line IPC-81	Human tumor cell line HepG2
198 [135]	0.275	19.0	14.6	1.58	92.3	100	45.3
199 [135]	0.217	23.8	16.4	2.34	227	44.9	47.3
200 [135]	2.34	115	15.84	402	5600	5000	>6200
201 [135]	>11,000	>1500	420	>2500	>2360	>5150	>5150
202 [128]		59		41	124	194	
203 [128]		6.3		21	38	112.2	
204 [128]		0.096		0.045	9.5	2.5	
205 [128]		146		199	134	1009	

Table 30
Clinical trials involving Re compounds.

Year started	Class of Re Compound	Status	Name of Clinical Trial Project	Condition/ illness	Treatment	Study location/ Organization
2018	Re-bisphosphonate	Recruiting	Rhenium-188-HEDP vs Radium-223-chloride in patients with advanced prostate cancer refractory to hormonal therapy	Prostate cancer metastatic to bone	$^{223}Ra^{188}Re$	VU U Medical Center Amsterdam NL
2013	Re(V)oxo BMEDA-labeled liposomes	Recruiting	Maximum Tolerated Dose, Safety, and Efficacy of Rhenium Nanoliposomes in Recurrent Glioblastoma	GlioblastomaAsrocytoma	^{186}Re-Liposomes	The Cancer Therapy and Research Center at UTHSCSA, San Antonio, Texas, US
2010	Re-SSS Lipiodol	Recruiting	188-Re-SSS Lipiodol to Treat Hepatocellular Carcinomas	Hepatocellular Carcinomas	^{188}Re	Centre Eugene MarquisRennes, France
2017	Re-poly-L-lysine dendrimer	Recruiting	Treatment of non-responding to conventional therapy inoperable liver cancers by in suit introduction of ImDendrim	Liver Cancer	^{188}Re ImDendrim	Tongji University Eastern Hospital, Shanghai, China
2004	Re(V)oxo labeled-peptide	Active – not recruiting	Rhenium Re-188 P2045 in Patients with lung cancer who have received or refused to receive prior chemotherapy	Lung NeoplasmsCarcinoma, Non-Small-Cell LungCarcinoma, Small CellNeoplasm Recurrence, Local	^{188}Re P2045	Iowa City, Iowa, US Baltimore, Maryland, US
2012	Re-sulfide	Active – not recruiting	Multicenter Canadian study to measure the safety and efficacy of radiosynoviorthesis	Arthritis	^{186}Re sulfide	12 locations in Canada
2014	Re(I)MAG_3-labeled MAB	Completed	Bio-distribution study with 186 Re-labeled humanized monoclonal antibody BIWA 4 in patients with adenocarcinoma of the breast	Adenocarcinoma	^{186}Re BIWA 4	
2014	Re(I)MAG_3-labeled MAB	Completed	Bio-distribution study with 186 Re-labeled humanized monoclonal antibody BIWA 4 in patients with non-small cell lung cancer	Carcinoma, non-small-cell lung cancer	^{186}Re hMAB BIWA 4	
2014	Re(I)MAG_3-labeled MAB	Completed	Dose escalation study with 99mTC - or 186 Re-labeled humanized monoclonal antibody (hMAB) BIWA 4 in patients with head and neck cancer	Head and Neck Neoplasms	^{186}Re hMAB BIWA 4	
2008	Colloidal Re sulfur	Completed	Intraoperative gamma camera for breast cancer surgery	Breast cancer,Ductal carcinoma in situ	Test performance of CarollReS camera	CHRU, Hôpital Civil, Service de Gynécologie-obstétriqueStrasbourg, France
2006	Re-sulfur	Completed	Identification of sentinel lymph nodes with methylene blue and isotope	Infiltrative Breast Cancer	^{186}Re sulfur and methylene blue	Service de Gynécologie-Obstétrique, Hôpital CivilStrasbourg, France
2008	Re-colloids	Completed	Added-value of SPECT/CT in patients undergoing LM/SL for gynecological cancers	Cervical CancerVulvar Cancer	^{99m}Tc-cystein rhenium colloids,	375, South Street Hospital - Dpt. of Nuclear MedicineLondon, Ontario, Canada
2014	Re-sulfide	Withdrawn	Diagnosis of micro aspiration in intubated critically Ill patients: Pepsin vs 99 m Technetium	Critical illness	^{99m}Tc-Re sulfide nanocolloid	ICU, Calmette Hospital, University Hospital of LilleLille, France
2014	Re(V)oxo labeled-peptide	Withdrawn	Phase I/II trial of rhenium 188-P2045 in small lung cancer and other advanced neuroendocrine carcinomas	Small Cell Lung Cancer (SCLC) Neuroendocrine (NE) TumorsLarge Cell Neuroendocrine (NE) Tumors	^{188}Re P2045	U Maryland Marlene & Stewart Greenebaum Cancer Center, Baltimore, Maryland, US

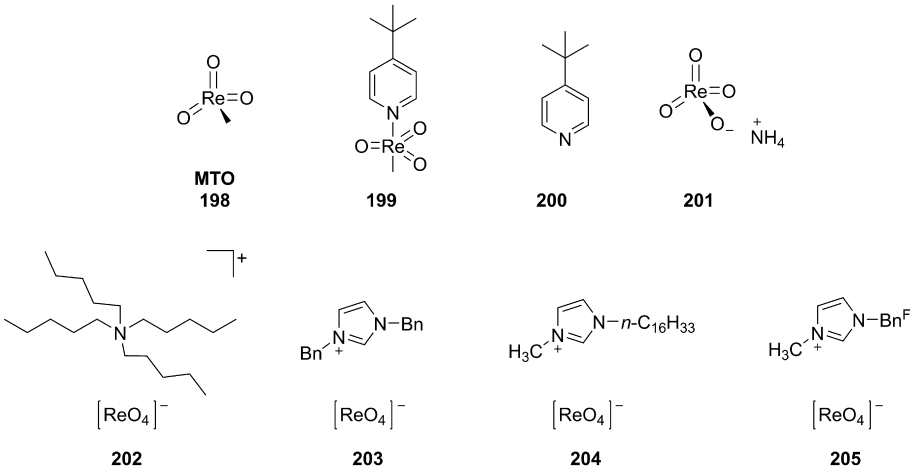

Fig. 31. Structures of Re(VII) trioxo compounds and perrhenate **198–205**. Corresponding IC_{50} values are given in Table 29.

pounds selected for the clinical trials was done, it became clear that many of the Re compounds investigated for potential therapeutic applications were not selected for clinical trials yet. This may suggest that the compounds in clinical trials are potentially more promising, however, since the other compounds are not yet tested in clinical trials, they are still interesting candidates.

At this time, 14 studies are listed on the NIH US National library of Medicine (https://clinicaltrials.gov/, last accessed 27 Nov 2018) and are documented in Table 30 showing that some Re compounds are approaching application in the clinic. The Re compounds investigated in clinical trials make use of the two different radioisotopes ^{188}Re and ^{186}Re, except for three studies. These two radioactive isotopes are suitable for radiopharmaceutical application, because they have β-emissions suitable for killing tumor cells and γ-emission for imaging [161–163]. ^{188}Re can conveniently be produced with high specific activity (high activity per unit mass) from a generator and with a reasonable half-life 16.9 h, an emission maximum energy of 2 MeV and an average energy of 764 keV [161–163]. ^{188}Re has been used to radiolabel peptides for targeted radiotherapy [120,164]. ^{186}Re on the other hand has a longer half-life (90 h) and a lower energy of emission than ^{188}Re. ^{186}Re also has β-emissions, and is produced at high specific activity in a cyclotron or accelerator [165]. Two clinical trials including ^{186}Re based compounds are currently ongoing with others having been completed or recently withdrawn (see Table 30) [165].

The focus of the ^{186}Re labeled nanoliposomes ongoing clinical trial [166] is to determine the maximum tolerated dose, safety and efficacy of ^{186}Re administered in nanoliposomes using brachytherapy for the ultimate use to treatment of recurrent glioblastoma [165]. ^{186}Re, like ^{99m}Tc, is not taken up by the bone and is cleared by the kidney. The energy of the γ-rays produced by ^{186}Re is suitable for external imaging using a gamma camera and the β-emission has suitable energy to penetrate solid tumors up to 2 mm. The 80–100 nm-sized nanoliposome is used as a convection-enhanced delivery system, which is directly injected into the tumor site. The liposome-encapsulated ^{186}Re is thus maintained at the target site and the majority of radiation is released to the tumor tissue making ^{186}Re labeled nanoliposomes desirable as a potential agent for treating glioblastoma [165].

Two other ongoing clinical trials focus on treatment of liver cancers. The use of a ^{188}Re coupled to an imidazole ligand and associated with a dendrimer, referred to as ImDendrim, is investigated to treat previously non-responding inoperable liver cancers [167]. In addition, application of ^{188}Re-SSS Lipiodol (general structure of Re-SSS is given in Fig. 33) is investigated for treatment of patients

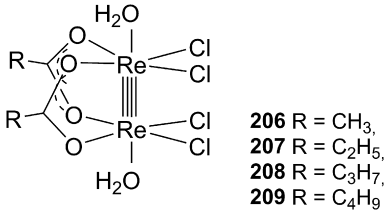

Fig. 32. Dirhenium dicarboxylates showing synergistic effects with cisplatin when encapsulated in liposomes.

with hepatocellular carcinoma. The hepatic intra-arterial administration of the radiolabeled lipiodol could potentially replace the ^{131}I labeled lipiodol, and the results are expected to reduce hospitalization from the current eight days to one day and thus lower costs and improve patient comfort [168].

A Re(V)oxo based compound of recent interest is the Re labeled peptide P2045 (Fig. 33). P2045 is a somatostatin-derived peptide targeting somatostatin receptor overexpressing cancers [161–163]. After the ^{188}Re labeled peptide binds to these receptors, the radioactivity will kill the cancer cells [161–163]. Unfortunately, the Phase I/II clinical trials of the ^{188}Re P2045 to treat patients with advanced small cell lung cancer that has recurred or in patients with advanced neuroendocrine cancers has been withdrawn [171]. However, a related clinical trial remains active involves ^{188}Re labeled P2045 being evaluated in patients with several different lung cancers [172]. The purpose of the study was to determine the safe dose of the compound (Phase II), potentially resulting in a larger Phase III study against the cancer(s) for which this treatment was most effective.

Another study (Phase I/II) that remains active is performed in Canada exploring the potential for a colloid of ^{90}Y citrate or a ^{186}Re sulfide for treatment of persistent active synovectomy [173]. Radiation synovectomy is considered a reliable and easy-to-perform therapy and involves intra-articular injection of β-emitting radionuclides of inflammatory joint disease. In addition, the absence of harmful side effects for the ^{90}Y citrate or ^{186}Re sulfide treatment make these potential alternative treatments to cases that are resistant to systemic therapy and intra-articular corticosteroid injections.

Other Phase I clinical trials recently completed include intravenous administration of ^{186}Re(I) labeled bivatuzumab to investigate the bio-distribution, pharmacokinetics and safety of a ^{186}Re

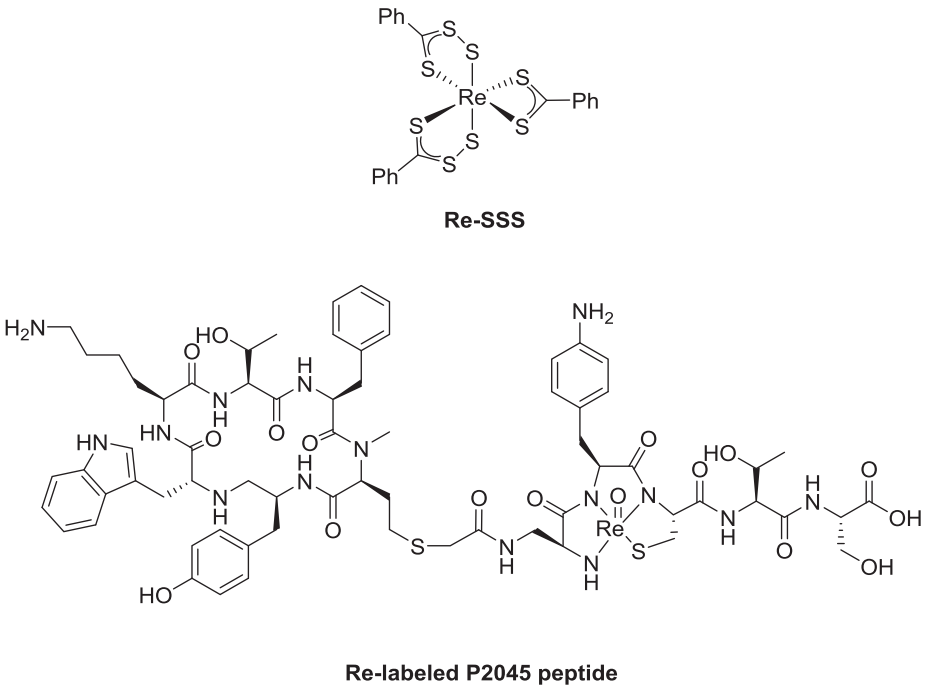

Fig. 33. Structures of Re-SSS and Re labeled P2045 peptide [163,169,170].

(I) labeled antibody in patients with adenocarcinoma of the breast. This represents an example of a Re antibody labeled using the mercaptoacetyltriglycine (MAG_3) chelate [174]. A similar study was also proposed using ^{186}Re(I) labeled bivatuzumab in patients with non-small cell lung cancer.

Finally, Re bisphosphonates and the corresponding ^{99m}Tc analogues are widely studied for their potential theranostics applications in bone metastases. The biological evaluation of this class of compounds is often based on pharmacokinetic and biodistribution studies focusing first on safety and the diagnostic part of the drug. Such studies are not included in the IC_{50}-listing tables. However, bisphosphonates are a prominent class of Re/Tc radiopharmaceuticals, which are currently used in the clinic and thus should be mentioned in this review. These compounds have been known to target bone cancer/metastases for over 30 years and clinical trials are ongoing [175–181]. Specifically, a clinical trial initiated in spring 2018 is currently recruiting patients and involve a combination of ^{223}Ra chloride and ^{188}Re-HEDP treatment. The studied clinical condition is prostate cancer metastatic to the bone. The study plans to involve 402 participants [182]. A detailed review on treatment of bone metastases/cancer has been reported by Finlay *et al.* [183] and the reader is directed there for more details on this topic.

8. Summary of most effective compounds in various cell lines

After the *in vitro* studies carried out on different Re compounds have been summarized in this work, it would be beneficial to compare the effects of the compounds to evaluate their effectiveness both in cell culture and *in vivo*.

In order to compare the results of the *in vitro* studies for evaluation of the most effective compounds and to be able to interpret the effects of the structure on cytotoxicity, the following issues should be considered. First, the different (cancer) cell lines cannot be directly compared since every cell line represents different characteristics, receptors, and surroundings. Although, a particular cell may originate from the same cancer tissue, the main characteristic of cancer cells is their ability to adapt to cytotoxic conditions and survive outside attacks, such as those from the body's immune system. Thus, independent evolution of separately treated cells cannot be excluded and could explain some differences observed in studies. While being aware of these factors, the enclosed data compilation here provides a fast and informative tool to evaluate biological effects of relevant compounds.

Importantly, comparison of IC_{50} values cannot be done across different cell lines, and comparison should be done using the same assay. Accordingly, a radioactive competitive binding assay is hardly comparable to the colorimetric MTT assay; however, both provide IC_{50} values, which can be compared within each assay. Furthermore, when comparing IC_{50} values obtained by the same assay, the cell number/concentration (which is infrequently given in experimental parts) and the incubation time (more frequently given but not always) with the test compound are also crucial factors making both positive and negative controls in the assay system relevant. Moreover, since the determination of the IC_{50} values is dependent on the concentration of the test sample, it is required for the compound to dissolve in the medium or DMSO. Besides solubility, the speciation of the complex and its stability under applied conditions is of great importance. Therefore, the bioprocessing and conversion/metabolism of the initially applied Re complex to other Re-containing species through ligand exchange and/or redox processes (referred to as the speciation of the compound) must be evaluated [184]. If the Re-system in question is not stable, other Re-derivatives will form and they may exert a response. At radiotracer or therapeutic concentrations, the Re-derivative that ultimately forms will be perrhenate due to its high thermodynamic stability. However, depending on the system, other Re intermediates may form before perrhenate is ultimately obtained, whereas all these compounds may have different effects on the cancer cells. Thus, the chemical processes occurring in the cell culture and its medium are critical for what is observed [37,184–186].

Table 31 gives a summary of the most cytotoxic compounds surveyed in this review and serves to summarize the topic that has been reviewed. For convenience of the reader, we have created Fig. 34 that shows the most toxic compounds.

Table 31
Most cytotoxic Re compounds and its IC_{50} values for each cell line.

Cancer cell type	Cell line	Most active compound + IC_{50} value [μM]	Assay + incubation time	Log *P* values
Cervical cancer	HeLa	**52** IC_{50} = 0.106	MTT; no time given	**1.05**
		125 IC_{50} = 0.03	MTT; 24 h after irradiation with $LED_{580\ nm}$	
Ovarian carcinoma cells	A2780	**167** IC_{50} = 0.150	MTT, 72 h	**0.95**
Cisplatin-resistant ovarian carcinoma cells	A2780R	**166** IC_{50} = 0.042	MTT, 72 h	**1.20**
Estrogen-positive breast cancer	MCF-7	**166** IC_{50} = 0.285	MTT, 72 h	**1.20**
Estrogen-negative breast cancer	MDA-MB-231	**97** IC_{50} = 0.248	Resazurin, 72 h	
Mammary epithelial cell line	MCF-10A	**98** IC_{50} = 0.023	Resazurin, 72 h	
Epidermoid carcinoma	A431	**130** IC_{50} = 2.0	MTT, 72 h	
Malignant melanoma	A375	**14** IC_{50} = 12.5	MTT, 72 h	
Lung adenocarcinoma epithelial cells	A549	**167** IC_{50} = 0.15	MTT, 72 h	**0.95**
Cisplatin-resistant lung carcinoma cells	A549cisR	**67e** IC_{50} = 0.75	MTT, 48 h, dark	
Murine lung carcinoma	LLC	**57** IC_{50} = 4.8	WST-1, 24 h	**0.98**
Colon carcinoma cells	HT-29	**166** IC_{50} = 0.085	MTT, 72 h	**1.20**
Pancreatic adenocarcinoma	PT-45	**18** IC_{50} = 25.8	MTT, 72 h	
Hepatocellular liver carcinoma	HepG2	**67b** IC_{50} = 2.1	MTT, 48 h, dark	**3.12**
Murine skin carcinoma	B16	**10** IC_{50} = 9.82	Resazurin, 24 h	
Myelogenous leukemia cell line	K562	**127** IC_{50} = 3.0	MTT, 48 h	
Human acute T lymphoblastic leukemia	MOLT-4	**157** IC_{50} = 1.0	MTT, 24 h	
	MOLT-3	**115** IC_{50} = 3.01	Trypan blue; no time given	
Leukemia monocytic cells	THP-1	**112** IC_{50} = 2.1	Trypan blue; no time given	
Human Osteosarcoma	U2OS	**167** IC_{50} = 0.209	MTT, 72 h	**0.95**
Prostate cancer cells	PC3	**166** IC_{50} = 0.27	MTT, 72 h	**1.20**
Healthy cell type				
Hepatic cells	LO2	**67c** IC_{50} = 3.1	MTT, 48 h	
Embryonic kidney cells expressing mutant SV40 large T antigen	HEK293T	**93** IC_{50} = 2.1	MTT, 48 h	**3.63**
Lung fibroblasts	MRC-5	**167** IC_{50} = 0.709	MTT, 72 h	**0.95**
Fibroblasts (murine)	Fibroblasts (like NIH/3T3)	**93** IC_{50} = 1.8	MTT, 48 h	**3.63**

Most of the compounds listed in Table 31 are organometallic Re (I) complexes, but there are also two Re(V)oxo complexes (**166** and **167**). The first part of the table lists different cancer cell lines and the corresponding most cytotoxic compounds. It has to be noted that the cell lines listed are those used in the studies reported and not necessarily the most suitable cell line to use to study a specific form of cancer. Cell culture studies will provide information on cytotoxicity but results and interpretation will depend in part on the cell line chosen. Cell culture studies provide some data, which allows for analysis of effects prior to embarking on more expensive and demanding *in vivo* studies. The second part of Table 31 contains a few different non-cancerous cell lines and the effects of Re compounds on these systems. A comparative evaluation of the compounds in healthy cells provides insight into the compounds' toxicity for healthy cells and therefore the possibility of side effects. Thus, the compounds having the lowest IC_{50} values in healthy cells, namely **67c**, **93** and **167**, are possibly too toxic for *in vivo* applications, although only the performance of *in vivo* experiments will demonstrate how toxic the compounds are. However, in the case of the Re(V)oxo complex **167** (IC_{50} = 0.709 in MRC-5 lung fibroblasts) no weight loss or other signs of toxicity was observed when administered to mice [116]. This important finding was addressed in the *in vivo* studies of these compounds countering the expectations that they would be toxic to healthy cells.

Phenyl-phenanthroline ligands, as used for Re(V)oxo coordination complexes **166** and **167**, are also used for Re(I) carbonyl organometallic complexes, like **67b**, **67c**, **67e**, **75**, **87**, **88** and **97**, which all have comparable IC_{50} values of 0.3 to 5 μM in HeLa, MCF7 or A549 cells, respectively (see Tables 24, 12, 13, and 16). Therefore, these phenanthroline based ligands were found to stabilize Re in different oxidation states, like Re(I), Re(V) and Re(VII)O_3, however, the latter was not tested for its IC_{50} value in different cell lines but in antibacterial assays, showing a certain amount of antibacterial activity. Therefore, it would appear that complexes with this ligand are very promising for the development of biologically highly active Re complexes. However, the toxicity of these complexes should not be considered without examining the phenanthroline ligands alone, as it is well-known that the phenanthroline ligand by itself is cytotoxic [187]. In this case, the stability and speciation of the compounds become very important in determining if the phenanthroline dissociates [184–186,188]. If so, the observed toxicity of these metal complexes are much less interesting and promising, because the likelihood that such systems would be further developed is very low.

Most of the compounds shown in Fig. 34 contain the $Re(I)(CO)_3^+$ unit. This demonstrates that most of potent effects have been observed with organometallic Re compounds. Furthermore, in large parts of the cell lines listed in Table 31, the more active Re complexes are coordinated to phenanthroline-based ligands. Moreover, **166** and **167** represent the most active compounds reviewed in here, as they display the highest activity in 7 out of 21 different cancer cell lines listed in Table 31. Investigations on the mechanism of action of these compounds suggest, among other characterized effects, a necroptotic cell death with mitochondrial damage. This is supported by a log P value between 0 and +5, which is consistent with mitochondrial accumulation. The determined log P values are 1.2 and 0.95 for compounds **166** and **167**, respectively (see Table 31). Mitochondria are essential for energy production in eukaryotic cells and therefore their survival. In addition, they regulate intrinsic pathways leading to apoptosis, necroptosis and non-apoptotic cell death. Consequently, the mitochondria regulate fundamental functions in healthy and cancerous cells. Therefore, it is not surprising that attributes of cancer cells like excessive proliferation are linked to mitochondrial dysfunction and that anticancer research is developing mitochondria-targeting compounds [189].

It is often observed that the higher the lipophilicity (positive log P value) of the compounds, the lower the IC_{50} value will be (see

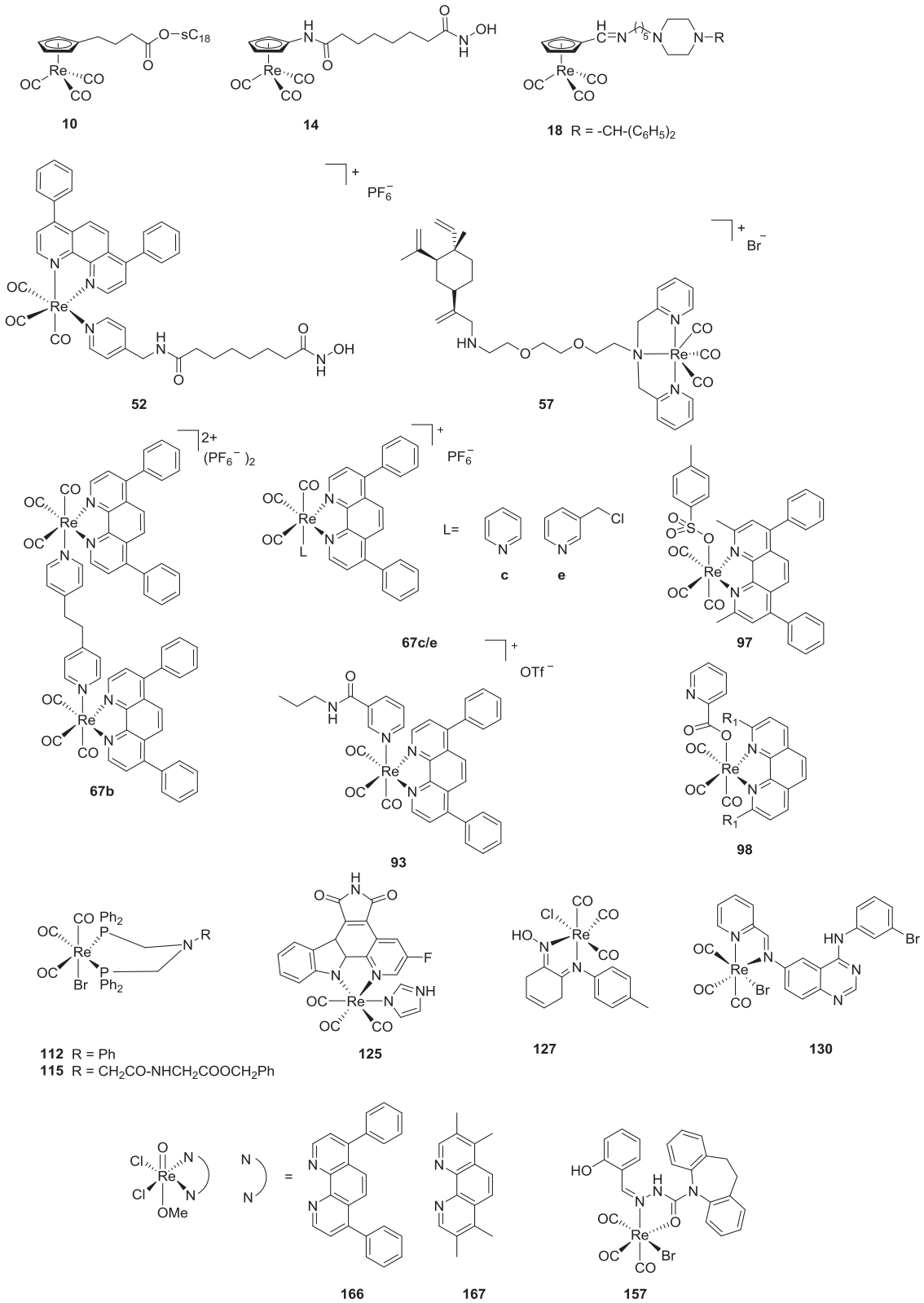

Fig. 34. Summary of the most cytotoxic compounds. Corresponding IC_{50} values are listed in Table 31.

Table 31). Nevertheless, an increased lipophilicity may lead to decreased solubility, enhanced liver uptake and may cause lower clearance from non-target tissues. However, the activity is also highly dependent on cellular uptake, molecular size, charge, and therefore speciation [184–186,188]. Even small changes in the constitution of the compounds can have a big influence, as it is shown for the compounds in Tables 12, 20 and 22. Accordingly, the complexes listed in Table 22 show formation of dimers in solution after loss of ancillary coordinated bromide, which results in increased lipophilicity and cytotoxicity. These results are supported by previ-

ous reports documenting that the speciation involved plays an important role, because any bioprocessing of the administered drug can affect uptake [185]. A possible explanation for increased cytotoxicity by such small molecular changes might be the increase in lipophilicity, and this is certainly the case for the compounds in Table 16. However, a good systematic study of the cytotoxicity of different $(CO)_3Re(I)$ compounds in ASCP-1 pancreatic cells show that a greater influence is observed by the exchange of the ancillary ligand. An increase in cytotoxicity was shown in the order Br < NCS < Cl < I in cancer cells. The order changed to Cl ≈ Br < I < NCS in healthy cells (see Tables 19 and 20). Furthermore, for Re(V)oxo compounds, similar observations were made by evaluating different structurally related ligands indicating that chelating ligands increase the stability, leading to a decrease in cytotoxicity (see Table 25). Therefore, for the development of potent cytotoxic compounds, the right balance between stability and lability as well as lipophilicity and hydrophilicity must be found.

Although $(CO)_3Re(I)$ complexes have been extensively studied in recent years, there are only a limited number of Re complexes that are studied *in vivo*. The reviewed *in vivo* studies include two studies on Re(I) tricarbonyl compounds, one study dealing with dirhenium(III) complexes encapsulated in liposomes, one study performed on Re(V)oxo complexes, two studies on hexarhenium cluster compounds and one on NIS addressing $^{188}ReO_4^-$.

Re compounds, which are currently in or have previously been in clinical trials include Re-bisphosphonates, Re-labeled liposomes, Re-peptide or Re-protein complexes, Re-sulfide material and Re(V) oxo complexes. The analysis shown in this work points to the fact that the organometallic $Re(I)(CO)_3$-containing compounds, particularly those with phenanthroline ligands, are particularly potent in cell culture work. However, none of these compounds made it to clinical trials. Some studies indicate, that this might be due to the high toxicity of the phenanthroline ligand, however, in other cases, *in vivo* studies have been done suggesting that the toxicity is not great for these systems.

9. Conclusions

The development of potent anticancer agents starts with the selection of compounds based on their *in vitro* activity. This is commonly evaluated by the effect of the compounds on the growth of appropriate cell lines and determination of the half-maximal inhibitory concentration (IC_{50}) after treatment with a test compound. Making use of results obtained by this method, this review focuses on the cytotoxicity of Re compounds classified by their oxidation state in order to identify the most cytotoxic Re complexes. In addition to providing IC_{50} data, this review also highlighted correlations and basic information on the systems and (if available) modes of action. Furthermore, the few *in vivo* studies reported for non-radioactive Re complexes are reviewed. Finally, the most cytotoxic Re compounds reported are compared to the classes of compounds that have made it to the 14 clinical trials, some of which are currently active while others have been completed. The compounds that have or are in clinical trials include Re-bisphosphonates, Re labeled liposomes, Re-peptides or Re-protein complexes, Re-sulfide materials and Re(V)oxo complexes. Surprisingly, no $(CO)_3Re(I)$ compounds have made it to clinical trials. Considering that this class of Re compounds is the one most frequently studied in cell culture, might be to expect that at least some one of these compounds would have been considered for human studies. As described in this review, the reasons for such discrepancy can be attributed to the toxicity on healthy cells, bioprocessing, compound stability, toxicity of the ligand itself or many other factors. However, this review demonstrates that the area of Re chemistry is of growing interest in medicine and provides guidelines for future applications.

Acknowledgments

EBB thanks the TUM Graduate School of Chemistry for financial support and AAH thanks Colorado State University. DCC and FEK thank the Bavarian State Ministry of Education, Science and the Arts for funding the Technische Universität München Visiting Professor Program given to DCC. DCC thanks the NSF (CHE-1709564) and The Arthur C. Cope Foundation, administered by the American Chemical Society for partial support.

Declaration of interest

None.

References

[1] R.L. Siegel, K.D. Miller, A. Jemal, CA-Cancer J. Clin. 68 (2018) 7–30.
[2] V.T. DeVita, S.A. Rosenberg, New Engl. J. Med. 366 (2012) 2207–2214.
[3] P.G. Corrie, Medicine 36 (2008) 24–28.
[4] D.-W. Shen, L.M. Pouliot, M.D. Hall, M.M. Gottesman, Pharmacol. Rev. 64 (2012) 706–721.
[5] R. Schibli, A.P. Schubiger, Eur. J. Nucl. Med. Mol. Imaging 29 (2002) 1529–1542.
[6] M. Frier, Mini-Rev. Med. Chem. 4 (2004) 61–68.
[7] F. Tisato, C. Bolzati, M. Porchia, F. Refosco, Mass Spectrom. Rev. 23 (2004) 309–332.
[8] U. Abram, R. Alberto, J. Brazil. Chem. Soc. 17 (2006) 1486–1500.
[9] G. Ferro-Flores, C.A. de Murphy, Adv. Drug Deliver. Rev. 60 (2008) 1389–1401.
[10] E.M. Hahn, A. Casini, F.E. Kühn, Coord. Chem. Rev. 276 (2014) 97–111.
[11] S. Jürgens, W.A. Herrmann, F.E. Kühn, J. Organomet. Chem. 751 (2014) 83–89.
[12] A. Boschi, P. Martini, L. Uccelli, Pharmaceuticals 10 (2017) 12.
[13] K.K.W. Lo, Acc. Chem. Res. 48 (2015) 2985–2995.
[14] S. Hostachy, C. Policar, N. Delsuc, Coord. Chem. Rev. 351 (2017) 172–188.
[15] A.M.H. Yip, K.K.W. Lo, Coord. Chem. Rev. 361 (2018) 138–163.
[16] A.G. Mayor, X. Gómez-Olivé, J.J. Aponte, S. Casimiro, S. Mabunda, M. Dgedge, A. Barreto, P.L. Alonso, J. Infect. Dis. 183 (2001) 1413–1416.
[17] A. Coleman, C. Brennan, J.G. Vos, M.T. Pryce, Coord. Chem. Rev. 252 (2008) 2585–2595.
[18] D. Gupta, M. Sathiyendiran, ChemistrySelect 3 (2018) 7439–7458.
[19] A. Leonidova, G. Gasser, A.C.S. Chem. Biol. 9 (2014) 2180–2193.
[20] W. Noddack, I. Tacke, O. Berg, Naturwissenschaften 13 (1925) 567.
[21] J.-C. Carlen, B.D. Bryskin, Mater. Manuf. Processes 9 (1994) 1087–1104.
[22] M. Fleischer, Econ. Geol. 54 (1959) 1406–1413.
[23] S. Liu, Chem. Soc. Rev. 33 (2004) 445–461.
[24] D.E. Polyak, 2015 Minerals Yearbook: Rhenium, United States Geological Survey, 2015.
[25] C.D. Anderson, P. Taylor, C.G. Anderson, Miner. Metall. Process 30 (2013) 59–73.
[26] A.D. Dobrzańska-Danikiewicz, W. Wolany, Arch. Mater. Sci. Eng. 82 (2016) 70–78.
[27] J.W. Kück, R.M. Reich, F.E. Kühn, Chem. Rec. 16 (2016) 349–364.
[28] C.C. Romão, F.E. Kühn, W.A. Herrmann, Chem. Rev. 97 (1997) 3197–3246.
[29] E. Deutsch, K. Libson, J.-L. Vanderheyden, A.R. Ketring, H.R. Maxon, Int. J. Rad. Appl. Instrum. B 13 (1986) 465–477.
[30] Y. He, Q. Zhu, M. Chen, Q. Huang, W. Wang, Q. Li, Y. Huang, W. Di, Oncotarget 7 (2016) 70803–70821.
[31] W. Li, J. Zhou, Y. Xu, Biomed. Rep. 3 (2015) 617–620.
[32] T.L. Riss, R.A. Moravec, A.L. Niles, S. Duellman, H.A. Benink, T.J. Worzella, L. Minor, Assay Guidance Manual (2016).
[33] J. O'Brien, I. Wilson, T. Orton, F. Pognan, Eur. J. Biochem. 267 (2000) 5421–5426.
[34] L. Śliwka, K. Wiktorska, P. Suchocki, M. Milczarek, S. Mielczarek, K. Lubelska, T. Cierpiał, P. Łyżwa, P. Kiełbasiński, A. Jaromin, PloS one 11 (2016) e0155772.
[35] R. Roskoski, Assays of protein kinase, Methods Enzymol., Elsevier (1983) 3–6.
[36] M.T. Makler, J.M. Ries, J.A. Williams, J.E. Bancroft, R.C. Piper, B.L. Gibbins, D.J. Hinrichs, Am. J. Trop. Med. Hyg. 48 (1993) 739–741.
[37] A.A. Haase, E.B. Bauer, F.E. Kühn, D.C. Crans, Coord. Chem. Rev. (2019), in press.
[38] D.A. Volpe, S.S. Hamed, L.K. Zhang, The AAPS Journal 16 (2014) 172–180.
[39] J.L. Sebaugh, Pharm. Stat. 10 (2011) 128–134.
[40] W. Hieber, H. Fuchs, Z. Anorg. Allg. Chem. 248 (1941) 269–275.
[41] Y.K. Yan, S.E. Cho, K.A. Shaffer, J.E. Rowell, B.J. Barnes, I.H. Hall, Pharm. 55 (2000) 307–313.
[42] R.G. Pearson, J. Am. Chem. Soc. 85 (1963) 3533–3539.
[43] B. Safi, J. Mertens, F. De Proft, P. Geerlings, J. Phys. Chem. A 110 (2006) 9240–9246.

[44] J. Oyarzo, A. Acuna, H. Klahn, R. Arancibia, C.P. Silva, R. Bosque, C. Lopez, M. Font-Bardia, C. Calvis, R. Messeguer, Dalton Trans. 47 (2018) 1635–1649.
[45] K. Kowalski, Ł. Szczupak, S. Saloman, D. Steverding, A. Jabłoński, V. Vrček, A. Hildebrandt, H. Lang, A. Rybarczyk-Pirek, ChemPlusChem 82 (2017) 303–314.
[46] R. Arancibia, F. Dubar, B. Pradines, I. Forfar, D. Dive, A.H. Klahn, C. Biot, Bioorg. Med. Chem. 18 (2010) 8085–8091.
[47] L. Glans, W.N. Hu, C. Jost, C. de Kock, P.J. Smith, M. Haukka, H. Bruhn, U. Schatzschneider, E. Nordlander, Dalton Trans. 41 (2012) 6443–6450.
[48] W. Hu, K. Splith, I. Neundorf, K. Merz, U. Schatzschneider, J. Biol. Inorg. Chem. 17 (2012) 175–185.
[49] D. Can, H.W. Peindy N'Dongo, B. Spingler, P. Schmutz, P. Raposinho, I. Santos, R. Alberto, Chem. Biodivers. 9 (2012) 1849–1866.
[50] M. Munoz-Osses, F. Godoy, A. Fierro, A. Gomez, N. Metzler-Nolte, Dalton Trans. 47 (2018) 1233–1242.
[51] D. Rosita, M.A. Dewit, L.G. Luyt, J. Med. Chem. 52 (2009) 2196–2203.
[52] C. Concha, C. Quintana, A.H. Klahn, V. Artigas, M. Fuentealba, C. Biot, I. Halloum, L. Kremer, R. López, J. Romanos, Y. Huentupil, R. Arancibia, Polyhedron 131 (2017) 40–45.
[53] A. Kondratskyi, K. Kondratska, F. Vanden Abeele, D. Gordienko, C. Dubois, R.-A. Toillon, C. Slomianny, S. Lemière, P. Delcourt, E. Dewailly, R. Skryma, C. Biot, N. Prevarskaya, Sci. Rep. 7 (2017) 15896.
[54] K. Splith, I. Neundorf, W. Hu, H.W.P. N'Dongo, V. Vasylyeva, K. Merz, U. Schatzschneider, Dalton Trans. 39 (2010) 2536–2545.
[55] G. Jaouen, S. Top, A. Vessieres, G. Leclercq, M.J. McGlinchey, Curr. Med. Chem. 11 (2004) 2505–2517.
[56] G. Jaouen, S. Top, A. Vessieres, P. Pigeon, G. Leclercq, I. Laios, Chem. Commun. (2001) 383–384.
[57] S. Top, A. Vessieres, P. Pigeon, M.N. Rager, M. Huche, E. Salomon, C. Cabestaing, J. Vaissermann, G. Jaouen, ChemBioChem 5 (2004) 1104–1113.
[58] I. Paterni, C. Granchi, J.A. Katzenellenbogen, F. Minutolo, Steroids 90 (2014) 13–29.
[59] A. Vessieres, S. Top, W. Beck, E. Hillard, G. Jaouen, Dalton Trans. (2006) 529–541.
[60] M. Patra, M. Wenzel, P. Prochnow, V. Pierroz, G. Gasser, J.E. Bandow, N. Metzler-Nolte, Chem. Sci. 6 (2015) 214–224.
[61] L. Quental, P. Raposinho, F. Mendes, I. Santos, C. Navarro-Ranninger, A. Alvarez-Valdes, H.Y. Huang, H. Chao, R. Rubbiani, G. Gasser, A.G. Quiroga, A. Paulo, Dalton Trans. 46 (2017) 14523–14536.
[62] S. Imstepf, V. Pierroz, P. Raposinho, M. Bauwens, M. Felber, T. Fox, A.B. Shapiro, R. Freudenberg, C. Fernandes, S. Gama, G. Gasser, F. Motthagy, I.R. Santos, R. Alberto, Bioconj. Chem. 26 (2015) 2397–2407.
[63] S. Imstepf, V. Pierroz, P. Raposinho, M. Felber, T. Fox, C. Fernandes, G. Gasser, I. R. Santos, R. Alberto, Dalton Trans. 45 (2016) 13025–13033.
[64] S. Imstepf, V. Pierroz, R. Rubbiani, M. Felber, T. Fox, G. Gasser, R. Alberto, Angew. Chem. Int. Ed. 55 (2016) 2792–2795.
[65] A. Leonidova, V. Pierroz, R. Rubbiani, J. Heier, S. Ferrari, G. Gasser, Dalton Trans. 43 (2014) 4287–4294.
[66] A. Leonidova, V. Pierroz, R. Rubbiani, Y. Lan, A.G. Schmitz, A. Kaech, R.K.O. Sigel, S. Ferrari, G. Gasser, Chem. Sci. 5 (2014) 4044–4056.
[67] T. Joshi, G. Gasser, Synlett 26 (2015) 275–284.
[68] G. Santoro, T. Zlateva, A. Ruggi, L. Quaroni, F. Zobi, Dalton Trans. 44 (2015) 6999–7008.
[69] K.M. Knopf, B.L. Murphy, S.N. MacMillan, J.M. Baskin, M.P. Barr, E. Boros, J.J. Wilson, J. Am. Chem. Soc. 139 (2017) 14302–14314.
[70] A. Luengo, V. Fernández-Moreira, I. Marzo, M.C. Gimeno, Inorg. Chem. 56 (2017) 15159–15170.
[71] I. Maisuls, E. Wolcan, O.E. Piro, E.E. Castellano, G. Petroselli, R. Erra-Balsells, F. M. Cabrerizo, G.T. Ruiz, ChemistrySelect 2 (2017) 8666–8672.
[72] R.-R. Ye, C.-P. Tan, Y.-N. Lin, L.-N. Ji, Z.-W. Mao, Chem. Commun. 51 (2015) 8353–8356.
[73] G. Mion, T. Gianferrara, A. Bergamo, G. Gasser, V. Pierroz, R. Rubbiani, R. Vilar, A. Leczkowska, E. Alessio, ChemMedChem 10 (2015) 1901–1914.
[74] Y. Ren, K. Cheng, G. Liu, Y. Sun, Y. Shen, Acta Chim. Sincia 66 (2008) 459.
[75] S. Clède, F. Lambert, R. Saint-Fort, M.A. Plamont, H. Bertrand, A. Vessières, C. Policar, Chem. Eur. J. 20 (2014) 8714–8722.
[76] A.W.-T. Choi, H.-W. Liu, K.K.-W. Lo, J. Inorg. Biochem. 148 (2015) 2–10.
[77] M. Strack, A. Bedini, K.T. Yip, S. Lombardi, D. Siegmund, R. Stoll, S.M. Spampinato, N. Metzler-Nolte, Chem. Eur. J. 22 (2016) 14605–14610.
[78] J. Yang, J.-X. Zhao, Q. Cao, L. Hao, D. Zhou, Z. Gan, L.-N. Ji, Z.-W. Mao, A.C.S. Appl. Mater. Interfaces 9 (2017) 13900–13912.
[79] R.R. Ye, C.P. Tan, M.H. Chen, L. Hao, L.N. Ji, Z.W. Mao, Chem. Eur. J. 22 (2016) 7800–7809.
[80] J. Yang, Q. Cao, H. Zhang, L. Hao, D. Zhou, Z. Gan, Z. Li, Y.-X. Tong, L.-N. Ji, Z.-W. Mao, Biomaterials 176 (2018) 94–105.
[81] I. Kitanovic, S.Z. Can, H. Alborzinia, A. Kitanovic, V. Pierroz, A. Leonidova, A. Pinto, B. Spingler, S. Ferrari, R. Molteni, A. Steffen, N. Metzler-Nolte, S. Wolfl, G. Gasser, Chem. Eur. J. 20 (2014) 2496–2507.
[82] C. Redshaw, S. Watkins, S.M. Humphrey, P.C.B. Page, S. Ashby, Y.M. Chao, C.J. Herbert, A. Mueller, RSC Advances 3 (2013) 23963–23966.
[83] A. Leonidova, V. Pierroz, L.A. Adams, N. Barlow, S. Ferrari, B. Graham, G. Gasser, A.C.S. Med. Chem. Lett. 5 (2014) 809–814.
[84] M.W. Louie, H.W. Liu, M.H.C. Lam, Y.W. Lam, K.K.W. Lo, Chem. Eur. J. 17 (2011) 8304–8308.
[85] M.-W. Louie, T.T.-H. Fong, K.K.-W. Lo, Inorg. Chem. 50 (2011) 9465–9471.
[86] A.W.T. Choi, M.W. Louie, S.P.Y. Li, H.W. Liu, B.T.N. Chan, T.C.Y. Lam, A.C.C. Lin, S.H. Cheng, K.K.W. Lo, Inorg. Chem. 51 (2012) 13289–13302.
[87] K. Yin Zhang, K. Ka-Shun Tso, M.-W. Louie, H.-W. Liu, K. Kam-Wing Lo, Organometallics 32 (2013) 5098–5102.
[88] L.C.-C. Lee, K.-K. Leung, K.K.-W. Lo, Dalton Trans. 46 (2017) 16357–16380.
[89] F.F. Zhong, X.L. Yuan, J.Z. Zhao, Q. Wang, Sci. China Chem. 59 (2016) 70–77.
[90] G. Balakrishnan, T. Rajendran, K. Senthil Murugan, M. Sathish Kumar, V.K. Sivasubramanian, M. Ganesan, A. Mahesh, T. Thirunalasundari, S. Rajagopal, Inorg. Chim. Acta 434 (2015) 51–59.
[91] P.T. Wilder, D.J. Weber, A. Winstead, S. Parnell, T.V. Hinton, M. Stevenson, D. Giri, S. Azemati, P. Olczak, B.V. Powell, T. Odebode, S. Tadesse, Y.C. Zhang, S.K. Pramanik, J.M. Wachira, S. Ghimire, P. McCarthy, A. Barfield, H.N. Banerjee, C. Chen, J.A. Golen, A.L. Rheingold, J.A. Krause, D.M. Ho, P.Y. Zavalij, R. Shaw, S.K. Mandal, Mol. Cell. Biochem. 441 (2018) 151–163.
[92] J. Zhang, J.J. Vittal, W. Henderson, J.R. Wheaton, I.H. Hall, T.S.A. Hor, Y.K. Yan, J. Organomet. Chem. 650 (2002) 123–132.
[93] W. Wang, Y.K. Yan, T.S. Andy Hor, J.J. Vittal, J.R. Wheaton, I.H. Hall, Polyhedron 21 (2002) 1991–1999.
[94] K. Wähler, A. Ludewig, P. Szabo, K. Harms, E. Meggers, Eur. J. Inorg. Chem. 2014 (2014) 807–811.
[95] S. Wirth, A.U. Wallek, A. Zernickel, F. Feil, M. Sztiller-Sikorska, K. Lesiak-Mieczkowska, C. Brauchle, I.P. Lorenz, M. Czyz, J. Inorg. Biochem. 104 (2010) 774–789.
[96] A. Bourkoula, M. Paravatou-Petsotas, A. Papadopoulos, I. Santos, H.-J. Pietzsch, E. Livaniou, M. Pelecanou, M. Papadopoulos, I. Pirmettis, Eur. J. Med. Chem. 44 (2009) 4021–4027.
[97] K. Lyczko, M. Lyczko, S. Meczynska-Wielgosz, M. Kruszewski, J. Mieczkowski, J. Organomet. Chem. 866 (2018) 59–71.
[98] S.C. Marker, S.N. MacMillan, W.R. Zipfel, Z. Li, P.C. Ford, J.J. Wilson, Inorg. Chem. 57 (2018) 1311–1331.
[99] D.-L. Ma, C.-M. Che, F.-M. Siu, M. Yang, K.-Y. Wong, Inorg. Chem. 46 (2007) 740–749.
[100] N. Margiotta, N. Denora, S. Piccinonna, V. Laquintana, F.M. Lasorsa, M. Franco, G. Natile, Dalton Trans. 43 (2014) 16252–16264.
[101] N. Denora, R.M. Iacobazzi, G. Natile, N. Margiotta, Coord. Chem. Rev. 341 (2017) 1–18.
[102] R. Govindarajan, R. Nagarajaprakash, V. Veena, N. Sakthivel, B. Manimaran, Polyhedron 139 (2018) 229–236.
[103] C.A. Kumar, R. Nagarajaprakash, W. Victoria, V. Veena, N. Sakthivel, B. Manimaran, Inorg. Chem. Commun. 64 (2016) 39–44.
[104] B. Ramakrishna, R. Nagarajaprakash, V. Veena, N. Sakthivel, B. Manimaran, Dalton Trans. 44 (2015) 17629–17638.
[105] A. Kermagoret, G. Morgant, J. d'Angelo, A. Tomas, P. Roussel, G. Bastian, P. Collery, D. Desmaele, Polyhedron 30 (2011) 347–353.
[106] P. Collery, A. Mohsen, A. Kermagoret, S. Corre, G. Bastian, A. Tomas, M. Wei, F. Santoni, N. Guerra, D. Desmaële, J. d'Angelo, Invest. New Drugs 33 (2015) 848–860.
[107] J.M. Ho, W.Y. Lee, K.J.T. Koh, P.P.F. Lee, Y.K. Yan, J. Inorg. Biochem. 119 (2013) 10–20.
[108] M.L. Low, G. Paulus, P. Dorlet, R. Guillot, R. Rosli, N. Delsuc, K.A. Crouse, C. Policar, Biometals 28 (2015) 553–566.
[109] E. Rodríguez Arce, I. Machado, B. Rodríguez, M. Lapier, M.C. Zúñiga, J.D. Maya, C. Olea Azar, L. Otero, D. Gambino, J. Inorg. Biochem. 170 (2017) 125–133.
[110] P.V. Simpson, I. Casari, S. Paternoster, B.W. Skelton, M. Falasca, M. Massi, Chem. Eur. J. 23 (2017) 6518–6521.
[111] S. Seifert, J.U. Künstler, E. Schiller, H.J. Pietzsch, B. Pawelke, R. Bergmann, H. Spies, Bioconjugate Chem. 15 (2004) 856–863.
[112] J. Martinez-Lillo, T.F. Mastropietro, R. Lappano, A. Madeo, M.E. Alberto, N. Russo, M. Maggiolini, G. De Munno, Chem. Commun. 47 (2011) 5283–5285.
[113] T.B.Y. Nguyen, C.T. Pham, T.N. Trieu, U. Abram, H.H. Nguyen, Polyhedron 96 (2015) 66–70.
[114] A. Maalaoui, O.B. Said, S.T. Akriche, S.S. Al-Deyab, M. Rzaigui, Z. Naturforsch. B. 67 (2012) 1178–1184.
[115] A. Davison, C. Orvig, H.S. Trop, M. Sohn, B.V. DePamphilis, A.G. Jones, Inorg. Chem. 19 (1980) 1988–1992.
[116] K. Suntharalingam, S.G. Awuah, P.M. Bruno, T.C. Johnstone, F. Wang, W. Lin, Y.-R. Zheng, J.E. Page, M.T. Hemann, S.J. Lippard, J. Am. Chem. Soc. 137 (2015) 2967–2974.
[117] P.I.d.S. Maia, H.H. Nguyen, A. Hagenbach, S. Bergemann, R. Gust, V.M. Deflon, U. Abram, Dalton Trans. 42 (2013) 5111–5121.
[118] B. Johannsen, M. Scheunemann, H. Spies, P. Brust, J. Wober, R. Syhre, H.J. Pietzsch, Nucl. Med. Biol. 23 (1996) 429–438.
[119] D.W. Demoin, A.N. Dame, W.D. Minard, F. Gallazzi, G.L. Seickman, T.L. Rold, N. Bernskoetter, M.E. Fassbender, T.J. Hoffman, C.A. Deakyne, S.S. Jurisson, Nucl. Med. Biol. 43 (2016) 802–811.
[120] C.J. Smith, G.L. Sieckman, N.K. Owen, D.L. Hayes, D.G. Mazuru, W.A. Volkert, T. J. Hoffman, Anticancer Res. 23 (2003) 63–70.
[121] Y. Barda, N. Cohen, V. Lev, N. Ben-Aroya, Y. Koch, E. Mishani, M. Fridkin, C. Gilon, Nucl. Med. Biol. 31 (2004) 921–933.
[122] A. Cappelli, A. Mancini, F. Sudati, S. Valenti, M. Anzini, S. Belloli, R.M. Moresco, M. Matarrese, M. Vaghi, A. Fabro, F. Fazio, S. Vomero, Bioconjugate Chem. 19 (2008) 1143–1153.
[123] C. Fernandes, I.C. Santos, I. Santos, H.J. Pietzsch, J.U. Kunstler, W. Kraus, A. Rey, N. Margaritis, A. Bourkoula, A. Chiotellis, M. Paravatou-Pestsotas, I. Pirmettis, Dalton Trans. (2008) 3215–3225.
[124] Y. Li, L. Ma, V. Gaddam, F. Gallazzi, H.M. Hennkens, M. Harmata, M.R. Lewis, C. A. Deakyne, S.S. Jurisson, Inorg. Chem. 55 (2016) 1124–1133.

[125] A.A. Krasilnikova, A.O. Solovieva, A.A. Ivanov, K.E. Trifonova, T.N. Pozmogova, A.R. Tsygankova, A.I. Smolentsev, E.I. Kretov, D.S. Sergeevichev, M.A. Shestopalov, Y.V. Mironov, A.M. Shestopalov, A.F. Poveshchenko, L.V. Shestopalova, Nanomedicine: NBM 13 (2017) 755–763.
[126] A.O. Solovieva, K. Kirakci, A.A. Ivanov, P. Kubat, T.N. Poznaogova, S.M. Miroshnichenko, E.V. Vorontsova, A.V. Chechushkov, K.E. Trifonova, M.S. Fufaeva, E.I. Kretov, Y.V. Mironov, A.F. Poveshchenko, K. Lang, M.A. Shestopalov, Inorg. Chem. 56 (2017) 13491–13499.
[127] M. Cokoja, M. Markiewicz, S. Stolte, F.E. Kühn, Toxicity Assessment of Molecular Rhenium(VII) Epoxidation Catalysts, Encycl. Inorg. Bioinorg. Chem. (2016).
[128] H.B.T. Thu, M. Markiewicz, J. Thöming, R.M. Reich, V. Korinth, M. Cokoja, F.E. Kühn, S. Stolte, New J. Chem. 39 (2015) 5431–5436.
[129] R.I. Eggen, R. Behra, P. Burkhardt-Holm, B.I. Escher, N. Schweigert, Environ. Sci. Technol. 38 (2004) 58a–64a.
[130] I. Pastan, D. Fitzgerald, Science 254 (1991) 1173–1177.
[131] A.A. Krasilnikova, M.A. Shestopalov, K.A. Brylev, I.A. Kirilova, O.P. Khripko, K. E. Zubareva, Y.I. Khripko, V.T. Podorognaya, L.V. Shestopalova, V.E. Fedorov, Y. V. Mironov, J. Inorg. Biochem. 144 (2015) 13–17.
[132] M.A. Shestopalov, K.E. Zubareva, O.P. Khripko, Y.I. Khripko, A.O. Solovieva, N. V. Kuratieva, Y.V. Mironov, N. Kitamura, V.E. Fedorov, K.A. Brylev, Inorg. Chem. 53 (2014) 9006–9013.
[133] C. Echeverria, A. Becerra, F. Nunez-Villena, A. Munoz-Castro, J. Stehberg, Z. Zheng, R. Arratia-Perez, F. Simon, R. Ramirez-Tagle, New J. Chem. 36 (2012) 927–932.
[134] S.J. Choi, K.A. Brylev, J.Z. Xu, Y.V. Mironov, V.E. Fedorov, Y.S. Sohn, S.J. Kim, J.H. Choy, J. Inorg. Biochem. 102 (2008) 1991–1996.
[135] S. Stolte, H.T.T. Bui, S. Steudte, V. Korinth, J. Arning, A. Bialk-Bielinska, U. Bottin-Weber, M. Cokoja, A. Hahlbrock, V. Fetz, R. Stauber, B. Jastorff, C. Hartmann, R.W. Fischer, F.E. Kühn, Green Chem. 17 (2015) 1136–1144.
[136] N. Shtemenko, P. Collery, A. Shtemenko, Anticancer Res. 27 (2007) 2487–2492.
[137] P.J. Blower, Int. J. Nucl. Med. Res. 4 (2017) 39–53.
[138] E. Boros, A.B. Packard, Chem. Rev. (2018).
[139] C.C. Konkankit, S.C. Marker, K.M. Knopf, J.J. Wilson, Dalton Trans. 47 (2018) 9934–9974.
[140] R. Alberto, R. Schibli, U. Abram, A. Egli, F.F. Knapp, P.A. Schubiger, Radiochim. Acta 79 (1997) 99–103.
[141] J.D.G. Correia, I. Santos, R. Alberto, K. Ortner, H. Spies, A. Drews, J. Label. Compd. Rad. 44 (2001) S507–S509.
[142] S.R. Banerjee, C.A. Foss, M. Castanares, R.C. Mease, Y. Byun, J.J. Fox, J. Hilton, S. E. Lupold, A.P. Kozikowski, M.G. Pomper, J. Med. Chem. 51 (2008) 4504–4517.
[143] S.R. Banerjee, M.K. Levadala, N. Lazarova, L. Wei, J.F. Valliant, K.A. Stephenson, J.W. Babich, K.P. Maresca, J. Zubieta, Inorg. Chem. 41 (2002) 6417–6425.
[144] H. Struthers, B. Spingler, T.L. Mindt, R. Schibli, Chem. Eur. J. 14 (2008) 6173–6183.
[145] B.A. Rhodes, C.R. Lambert, M.J. Marek, F.F. Knapp, E.B. Harvey, Appl. Radiat. Isot. 47 (1996) 7–14.
[146] S.M. Quadri, B.W. Wessels, Int. J. Rad. Appl. Instrum. B 13 (1986) 447–451.
[147] R. Schibli, R. Schwarzbach, R. Alberto, K. Ortner, H. Schmalle, C. Dumas, A. Egli, P.A. Schubiger, Bioconjugate Chem. 13 (2002) 750–756.
[148] A. Varvarigou, S. Archimandritis, M. Fani, P. Bouziotis, S. Vranjez, S. Xanthopoulos, A. Leonti, T. Sourlingas, M. Sotiropoulou, IAEA-TECDOC-1359 (2003) 85.
[149] P. Collery, G. Bastian, F. Santoni, A. Mohsen, M. Wei, T. Collery, A. Tomas, D. Desmaele, J. D'Angelo, Anticancer Res. 34 (2014) 1679–1689.
[150] P. Collery, F. Santoni, J. Ciccolini, T.N.N. Tran, A. Mohsen, D. Desmaele, Anticancer Res. 36 (2016) 6051–6057.
[151] A. Shtemenko, A. Golichenko, S. Tretyak, N. Shtemenko, M. Randarevich, Synthesis and antiradical properties of dirhenium cluster compounds, Metal Ions in Biology and Medicine (2008) 229–234.
[152] A.V. Shtemenko, P. Collery, N.I. Shtemenko, K.V. Domasevitch, E.D. Zabitskaya, A.A. Golichenko, Dalton Trans. (2009) 5132–5136.
[153] A.V. Shtemenko, N.I. Shtemenko, S.A. Oliynik, M.A. Zelenuk, Lyposome forms of rhenium cluster compounds in models of haemolytic anemia, in: L. Khassanova, P. Collery, I. Maymard, Z. Khassanova, J.C. Etienne (Eds.), Metal Ions in Biology and Medicine, 2002, pp. 558–561.
[154] N.I. Shtemenko, H.T. Chifotides, K.V. Domasevitch, A.A. Golichenko, S.A. Babiy, Z. Li, K.V. Paramonova, A.V. Shtemenko, K.R. Dunbar, J. Inorg. Biochem. 129 (2013) 127–134.
[155] N.I. Shtemenko, E.D. Zabitskaya, O.V. Berzenina, D.E. Yegorova, A.V. Shtemenko, Chem. Biodivers. 5 (2008) 1660–1667.
[156] A.V. Shtemenko, N.I. Shtemenko, Ukr. Biochem. J. 89 (2017) 5–30.
[157] M. Zhang, S. Shi, R. Guo, Y. Miao, B. Li, Oncol. Rep. 36 (2016) 2289–2297.
[158] K. Brylev, M. Shestopalov, O. Khripko, V. Trunova, V. Zvereva, C. Wang, Y.V. Mironov, V. Fedorov, Bull. Exp. Biol. Med. 155 (2013) 741–744.
[159] T.N. Pozmogova, A.A. Krasilnikova, A.A. Ivanov, M.A. Shestopalov, S.N. Gyrylova, L.V. Shestopalova, A.M. Shestopaloiv, V.A. Shkurupy, Bull. Exp. Biol. Med. 161 (2016) 64–68.
[160] P.L. Esquinas, C.F. Uribe, M. Gonzalez, C. Rodriguez-Rodriguez, U.O. Hafeli, A. Celler, Phys. Med. Biol. 62 (2017) 6379–6396.
[161] J.E. Cyr, D.A. Pearson, D.M. Wilson, C.A. Nelson, M. Guaraldi, M.T. Azure, J. Lister-James, L.M. Dinkelborg, R.T. Dean, J. Med. Chem. 50 (2007) 1354–1364.
[162] D.A. Pearson, J. Lister-James, W.J. McBride, D.M. Wilson, L.J. Martel, E.R. Civitello, J.E. Taylor, B.R. Moyer, R.T. Dean, J. Med. Chem. 39 (1996) 1361–1371.
[163] M.J. Edelman, G. Clamon, D. Kahn, M. Magram, J. Lister-James, B.R. Line, J. Thorac. Oncol. 4 (2009) 1550–1554.
[164] Y. Miao, N.K. Owen, D.R. Fisher, T.J. Hoffman, T.P. Quinn, J. Nucl. Med. 46 (2005) 121–129.
[165] W.T. Phillips, B. Goins, A. Bao, D. Vargas, J.E. Guttierez, A. Trevino, J.R. Miller, J. Henry, R. Zuniga, G. Vecil, Neuro-oncology 14 (2012) 416–425.
[166] NIS, US Library of Medicine, ClinicalTrials.gov Identifier NCT01906385, Maximum Tolerated Dose, Safety, and Efficacy of Rhenium Nanoliposomes in Recurrent Glioblastoma, https://clinicaltrials.gov/ct2/show/NCT01906385?term=rhenium&rank=3 (last accessed 28 Nov 2018).
[167] NIS, US Library of Medicine, ClinicalTrials.gov Identifier NCT03255343, Treatment of Non-responding to Conventional Therapy Inoperable Liver Cancers by in Situ Introduction of ImDendrim (ImDendrim), https://clinicaltrials.gov/ct2/show/NCT03255343?term=rhenium&draw=3&rank=8 (last accessed 28 Nov 2018).
[168] NIS, US Library of Medicine, ClinicalTrials.gov Identifier NCT01126463, 188RE-SSS Lipiodol to Treat HepatoCellular Carcinomas (LIP-RE-I), https://clinicaltrials.gov/ct2/show/NCT01126463?term=rhenium&rank=7 (last accessed 28 Nov 2018).
[169] E. Garin, B. Denizot, N. Noiret, N. Lepareur, J. Roux, M. Moreau, J.-Y. Herry, P. Bourguet, J.-P. Benoit, J.-J. Lejeune, Nuc. Med. Commun. 25 (2004) 1007–1013.
[170] N. Lepareur, V. Ardisson, N. Noiret, E. Garin, Int. J. Mol. Im. 2012 (2012).
[171] NIS, US Library of Medicine, ClinicalTrials.gov Identifier NCT02030184, Phase I/II Trial of Rhenium 188-P2045 in Small Cell Lung Cancer and Other Advanced Neuroendocrine Carcinomas, https://clinicaltrials.gov/ct2/show/NCT02030184?term=rhenium&rank=2 (last accessed 28 Nov 2018).
[172] NIS, US Library of Medicine, ClinicalTrials.gov Identifier NCT00100256, Rhenium Re 188 P2045 in Patients With Lung Cancer Who Have Received or Refused to Receive Prior Chemotherapy, https://clinicaltrials.gov/ct2/show/NCT00100256?term=rhenium&rank=4 (last accessed 28 Nov 2018).
[173] NIS, US Library of Medicine, ClinicalTrials.gov Identifier NCT01615991, Multicentre Canadian Study to Measure the Safety and Efficacy of Radiosynoviorthesis (RSO), https://clinicaltrials.gov/ct2/show/NCT01615991?term=rhenium&draw=3&rank=5 (last accessed 28 Nov 2018).
[174] M. Koppe, F.v. Schaijk, J. Roos, P.v. Leeuwen, K.-H. Heider, H. Kuthan, R. Bleichrodt, Cancer Biother. Radiopharm. 19 (2004) 720–729.
[175] A.M. Denis-Bacelar, S.J. Chittenden, D.P. Dearnaley, A. Divoli, J.M. O'Sullivan, V.R. McCready, B. Johnson, Y. Du, G.D. Flux, Eur. J. Nucl. Med. Mol. Imaging 44 (2017) 620–629.
[176] J.M. O'Sullivan, V.R. McCready, G. Flux, A.R. Norman, F.M. Buffa, S. Chittenden, M. Guy, K. Pomeroy, G. Cook, J. Gadd, J. Treleaven, A. Al-Deen, A. Horwich, R.A. Huddart, D.P. Dearnaley, Br. J. Cancer 86 (2002) 1715.
[177] H. Maxon, E. Deutsch, S. Thomas, K. Libson, S. Lukes, C. Williams, S. Ali, Radiology 166 (1988) 501–507.
[178] H.R. Maxon, S.R. Thomas, V.S. Hertzberg, L.E. Schroder, E.E. Englaro, R. Samaratunga, H.I. Scher, J.S. Moulton, E.A. Deutsch, K.F. Deutsch, Semin. Nucl. Med., Elsevier (1992) 33–40.
[179] M.C. Graham, H.I. Scher, G.-B. Liu, S.D. Yeh, T. Curley, F. Daghighian, S.J. Goldsmith, S.M. Larson, Clin. Cancer Res. 5 (1999) 1307–1318.
[180] M. Erfani, N. Rahmani, A. Doroudi, M. Shafiei, Nucl. Med. Biol. 49 (2017) 1–7.
[181] C. Fernandes, S. Monteiro, A. Belchior, F. Marques, L. Gano, J.D.G. Correia, I. Santos, Nuc. Med. Bio. 43 (2016) 150–157.
[182] NIS, US Library of Medicine, ClinicalTrials.gov Identifier NCT03458559, Rhenium-188-HEDP vs. Radium-223-chloride in Patients With Advanced Prostate Cancer Refractory to Hormonal Therapy (RaRe), https://clinicaltrials.gov/ct2/show/NCT03458559?term=rhenium&rank=1 (last accessed 28 Nov 2018).
[183] I.G. Finlay, M.D. Mason, M. Shelley, Lancet Oncol. 6 (2005) 392–400.
[184] A. Levina, D.C. Crans, P.A. Lay, Coord. Chem. Rev. 352 (2017) 473–498.
[185] D.C. Crans, K.A. Woll, K. Prusinskas, M.D. Johnson, E. Norkus, Inorg. Chem. 52 (2013) 12262–12275.
[186] K.A. Doucette, K.N. Hassell, D.C. Crans, J. Inorg. Biochem. 165 (2016) 56–70.
[187] M. Le, O. Rathje, A. Levina, P.A. Lay, J. Biol. Inorg. Chem. 22 (2017) 663–672.
[188] N. Samart, Z. Arhouma, S. Kumar, H.A. Murakami, D.C. Crick, D.C. Crans, Front. Chem. 6 (2018).
[189] S. Fulda, L. Galluzzi, G. Kroemer, Nat. Rev. Drug Discov. 9 (2010) 447.